The Dissertation Committee for Ijung Kim Certifies that this is the approved version of the following dissertation:

TRANSPORT AND RETENTION OF SILVER NANOPARTICLES IN GRANULAR MEDIA FILTRATION

Committee:

Desmond F. Lawler, Supervisor

Howard M. Liljestrand

Lynn E. Katz

Brian A. Korgel

Boris L. T. Lau

TRANSPORT AND RETENTION OF SILVER NANOPARTICLES
IN GRANULAR MEDIA FILTRATION

by

Ijung Kim, B.S., M.S.

Dissertation

Presented to the Faculty of the Graduate School of

The University of Texas at Austin

in Partial Fulfillment

of the Requirements

for the Degree of

Doctor of Philosophy

The University of Texas at Austin

August 2014

I have been crucified with Christ and I no longer live, but Christ lives in me. The life I now live in the body, I live by faith in the Son of God, who loved me and gave himself for me.

Galatians 2:20

Acknowledgements

I would like to express my deep gratitude to my advisor, Professor Desmond Lawler who inspired me to think as a researcher and to encounter the unsolved research problems. I am sure this training will be the strong foundation for my future research. Also, I appreciate all his supports that enabled me to complete my graduate study.

I would like to offer my sincere thanks to my committee members, Professors Howard Liljestrand, Lynn Katz, Brian Korgel, and Boris Lau, for their guidance and comments on my dissertation.

I am pleased to acknowledge the support of my research group members. Especially, Tongren worked with me day and night, and his help was tremendous to complete this work. I also would like to thank Sungmin and Anne who encouraged and helped me to overcome the struggles in my research. I would like to acknowledge Chanhoo who helped me to figure out the modeling. EWRE friends including my wonderful officemates, Aurore, Celina and Shahana, have made my ECJ life more enjoyable and comfortable. I also thank all my Korean friends for their help and the pleasant memories we shared.

Special gratitude is extended to my family church members. Their prayers and supports have encouraged me to be on the faith. I owe a debt of love to Pastor Ilsun Kim, Inhye Park, Sungtae Son, Insook Son, Youngmi Choi, and Keumhwa Chun for their unforgettable loving care which saved my life when I was seriously sick. Halleluja choir was always my comfort and I thank all the choir members for sharing kind and warm greetings which have strengthened me spiritually.

TRANSPORT AND RETENTION OF SILVER NANOPARTICLES IN GRANULAR MEDIA FILTRATION

Ijung Kim, Ph.D.

The University of Texas at Austin, 2014

Supervisor: Desmond F. Lawler

The increasing use of engineered nanoparticles such as silver nanoparticles (AgNPs) has focused more attention on the transport of nanoparticles in natural and engineered systems. Despite a substantial number of studies on the transport of nanoparticles in groundwater flow conditions, other conditions such as those in granular media filtration in water treatment plant have not been fully explored. This study was designed to investigate the transport of AgNPs in granular media filtration with a relatively high filtration velocity (~2 m/hr) and a low influent AgNP concentration (~100 µg/L). Effects of several physical and chemical parameters on the transport and attachment of AgNPs were examined, focusing on the colloidal filtration theory and particle-particle interaction, respectively.

Regarding the transport of AgNPs, four physical parameters (filter depth, filtration velocity, filter media size, and AgNP size) were varied at a fixed chemical condition. Positively charged branched polyethylenimine (BPEI) capped AgNPs were chosen to examine the transport of AgNPs under electrostatically favorable attachment conditions. The effects of filter depth, filtration velocity, and filter media size on transport of AgNPs were adequately described by the well-known colloidal filtration model. However, deviation from the model prediction was apparent as the AgNP size

became smaller, implying a possible variation of nanoparticle properties in the smaller size such as 10 nm.

In the AgNP attachment study, negatively charged citrate- and polyvinylpyrrolidone (PVP)-capped AgNPs were employed to examine the chemical effects on particle (AgNP)-particle (filter media) interaction. When the ionic strength and ion type in the background water were varied, the attachment of citrate AgNPs followed the DLVO theory. Ca- or Mg-citrate complexation was found to lead to charge neutralization, resulting in a greater AgNP deposition onto the filter media. However, PVP AgNPs were only marginally affected by the electrostatic effect, demonstrating a stronger stabilizing effect by PVP than citrate.

When natural organic matter (NOM) was introduced in the background water, the deviation from the DLVO theory was considered primarily due to the steric interaction by NOM coating onto particles. Different amounts of AgNP deposition for different types of NOM suggest the variation of steric effects according to the molecular weight of NOM. The deposition of humic acid-coated AgNPs was similar regardless of the capping agent, indicating the possible displacement of the capping agent by NOM.

The electrostatic and steric interactions affected the detachment of AgNPs as well as the attachment of AgNPs. The amount of detachment depended on the depth and width of the secondary energy minimum. Also, the detachment was enhanced with NOM coating, probably due to a weak attachment by the steric effect. However, the hydrodynamic force employed in this study was insufficient to yield a remarkable detachment.

Overall, the retention profile was a relatively vertical line (i.e., equal deposition with depth) when the AgNP aggregation was prevented by the electrostatic or steric repulsion, implying homogeneous AgNP capture throughout the filter bed. On the other

hand, ripening (the capture of particles by attraction to previously retained particles) was favored at the top of the filter bed when the AgNP aggregation was allowable.

Table of Contents

List of Tables

List of Figures

Chapter 1: INTRODUCTION

1.1. Background

With technical advances in both the synthesis and analysis of chemicals, an increasing number of emerging compounds have been found in surface water. Their beneficial uses for humans can be cancelled out by returning them as a threat to the environment and ultimately to humans. One of the governing rules in nature is that every material has its own cycle. If the concentration of one chemical increases beyond the threshold that nature can stand, the resulting pollution would ruin the balance in the environment. In this sense, the increasing use of engineered nanoparticles all over the world and their release into water lead to a concern about possible harm to the aquatic environment. While the mechanism of engineered nanoparticles toxicity is still debatable (Xiu et al. 2012), the commercial products containing various nanoparticles have been growing in the market because of their perceived beneficial uses for humans. Beyond toxicity studies, it is important to understand how nanoparticles are transported and retained in natural and engineered systems to get a broader knowledge for decision-making on their future use.

Due to their ability to disinfect (Morones et al. 2005), silver nanoparticles (AgNPs) have become one of most widely used nanoparticles in consumer products (Benn and Westerhoff 2008, Rai et al. 2008). Silver is 'not classified as to human carcinogenicity' (EPA 2014), and the silver regulation in drinking water is 0.1 mg/L (NARA 2014) just to prevent skin discoloration; the regulations do not account for any other possible public health or environmental concerns. Because the prolonged and publicly accepted image is that silver is safe enough to use in human life, silver colloidal products have even been used as health supplements (Panyala et al. 2008). However,

AgNPs are accumulating in the environment, particularly in sediment and sludge treated soil with an approximately 300% increase in four years (Gottschalk et al. 2009). When highly accumulated, AgNPs can be toxic by releasing silver ions or damaging cell behavior (Lubick 2008), eventually posing a negative impact, e.g., on the performance of wastewater treatment facilities (Liang et al. 2010). Even after treatment, some AgNPs can be released into larger water streams (Kaegi et al. 2011, Nowack 2010).

A strict regulation can be found in Australia where the water quality limit for silver has been set at 0.05 μg/L due to the toxicity to aquatic species (Cornelis et al. 2012). Therefore, it seems likely that the removal of AgNPs from water will be considered desirable throughout the world in the near future to protect aquatic life and human health. Since 2010, official action within the Unites States has been taken to collect more information about AgNPs, and the regulation of AgNPs is still under investigation (Regulations 2014). With regard to research on the transport of nanoparticles, a considerable amount of research (Appendix A) has been focused on the transport of various nanoparticles in porous media. Most of these previous studies were aimed at understanding their movement in groundwater and hence have been done at very low filtration velocity. Also, because of the analytical challenge of measuring AgNPs at low concentrations, most studies have been performed with a high influent concentration (milligrams per liter) although actual AgNP concentrations in water are generally in the range of μg/L (Fabrega et al. 2011). Therefore, it is desirable to study the capacity of existing filtration technology in most drinking water treatment plants to remove emerging contaminants such as nanoparticles at low concentrations. Taking this background into consideration, it is necessary to investigate the granular media filtration of AgNPs in the physical and chemical conditions that are commonly found in drinking water treatment plants.

1.2. Research objectives

Though the definition of a nanoparticle is on the basis of the particle size (usually defined as a particle between 1 and 100 nm in at least one dimension), differences in behavior between nanoparticles and bigger particles might be caused by more than simply an increase in specific surface area. For example, the greater surface reactivity of nanoparticles due to changes in local electronic structure (Raimondi et al. 2005) could lead to differences in the attachment of nanoparticles to filter surfaces in comparison to that of larger particles. The primary concern about the transport and attachment of nanoparticles in granular media filtration is how they are influenced by the physical and chemical conditions of the filter media, the nanoparticles, and the filter operation. Assuming Brownian motion is the dominant mechanism of collision can lead to certain expectations about the effects of several parameters on the transport and attachment of nanoparticles. Therefore, experimental verification is necessary to test whether those theoretical expectations are met. The overall purpose of this study was to elucidate the transport and attachment of nanoparticles in granular media filtration in conditions resembling those at water treatment plants. Separate approaches were adopted to study attachment and transport.

With regard to attachment of particles onto the media, chemical parameters such as ionic strength (and the type of ion making up that ionic strength) and the surface chemistry of the particles (or any coating on those particles) are known to have the greatest effect. These parameters affect the level of attraction and repulsion forces (electrostatic, steric, and perhaps others) between particles and media. The simplified forces between a particle and a media are shown in Figure 1.1 (a). Once a nanoparticle is captured in the granular media filter, it is crucial to see whether the attachment is reversible and how such reversibility is affected by the physical or chemical conditions.

Therefore, detachment of previously captured nanoparticles is required to study as well; substantial detachment could suggest that the original retention is in the secondary energy minimum. Findings from attachment under one set of chemical conditions and detachment (release of captured particles) under different conditions can be used to evaluate how many particles are strongly or loosely captured and what factor is the most influential to the attachment of the nanoparticles.
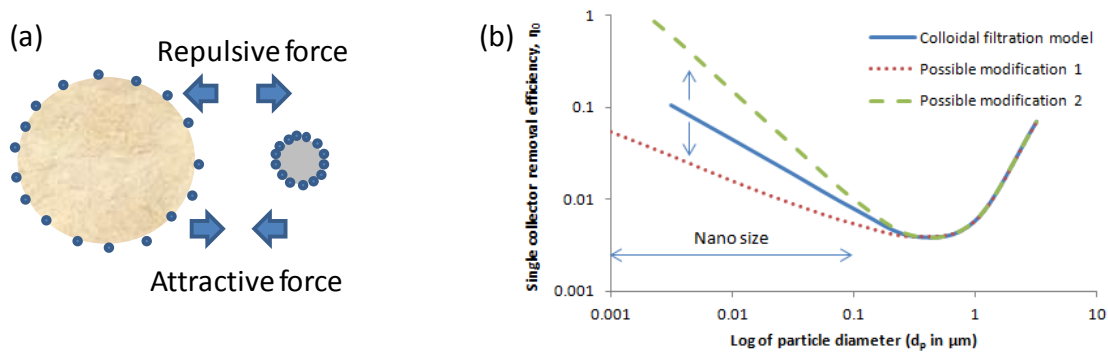
Figure 1.1:   Research concept of (a) attachment, (b) transport aspects.

Although many studies of nanoparticle deposition have been performed, few have been done at conditions that emulate water or wastewater filtration, and to our knowledge, few have been done to study the pattern of nanoparticle deposition onto the media. A greater knowledge of the pattern of particle deposition (i.e., the distribution of attachment with depth) is desirable to elucidate how ripening can be achieved in granular media filtration of nanoparticles. Nanoparticles captured in the filter bed can be measured as a function of depth to provide the concentration profile of nanoparticles.

With regard to transport, an existing colloidal filtration model has been used by many investigators to derive the filtration parameters such as contact efficiency (η_0) and attachment efficiency (α) from the experimental data. However, the model was

4

established mostly with particles greater than 1 µm. Figure 1.1(b) conceptually shows the possible deviations from the colloidal filtration model where the particle size is less than 1 µm. Therefore, further experimental evaluation with nanoparticles is needed to examine whether the existing model fits to transport of the nanoparticles. Under favorable conditions with the oppositely charged particles, the colloidal filtration model can be used to scrutinize whether the transport of nanoparticles differs from the expectations of the model.

In summary, the overall objective of this research was to study the granular media filtration of silver nanoparticles in conditions resembling filtration at water treatment plants. The specific objectives of this research were as follows:

- To evaluate the validity of the colloidal transport model with the nanoparticles under varying conditions of nanoparticle size, media size, filter depth and velocity;

- To investigate the effect of ionic strength and the type of ion on the attachment of nanoparticles to a granular media filter;

- To investigate the effect of natural organic matter coating on the attachment of nanoparticles to a granular media filter; and,

- To study the detachment (release) of the captured nanoparticles under different ionic strengths and filtration velocities.

References

Benn, T.M. and Westerhoff, P. (2008) Nanoparticle silver released into water from commercially available sock fabrics. Environmental Science & Technology 42(18), 7025-7026.

Cornelis, G., Doolette, C., Thomas, M., McLaughlin, M.J., Kirby, J.K., Beak, D.G. and Chittleborough, D. (2012) Retention and dissolution of engineered silver nanoparticles in natural soils. Soil Science Society of America Journal 76(3), 891-902.

EPA (2014) Integrated risk information system. Available at http://www.epa.gov/iris/subst/0099.htm.

Fabrega, J., Luoma, S.N., Tyler, C.R., Galloway, T.S. and Lead, J.R. (2011) Silver nanoparticles: Behaviour and effects in the aquatic environment. Environment International 37(2), 517-531.

Gottschalk, F., Sonderer, T., Scholz, R.W. and Nowack, B. (2009) Modeled environmental concentrations of engineered nanomaterials (TiO_2, ZnO, Ag, CNT, fullerenes) for different regions. Environmental Science & Technology 43(24), 9216-9222.

Kaegi, R., Voegelin, A., Sinnet, B., Zuleeg, S., Hagendorfer, H., Burkhardt, M. and Siegrist, H. (2011) Behavior of metallic silver nanoparticles in a pilot wastewater treatment plant. Environmental Science & Technology 45(9), 3902-3908.

Liang, Z.H., Das, A. and Hu, Z.Q. (2010) Bacterial response to a shock load of nanosilver in an activated sludge treatment system. Water Research 44(18), 5432-5438.

Lubick, N. (2008) Nanosilver toxicity: ions, nanoparticles-or both? Environmental Science & Technology 42(23), 8617-8617.

Morones, J.R., Elechiguerra, J.L., Camacho, A., Holt, K., Kouri, J.B., Ramirez, J.T. and Yacaman, M.J. (2005) The bactericidal effect of silver nanoparticles. Nanotechnology 16(10), 2346-2353.

NARA (2014) e-CFR Title-40 Part 143.3 Secondary maximum contaminant level. Available at http://www.ecfr.gov/cgi-bin/text-idx?SID=5c2f71fbc4c7e6fc033d5ad9787e0e61&node=40:23.0.1.1.5.0.39.3&rgn=div8.

Nowack, B. (2010) Nanosilver revisited downstream. Science 330(6007), 1054-1055.

Panyala, N.R., Pena-Mendez, E.M. and Havel, J. (2008) Silver or silver nanoparticles: a hazardous threat to the environment and human health? Journal of Applied Biomedicine 6(3), 117-129.

Rai, M., Tadav, A. and Gade, A. (2008) Silver nanoparticles as a new generation of antimicrobials. Biotechnology Advances 27(1), 76-83.

Raimondi, F., Scherer, G.G., Kotz, R. and Wokaun, A. (2005) Nanoparticles in energy technology: Examples from electrochemistry and catalysis. Angewandte Chemie-International Edition 44(15), 2190-2209.

Regulations (2014). Silver nanoparticles; information and comment request. Available at http://www.regulations.gov/#!documentDetail;D=CDC-2012-0014-0001.

Xiu, Z.M., Zhang, Q.B., Puppala, H.L., Colvin, V.L. and Alvarez, P.J.J. (2012) Negligible particle-specific antibacterial activity of silver nanoparticles. Nano Letters 12(8), 4271-4275.

Chapter 2: LITERATURE REVIEW

2.1. Silver Nanoparticles

2.1.1. Application and synthesis

AgNPs are not a new product and, in fact, they have been used for a long time in various fields, most notably photography (Debnath et al. 2010). Recently, however, the application of AgNPs in customer products has rapidly increased, due to their strong ability to inactivate a wide range of bacteria (Tolaymat et al. 2010). The data in Figure 2.1 indicate the dramatic rise in the use of AgNPs, as well as the rise in use of various other nanoparticles.
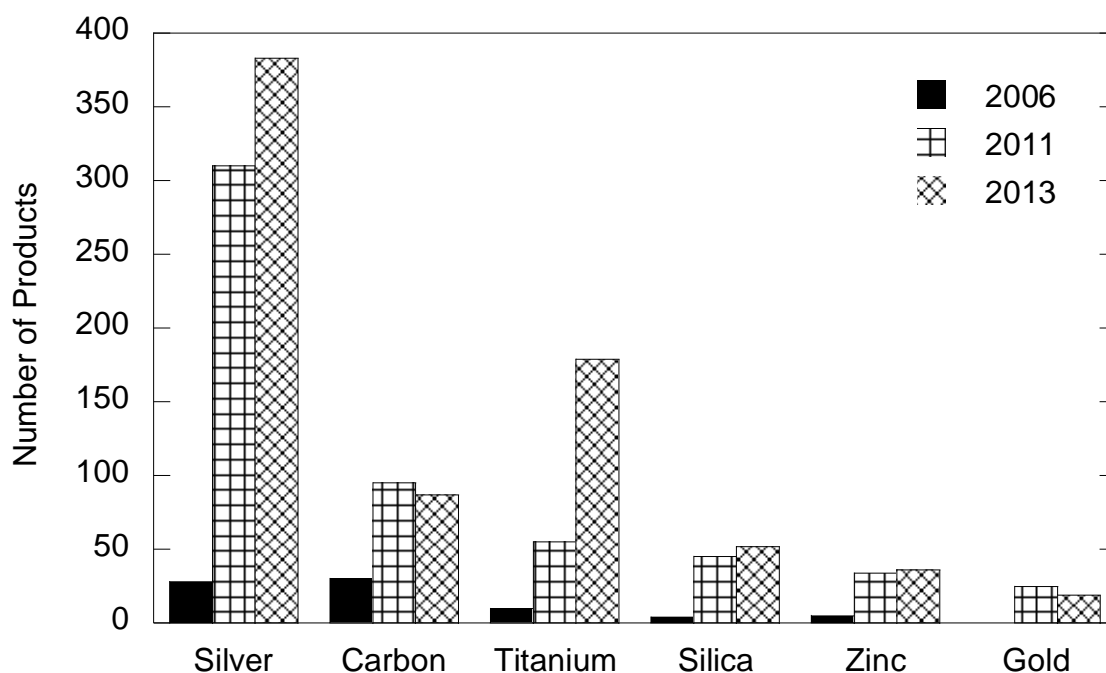
Figure 2.1:   Growth of products associated with specific nanomaterials (available at http://www.nanotechproject.org/cpi/about/analysis).

Several recent studies have focused on synthesis of AgNPs due to their increasing use. AgNPs are made of pure silver, i.e., silver in the zero oxidation state. One of the

commonly used synthesis methods in AgNPs research is to reduce Ag ions in solution with a reducing agent such as sodium borohydride, as shown in Equation 2-1.

$$AgNO_3 + NaBH_4 \rightarrow Ag^0 + \frac{1}{2}H_2 + \frac{1}{2}B_2H_6 + NaNO_3 \tag{2-1}$$
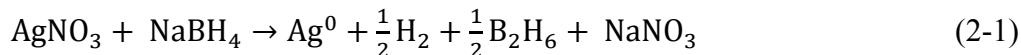
Though borohydride can adsorb onto the surface of AgNPs and provide negative surface charges that make the particles stable to some degree (Solomon et al. 2007), AgNPs can aggregate during the synthesis process. Therefore, it is normally required to add surface capping agents as well as the reducing agents to prevent aggregation during AgNP synthesis (Khanna et al. 2007). The capping agents play a role in controlling particle shape and size as well as providing stability during AgNP synthesis. The most widely used capping agents are citrate and polyvinylpyrrolidone (PVP) (Tolaymat et al. 2010).

A single AgNP is a cluster containing many Ag atoms. The number of atoms packed in an AgNP can be estimated by comparing the volumes of an Ag atom and an AgNP, assuming the diameter of an Ag atom is 0.288 nm (Key and Maass 2001). By high-resolution electron microscopy, the arrangement of Ag atoms in a AgNP was shown to be a cuboctahedron (Hofmeister et al. 2005). As a reference, the number of Ag atoms in a single AgNP is shown in Table 2.1, assuming the packing density is 0.74 from densest sphere packing form (Sloane 1998).

Table 2.1:   Number of Ag atoms in a single AgNP.

AgNP diameter (nm)	Estimated number of Ag atoms per particle	Estimated number of Ag atoms on surface
1	30	28
10	30,000	5,000
50	3,870,000	132,000
100	30,000,000	532,000

2.1.2. Fate and speciation

The fate of AgNPs when they are released into water is of particular interest in AgNP research. First, the oxidation of AgNPs (i.e., Ag^{+} ion release) has been suggested as a thermodynamically favored reaction at room temperature in oxygenated water (Liu and Hurt 2010), as shown in Equation 2-2.

$$2Ag_{(s)} + \frac{1}{2}O_{2(aq)} + 2H^{+}_{(aq)} \rightarrow 2Ag^{+}_{(aq)} + H_2O_{(l)} \, , \Delta G^0_{rxn} = -91.3 \text{ kJ/mol} \quad (2\text{-}2)$$
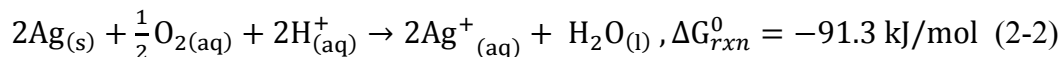
The authors suggested that, through this reaction, the complete dissolution of AgNPs could occur at the dissolved oxygen level of natural water if they were exposed for a long time (e.g., several to over 100 days).

Second, reaction with inorganic compounds can transform AgNPs into inorganic silver solids. The probable species after the dissolution of AgNP are Ag$_2$S or AgCl based on the thermodynamics, though most of AgNPs still can be stable in natural waters above pH 8 (Levard et al. 2012). AgNPs were found in sewage sludge as Ag$_2$S (Kaegi et al. 2011, Kim et al. 2010), implying AgNPs can be sulfidized when they encounter high sulfide concentration water like in reduced (de-oxygenated) wastewater. Several studies about fate and stability of engineered AgNPs in natural waters or wastewater also suggest the likely transformation of AgNPs (Kaegi et al. 2012, Li and Lenhart 2012, Lowry et al. 2012).

However, the stability of AgNPs can be enhanced when capped by the stabilizing agents in the synthesis process or coated by NOM in the environment (Delay et al. 2011). Even if dissolved, Ag ions can be turned back into AgNPs when they are exposed to humic acids in natural water (Akaighe et al. 2011). Also, some AgNPs were so persistent that they could flow through surface water until reaching marine water (Chinnapongse et al. 2011). It is difficult to make any conclusive statement about the fate of AgNPs in the environment at this moment and further studies are required.

2.1.3. Existing concentration and harmful effect on the environment

A few studies have reported existing Ag concentrations in surface waters: 0.2~0.3 µg/L in natural waters (WHO 2003), 38 µg/L in the Colorado River (Wijnhoven et al. 2009), 8~25 µg/L in California waters (Environmental_Working_Group 2014) and 10~200 µg/L in US waters (Fleischer 1963). Assuming Ag emission from AgNPs products as well as naturally existing Ag, the predicted Ag concentration is 0.04~0.32 µg/L in river water and 2~18 µg/L in sewage treatment plants (Blaser et al. 2008). It seems that the currently available data do not show a high level of Ag concentration in natural waters. However, locally accumulated Ag concentration in soils was predicted to increase up to 2~8 µg/kg on the basis of Ag release from AgNP products (Gottschalk et al. 2009).

Ag has been known for its adverse effects on microorganisms in the environment (Liau et al. 1997). For AgNPs, their negative effect can occur by producing reactive oxygen species (Carlson et al. 2008, Choi and Hu 2008, Foldbjerg et al. 2009) and releasing Ag ions (Kittler et al. 2010). Even at very low concentrations of AgNPs (e.g., 140 µg/L of AgNPs), nitrifying bacteria can be inhibited (Choi and Hu 2008). In addition, fish can be affected by interacting with Ag, because silver ions can inhibit the activity of enzymes (Wood et al. 1999). Furthermore, AgNPs could pose a threat to human health because prolonged exposure to Ag could cause damage to human organs such as the kidney and liver (Panyala et al. 2008).

2.2. Granular Media Filtration

Granular media filtration is the most commonly used process to remove particles that remain in water after sedimentation in a drinking water treatment plant. Historically, it has been applied for the protection of public health; the extensive application of

granular media filtration to remove pathogens from drinking water was achieved in the late 1800's in Europe and early 1900's in United States (Baker 1948). Since then, it has been thought of as a key process in water treatment.

Usually, the water flow in granular media filtration in water treatment plants is downflow, as shown in Figure 2.2. Granular media filtration can be accomplished either as slow sand filtration or rapid filtration. Slow sand filtration operates at filtration velocities less than 0.3 m/hr. Though slow filtration cannot be used for treating high turbidity water, it has been effective in removing pathogens like G. *Lamblia*. In addition, because of its low cost and simple configuration, slow sand filtration became an efficient process in the early years of water treatment. However, in modern large water treatment plants, rapid filtration became required and filtration velocities from 5 to 20 m/hr are used to achieve the required performance. The selection of operating parameters such as filtration velocity, filter media size, and filter depth depends on the objective of the operation as well as the costs.
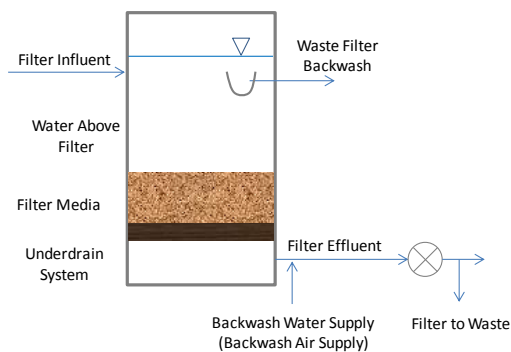
Figure 2.2:   Schematic view of granular media filter.

The most commonly used media in granular media filters are silica sand and anthracite coal, and the recommended media size is 0.25~0.35 mm for slow filtration (EPA 1990) and 0.45 mm or greater for rapid filtration (Schulz and Okun 1984). Most

modern water treatment plants use dual media filters (Curley 2010), with a layer of coarser anthracite coal on the top and finer sand on bottom. The target contaminants are the original particles in the water (including microorganisms) and those formed in prior treatment steps such as precipitative coagulation and softening. The particle size ranges of those contaminants are shown in Figure 2.3 along with the treatment options for those particles in accordance with common knowledge. Nanoparticles are in the range of 1~100 nm which is smaller than what a granular media filter is supposed to remove (typically particle size greater than 2 μm in drinking water applications). However, Yao et al. 1971 suggested that the removal efficiency in granular media filtration would be minimized at a particle size of approximately 1 μm and that the removal would be better with decreasing particle size due to diffusion (Brownian motion).
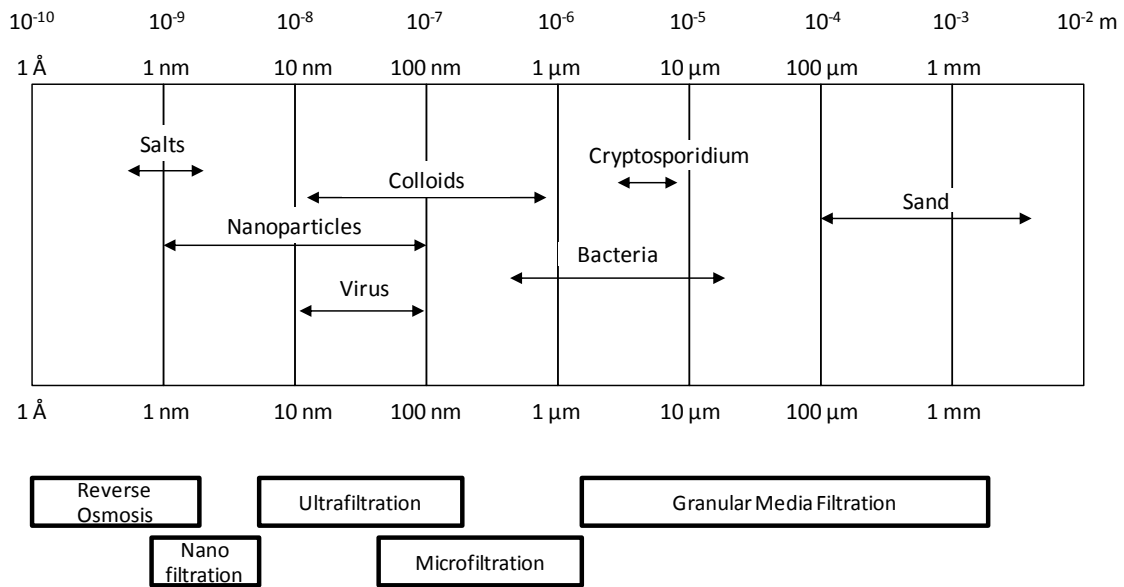
Figure 2.3: General particle size distribution of particulate contaminants with various treatment options (EPA 1999).

2.3. Filtration Mechanisms and Models

Though granular media filters can be designed in many ways, the basic mechanism to remove particles is the same. Focusing on a single grain of the media (i.e., a collector), many researchers have tried to get some insights of the transport model of the particles in the filtration. The filtration mechanism can be divided into two parts: transport and attachment. The two concepts can be found in the mathematical terms of Equation 2-3 for a single collector efficiency (all variables in following equations are defined in Appendix B).

$$\eta = \alpha \eta_0 \tag{2-3}$$

The single collector removal efficiency (η) of particles is expressed as the product of the particle-media attachment efficiency (α) and the particle-media contact efficiency (η_0).

In the single collector model, α is defined as the ratio of the particles attaching to a media grain to the particles contacting a grain. η_0 is defined as the ratio of the rate at which particles contact a media grain to the rate at which particles approach that grain, and is approximated as the sum of separate values for particle transport by interception, sedimentation, and Brownian motion. When the attachment is favorable ($\alpha=1$), that is, under the absence of an energy barrier, the removal efficiency becomes equal to the particle-media contact efficiency ($\eta=\eta_0$). So far, most models to predict η are based on the assumption of $\alpha=1$ (Long and Hilpert 2009, Ma et al. 2009, Nelson and Ginn 2011, Tufenkji and Elimelech 2004, Yao et al. 1971).

2.3.1. Transport model in granular media filtration

The transport of nanoparticles in filtration can be derived from the convective-diffusion equation (Li et al. 2008, Wang et al. 2008b).

$$\frac{\partial N}{\partial t} = D \frac{\partial^2 N}{\partial x^2} - v_0 \frac{\partial N}{\partial x} - \frac{\rho_c}{\varepsilon} \frac{\partial S}{\partial t} \tag{2-4}$$

14

Since the filtration model is derived from the interactions between individual particles and a single collector (Benjamin and Lawler 2013), it is required to use number concentration (N) instead of mass concentration (C). It is impossible to get the analytical solution when considering various parameters of the particles and the fluid. However, many efforts have been made to describe the transport in mathematical terms. As a first step, the single collector efficiency was suggested as the combination of the analytical expression of diffusion (Brownian motion), interception, and sedimentation (Yao et al. 1971).

$$\eta_0 = \eta_D + \eta_I + \eta_G = 0.9 \left(\frac{kT}{\mu d_p d_c v_o} \right)^{\frac{2}{3}} + \frac{3}{2} \left(\frac{d_p}{d_c} \right)^2 + \frac{\left(\rho_p - \rho_f \right) g d_p^2}{18 \mu v_0} \tag{2-5}$$

Since then, the concept of combining diffusion, interception, and sedimentation has been accepted. The single-collector contact efficiency of Brownian-sized particles has been modified by several researchers as below. They solved the convective-diffusion equation numerically and performed nonlinear regression to obtain the parameters (the coefficients of each term and the power of each dimensionless parameter such as N_R, N_{Pe}, etc).

From Tufenkji and Elimelech, 2004:

$$\eta_0 = 2.4 A_s^{\frac{1}{3}} N_R^{-0.081} N_{Pe}^{-0.715} N_{vdW}^{0.052} + 0.55 A_s N_R^{1.675} N_A^{0.125} \\ + 0.22 N_R^{-0.24} N_G^{1.11} N_{vdW}^{0.053} \tag{2-6}$$

From Long and Hilpert, 2009:

$$\eta_0 = \left(15.56 \pm 0.21 \right) \frac{\left(1 - \varepsilon \right)^3}{\varepsilon^2} N_{Pe}^{-0.65 \pm 0.023} N_R^{0.19 \pm 0.03} + 0.55 A_s N_R^{1.675} N_A^{0.125} \\ + 0.22 N_R^{-0.24} N_G^{1.11} N_{vdW}^{0.053} \tag{2-7}$$

From Ma et al., 2009:

$$\eta_0 = \gamma^2 [2.3 A_s^{1/3} N_R^{-0.028} N_{Pe}^{-0.66} N_A^{0.052} + 0.55 A_s N_R^{1.8} N_A^{0.15}$$
$$+ 0.2 N_R^{-0.047} N_G^{1.1} N_{Pe}^{0.053} N_A^{0.053}]$$

(2-8)

where $\gamma = (1-\varepsilon)^{\frac{1}{3}}$.

From Nelson and Ginn, 2011:

$$\eta_0 = \gamma^2 [2.4 A_s^{1/3} \left(\frac{N_{Pe}}{N_{Pe}+16}\right)^{0.75} N_{Pe}^{-0.68} N_{Lo}^{0.015} N_{Gi}^{0.8} + A_s N_{LO}^{1/8} N_R^{15/8}$$
$$+ 0.7 \left(\frac{N_{Gi}}{N_{Gi}+0.9}\right) N_G N_R^{-0.05}]$$

(2-9)

Normally, the single collector removal efficiency (η) can be scaled up to that of a full filter as follows.

$$\ln \frac{N}{N_0} = -\frac{3}{2}(1-\varepsilon)\eta \left(\frac{L}{d_c}\right)$$

(2-10)

Assuming the absence of an energy barrier and Brownian motion as dominant mechanism in transport for nanoparticles, η becomes η_D and the relative concentration (N/N_0) of a full filter can be a function of the parameters such as d_c, d_p, v_0, and L. Using the five models mentioned above (Equations 2-5 through 2-9), the results for nanoparticles (i.e., particles whose transport is dominated by Brownian motion) are as follows:

From Yao et al., 1971:

$$\ln\left(\frac{N}{N_0}\right) = -\frac{3}{2}(1-\varepsilon)0.9\left(\frac{kT}{\mu d_p d_c v_0}\right)^{\frac{2}{3}}\left(\frac{L}{d_c}\right) = 0.9\left(\frac{kT}{\mu}\right)^{\frac{2}{3}}\left(\frac{L}{d_c^{\frac{5}{3}} d_p^{\frac{2}{3}} v_0^{\frac{2}{3}}}\right)$$
$$= a\left(\frac{L}{d_c^{1.67} d_p^{0.67} v_0^{0.67}}\right)$$

(2-11)

From Tufenkji and Elimelech, 2004:

$$\ln\left(\frac{N}{N_0}\right) = -\frac{3}{2}(1-\varepsilon)2.4A_s^{\frac{1}{3}}\left(\frac{d_p}{d_c}\right)^{-0.081}\left(\frac{3\mu\pi v_0 d_c d_p}{kT}\right)^{-0.715}\left(\frac{A}{kT}\right)^{0.052}\left(\frac{L}{d_c}\right)$$

$$= b\left(\frac{L}{d_c^{1.634}d_p^{0.796}v_0^{0.715}}\right) \tag{2-12}$$

From Long and Hilpert, 2009:

$$\ln\left(\frac{N}{N_0}\right) = -\frac{3}{2}(1-\varepsilon)15.56\frac{(1-\varepsilon)^3}{\varepsilon^2}\left(\frac{3\mu\pi v_0 d_c d_p}{kT}\right)^{-0.65}\left(\frac{d_p}{d_c}\right)^{0.19}\left(\frac{L}{d_c}\right)$$

$$= c\left(\frac{L}{d_c^{1.84}d_p^{0.46}v_0^{0.65}}\right) \tag{2-13}$$

From Ma et al., 2009:

$$\ln\left(\frac{N}{N_0}\right) = -\frac{3}{2}(1-\varepsilon)2.3A_s^{\frac{1}{3}}\left(\frac{d_p}{d_c}\right)^{-0.028}\left(\frac{3\mu\pi v_0 d_c d_p}{kT}\right)^{-0.66}\left(\frac{A}{3\pi\mu d_p^2 v_0}\right)^{0.052}\left(\frac{L}{d_c}\right)$$

$$= d\left(\frac{L}{d_c^{1.532}d_p^{0.792}v_0^{0.712}}\right) \tag{2-14}$$

From Nelson and Ginn, 2011:

$$\ln\left(\frac{N}{N_0}\right) = -\frac{3}{2}(1-\varepsilon)\gamma^2 2.4A_s^{\frac{1}{3}}\left(\frac{3\mu\pi v_0 d_c d_p}{kT}\right)^{-0.68}\left(\frac{4A}{9\pi\mu d_p^2 v_0}\right)^{0.015}\left(\frac{L}{d_c}\right)$$

$$= e\left(\frac{L}{d_c^{1.68}d_p^{0.98}v_0^{0.695}}\right) \tag{2-15}$$

Overall, the powers of each parameter look similar in those models, and the single collector contact efficiencies from all of the models also nearly agree in the nanoparticle size range, except for the model of Tufenkji and Elimelech (Figure 2.4). However, it should be noted that these results are based on mathematical simulations, and the support of experimental data is needed to prove the validity of the classical colloidal filtration theory with nanoparticles.
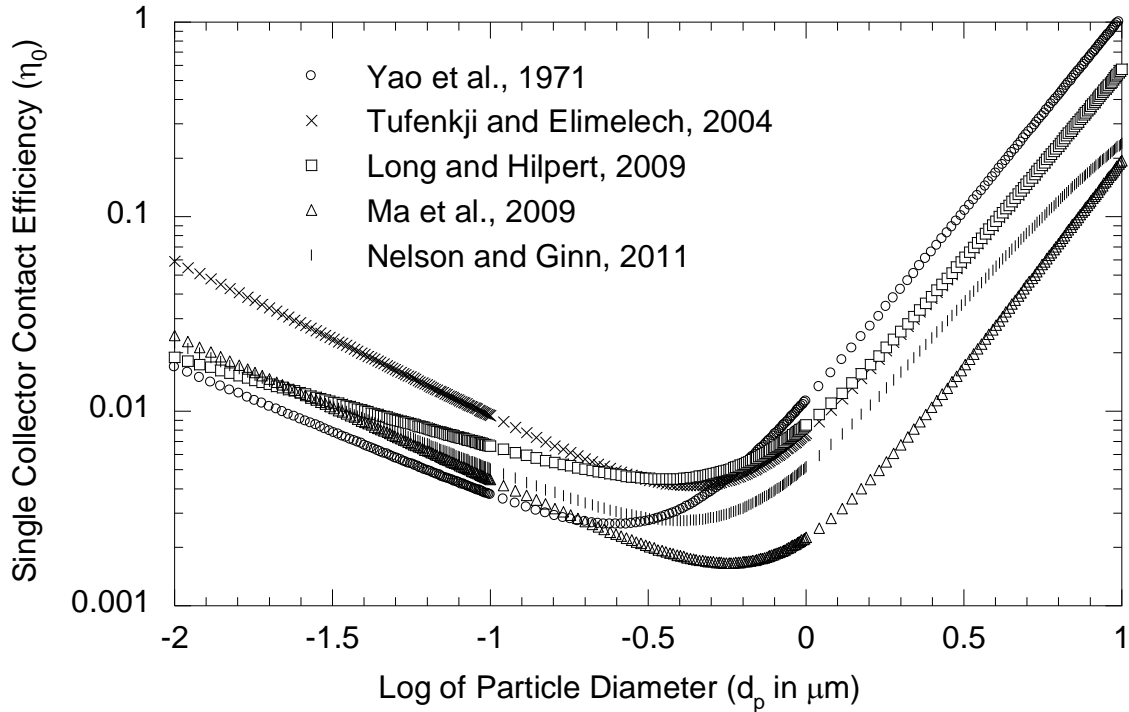
Figure 2.4: The single collector contact efficiency values calculated by the five models (A=10^{-20} J, μ=8.91×10^{-3} g/cm/s, k=1.38×10^{-16} g·cm^2/s^2/K, T=298 K, d_c=325 μm, ρ_p=10.49 g/cm^3, ρ_f=0.997 g/cm^3, v_0=2 m/hr, L=10 cm and ε=0.37).

2.3.2. Attachment model in granular media filtration

Likewise, various forms of equations have been suggested to describe the attachment efficiency. As mentioned above, when the attachment is favorable, the attachment efficiency is assumed to be 1. However, when the attachment becomes unfavorable, it becomes difficult to predict. Because the attachment is primarily governed by electrostatic parameters such as the surface potentials of the particles and media, a relationship was proposed between the attachment efficiency and the magnitude of the repulsive force for the prediction in cases of unfavorable attachment (Elimelech 1992). Equation 2-16 was also proposed as a correlation between the attachment efficiency and the parameter (N_{col}) which incorporates the Debye length, Hamaker constant, and the surface potentials of both the particle and media.

18

$$\alpha = 2.57 \times 10^{-2} N_{col}^{1.19} \tag{2-16}$$

A modified equation (Equation 2-17) was suggested using several data sets reported in the literature (Bai and Tien 1999):

$$\log \alpha = 2.527 \times 10^{-3} N_{Lo}^{0.7031} N_{E1}^{-0.3121} N_{E2}^{3.5111} N_{DL}^{1.352} \tag{2-17}$$

Phenrat et al. (2010) proposed Equation 2-18 for nanoparticles including the steric repulsion and decreased friction forces by organic coating.

$$\alpha = 10^{-1.35} N_{Lo}^{0.39} N_{E1}^{-1.17} N_{LEK}^{-0.10} \tag{2-18}$$

Finally, the experimental attachment efficiency (α_{exp}) has been obtained using the experimental removal efficiency at the initial stage of filtration, according to Equation 2-19.

$$\alpha_{exp} = -\frac{2}{3} \frac{d_c}{(1-\varepsilon)L\eta_0} \ln\left(\frac{N}{N_0}\right) \tag{2-19}$$

Because a typical filter produces numerous contact opportunities between particles and the media, it can be assumed that the successful filtration of particles is affected more by the attachment than by the transport. That is why the most frequently reported α is based on Equation 2-19 using experimental results. However, it has been suggested that α could be erroneously predicted under the presence of an energy barrier due to more complicated transport (such as wedging in grain-to grain contact areas) or attachment with repulsion (such as in the secondary energy minimum) (Johnson et al. 2007). If the experimental attachment efficiency deviates from the theoretical one, it implies that forces other than electrostatic repulsion occur between the nanoparticles and the media (Phenrat et al. 2010). These arguments necessitate a careful approach to modifying the model for η_0 and α.

2.4. Chemical Parameters in Granular Media Filtration of Nanoparticles

The chemical parameters that have been widely investigated in granular filtration are ionic strength, pH, and ion type of the background solution. These parameters can affect the surface characteristic of the particles and media, as well as the charge density in the solution immediately surrounding the particles, which in turn affect the electrostatic interactions expressed in the classical DLVO theory. This theory has often been used to explain the attachment (or non-attachment) of particles to the filter media.

2.4.1. Electrostatic interaction based on DLVO theory

DLVO theory was established by the works of Derjaguin, Landau, Verwey, and Overbeek to describe how colloidal stability was affected by the interaction between two particles. Repulsive energy is created by the charge of each particle when both have the same kind (sign) of charge. On the other hand, van der Waals energy causes an attraction between two particles at close separation distances. Therefore, there can be either a net repulsive or attractive energy acting on the particles according to the distance between the surfaces of two particles. The total interaction energy is expressed as the sum of electrostatic repulsive energy and van der Waals attractive energy.

In the case of the interaction between a particle and flat plate (Hogg et al. 1966), both the repulsive and attractive energy can be calculated using the following equations; this model is a good approximation for the interaction between a nanoparticle and a filter grain, since the filter grain is so much larger than the particles to be collected that its curved surface appears essentially flat in comparison to the particle.

- Electrostatic repulsive energy

$$V_R = \pi\varepsilon_0\varepsilon_r a_p \left(2\psi_c\psi_p \ln\left[\frac{1+\exp(-\kappa s)}{1-\exp(-\kappa s)}\right] + \left(\psi_c^{\,2}+\psi_p^{\,2}\right)\ln\left[1-\exp(-2\kappa s)\right]\right) \quad (2\text{-}20)$$

- Van der Waals attractive energy

$$V_A = \frac{Aa_p}{6s}\left(1+\frac{14s}{\lambda}\right)^{-1} \tag{2-21}$$

In Figure 2.5, the net energy moves deeply downward (toward attraction) as the separation distance decreases to quite small values. This region is the primary energy minimum where the attractive force becomes dominant and the attachment becomes (essentially) irreversible. As the separation distance increases, the net energy passes the peak point which indicates the energy barrier. The energy barrier causes particle stability (i.e., prevents attachment) unless the particle has sufficient momentum to overcome it. However, in some cases, no energy barrier exists, when the net energy curve is attractive at all separation distances; this condition is referred to as favorable attachment. Further, under generally unfavorable conditions, as the separation distance further increases, there can be a region where the net energy curve dips slightly into an attractive region. This condition is known as the secondary energy minimum, and it has been reported that weak but reversible attachment can occur in this region. Because of the (generally) low net energy value in the secondary energy minimum, most of the attachment in granular media filtration has been considered to be in the primary energy minimum. However, the attachment in the secondary energy minimum has been suggested when the attachment was higher than expected (Tufenkji and Elimelech 2005) or detachment was observed after ionic strength was decreased (Tian et al. 2010), providing further evidence of the weak and reversible attachment of nanoparticles in the secondary energy minimum. Also, the attachment in the secondary energy minimum has been pointed out to explain the difference between theoretical and experimental attachment efficiency (α) (Hahn and O'Melia 2004). According to those researchers, attachment in the secondary energy minimum can explain the release and reentrainment of particles.
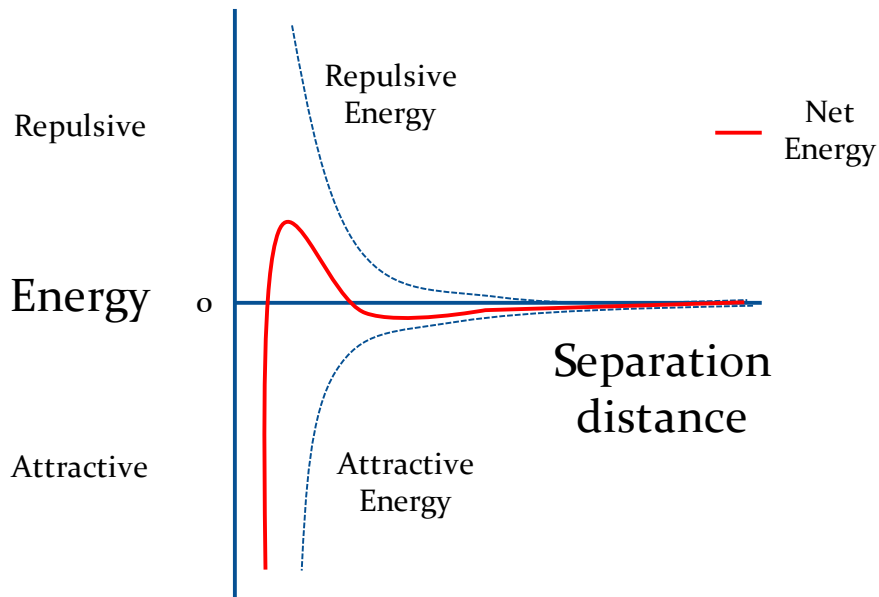
Figure 2.5:   General example of the energy curves in DLVO theory.

2.4.2. Water chemistry

DLVO theory has been widely used to describe particle-particle interactions, as in flocculation. As mentioned above, because the water chemistry parameters such as ionic strength, ion type, and pH of the background solution can affect the surface charge of the particle (which is one of key parameters in DLVO theory), it has been reported that the attachment of various nanoparticles in granular media filtration can be expected form DLVO as follows.

When the ionic strength increased, the attachment efficiency was greatly increased in the case of carbon nanotubes (Jaisi and Elimelech 2009) and nC_{60} (Espinasse et al. 2007). These results were explained well by DLVO theory; that is, comparison of the diffuse layer and weakened repulsive interaction led to increased attachment. By the increase of the ionic strength from 3 mM to 55 mM as KCl, there was a change in the deposition regime from unfavorable to favorable (Jaisi et al. 2008).

22

Also, the kind of background ions in the solution can affect the attachment of the nanoparticles because of the association between the ions and the charged functional group on the particle surface. In case of tri-p-tolylamine extracted C_{60}, the ability of the divalent ions (Ca^{2+}, Mg^{2+}) to associate with charged functional groups led to higher attachment efficiency than with monovalent ions (Espinasse et al. 2007). The fact that higher attachment can be achieved with divalent ions than monovalent ions, even at the same ionic strength (Saleh et al. 2008), implies that the greater adsorption or complexation of divalent ions to the surface coating layer can result in stronger (nearly irreversible) attachment in the primary energy minimum (Jaisi et al. 2008). These results suggest that charge neutralization due to ion adsorption was at work, and so they are not a direct test of DLVO theory which assumes indifferent electrolytes that do not adsorb.

The surface charge of nanoparticles and media can be a function of pH. If the pH is near the pH_{pzc} of the nanoparticles, the charge neutralization causes more aggregation of the nanoparticles (Guzman et al. 2006). And if the pH_{pzc} of the media and the nanoparticle have different values, then there is a possibility that nanoparticles and media would have the opposite charges at some pH range, resulting in more attachment of nanoparticles onto the media (Guzman et al. 2006, Lin et al. 2011, Solovitch et al. 2010). In addition, when the surface of AgNPs is coordinatively unsaturated, more OH^- can be adsorbed on the surface as pH increases, resulting in high negative surface charge which leads to the particles being stabilized (El Badawy et al. 2010).

Many of the experimental results that focused on the attachment of nanoparticles can be explained by DLVO theory. From the parameters mentioned above, it is possible to design experimental chemical conditions to make the nanoparticles attach more favorably to the media. It can be generally suggested that higher ionic strength (because of double layer compression) and low pH (because of lower surface charge) can lead to

greater attachment of nanoparticles. However, additional factors such as ion adsorption which leads to charge neutralization can influence attachment in ways besides those incorporated into DLVO theory, as explained in the next section.

2.4.3. Surface modification

Several researchers have found that the classical DLVO theory is insufficient to predict attachment in granular media filtration. This discrepancy can be explained by surface modification. Surface modification can change the attachment by adding repulsive forces. One possible result of surface modification is the steric effect caused by a surface coating of macromolecules. The steric effect generally provides repulsion in particle-particle interactions due to elastic and osmotic repulsion (Vincent et al. 1986). When the coating layers from different particles are overlapped, the compression of the coating layers results in a loss of entropy and an increase in elasticity. Also, the increase of macromolecule concentration in the overlapped zone leads to a local osmotic pressure increase which causes another repulsive source. The added (capping) layer on the nanoparticles can also play a role as a lubricant, so the friction between the particle and the media becomes less (Phenrat et al. 2010).

Surface modification can also change the surface charge as well as cause steric effects, which is called the electrosteric effect. NOM such as humic acid and organics such as carboxymethylcellulose (Joo et al. 2009) decrease the attachment efficiency by the steric effect since little change on the surface charge was observed. However, it was reported that the addition of humic acid reduced the filtration efficiency by increasing electrostatic and steric repulsion in the transport of carbon nanotubes (CNTs) in granular media filtration (Jaisi et al. 2008). Also, polymer coating could reduce the surface charge on nanoscale zerovalent iron (NZVI) (Saleh et al. 2008). Likewise, coating with

polyacrylic acid enhanced Fe^0 mobility by electrosteric stabilization (Kanel et al. 2008). These investigations suggested that surface coating could cause both steric and electrostatic stabilization.

On the other hand, the steric effect can be reduced when the cations from the background solution are adsorbed onto the surface of the particle through complexation with the functional groups on the surface, neutralizing the surface charge of the particle (Liu et al. 2003). However, the charge (de)stabilization does not always work because the effect of surface coating on the surface charge can be different depending on parameters such as particle size (Pelley and Tufenkji 2008) and ion valence (Saleh et al. 2008).

Sometimes, organic coatings can enhance the attachment of nanoparticles to the media by the bridging effect; that is, the polymers extend sufficiently from the particle surface that they can "bridge" the electrical double layer and attach to the media or previously-captured particle surface (Espinasse et al. 2007). However, organic coatings more commonly prevent the attachment by electrosteric stabilization.

Surface composition of the media can be another factor affecting the attachment of nanoparticles to the media. FeO coated glass bead media yielded a partially positive charge, thereby attracting negatively charged particles more (Lin et al. 2011). To explain the experimental results with DLVO, the correlation between the attachment efficiency and the portion of the media modified was required. Also, getting higher surface area of the media by the formation of metal chelate (Joo et al. 2009) or increasing hydrophobicity (Lecoanet et al. 2004) were reported to enhance the attachment.

Attachment can also be affected by the arrangement of the particle layers attached to the media. Covering the media with multiple particle layers is possible due to the available attractive force from the particle-covered media (Lecoanet and Wiesner 2004) or the attachment of particle aggregates. These researchers found that fullerene attached

to the media surface could be rearranged to get more favorable sites. Or the media covered by fullerene could be available to attract more fullerene; that is, previously attached nanoparticles can be another site for the next attachment, resulting in multiple layer attachment (Solovitch et al. 2010). And at higher ionic strength, particle aggregates can first form and then attach to the media, particularly if the particle concentration in the suspension to be filtered is high.

While the surfaces of particles and media are generally assumed to be smooth, the actual surface can have some irregular shape. This surface roughness was suggested as another factor affecting the attachment efficiency (Hahn and O'Melia 2004). In the case of a spherical particle with a number of uneven surfaces, an increased attachment efficiency was ascribed to an increased van der Waals force at close distance (Suresh and Walz 1996). The energy barrier was found to be significantly lowered with rough surfaces as the size and number of asperities increased (Bhattacharjee et al. 1998). If the nanoparticles can form an aggregate, the surface roughness of the aggregate can be a significant parameter affecting attachment.

Another common assumption is that the charge on the particle surface is uniformly distributed, so that there is one numerical value of charge density on each particle surface. However, just as every atom can create an induced dipole moment by the nonsymmetrical electron distribution on its surface, the charge on the surface of the particle is not uniformly distributed in nature. Therefore, even if the same kind of media is used, one part of the surface can have a different charge value from another part, even the opposite one. The heterogeneity in surface charge can contribute to more attachment by making a favorable condition especially at the initial stage of a filter run and can cause a huge discrepancy between the model and the experiment (Tufenkji and Elimelech 2005).

Overall, more detailed investigation on the surface of the nanoparticles and the filter media is required to describe the gap between the model expectation and the experimental result. However, among these, the NOM coating, which is expected to be ubiquitous in natural surface waters, needs to be investigated further to elucidate the role of NOM in the granular media filtration of nanoparticles.

2.5. Physical Parameters in Granular Media Filtration of Nanoparticles

In granular media filtration, the parameters generally considered in the operation are the media size, filtration velocity, and filter depth. These parameters are in the transport model of granular media filtration as mentioned in section 2.3.1. Though it is general knowledge that the filtration efficiency is lowered at higher velocity, less filter depth, and greater media size (Elimelech 1990), it is desirable to see how these parameters can be used in the research of granular media filtration of nanoparticles.

According to the previous literature (Appendix A), most of granular media filtration studies were done at low velocity, less than 2 m/hr (the range of filtration velocities used in conventional drinking water treatment plants) since their research interest was in the transport of nanoparticles in groundwater flow. Some of them used various filtration velocities to investigate the effects of velocity on nanoparticle removal, but showed a contradiction in results. It was reported higher velocity (4.32 m/hr) resulted in less retention of nC_{60} (Espinasse et al. 2007). However, in another study with nC_{60}, the slow (1.44 m/hr) and fast (5.04 m/hr) velocities did not show a noticeable difference in the plateau of C/C_{in} which reflects removal efficiency (Lecoanet and Wiesner 2004). When the completely mixed reactor and filtration tests of TiO_2 were compared under the presence of an energy barrier, the mixed reactor led to greater attachment due to the

27

overcoming of the energy barrier by higher relative velocities. Furthermore, the deposition of colloids could be reversible due to the fluid drag force caused by high flow rate (Bergendahl and Grasso 2000). Therefore, the filtration of nanoparticles at high velocity is required to see how velocity could affect the transport and attachment of nanoparticles.

Various filter depths (3~45 cm) have been used in the research on granular media filtration of the nanoparticles (Appendix A). However, few studies have compared several filter depths, presumably because it is known that shorter depth yields less attachment. Rather, the distance to remove 99% of the influent concentration of nanoparticles was used in some studies to describe the expectations in groundwater flow (Guzman et al. 2006, Lecoanet et al. 2004, Tiraferri and Sethi 2009). Filter depth can be a tool to measure the transport of nanoparticles, either indirectly by sectioning the filter bed after filtration or directly by taking samples at several depths (Darby and Lawler 1990, Liang et al. 2013b). Therefore, the trajectory of nanoparticles and the filter ripening development can be indirectly investigated using various filter depths in granular media filtration.

Normally, the media size (diameter) in filtration of nanoparticles has been in the range of 100-1000 μm (Appendix A), which is still 100 to 1000 times the size of the nanoparticles. In the case of particles greater than 1 μm, it was reported that straining occurred even when the ratio of particle to media size was as low as 0.003 (Bradford et al. 2007). Also, due to the aggregation of nanoparticles before or after deposition onto the media, straining could occur when the aggregates grow enough to block the pores (Saleh et al. 2007, Solovitch et al. 2010, Tiraferri and Sethi 2009). Therefore, it is necessary to study how many nanoparticles could deposit on the media surface and how much the media size affects the capture of nanoparticles in filtration.

2.6. Summary of filtration of nanoparticles

The transport of various nanoparticles in porous media has been one of the most active research fields with a substantial number of articles (Appendix A). In most cases, column studies were conducted under varying chemical parameters such as ionic strength and pH. Several different target compounds (type of nanoparticles) have been studied, but all with a similar research scope. Since 2010, studies have focused more on the metal nanoparticles such as AgNPs, TiO_2, and quantum dot. This trend is considered to be the consequence of spotlighting on the emerging nanoparticles.

As mentioned earlier, most studies adopted a relatively low filtration velocity to emulate groundwater flow conditions. However, assuming the existence of nanoparticles in surface water (and which might happen to flow into water treatment plants), further investigation on the transport of nanoparticles is desirable with a higher filtration velocity to mimic the granular media filtration process.

Also, the limited number of studies on natural organic matter (NOM) application indicates another research gap in the transport of nanoparticles. Though more studies on NOM coating of nanoparticles have been reported recently, the overall NOM application is seemingly low considering its ubiquitous presence in the environment.

2.7. Summary with Research Gap

In summary, the transport and attachment of nanoparticles in granular media filtration can be affected by physical and chemical parameters. The physical parameters are largely associated with the operational parameters such as media size, filtration velocity, and filter depth which are also embedded in the colloidal filtration models. In

other words, the physical parameters are closely related with the colloidal filtration model which describes the transport of nanoparticles. However, the development of colloidal filtration theory with nanoparticles was mostly accomplished by mathematical simulation. Also, in most filtration experiment studies, an existing model has been used to calculate η_0, and α was estimated from the experimental results. To validate the model with nanoparticles, more experimental data are required to see if the reported η_0 or α model is applicable for the nanoparticles. Once η_0 model is updated or confirmed, α can also be evaluated under various experimental conditions. Therefore, it is desirable to conduct the granular media filtration of nanoparticles with varying values of these physical parameters.

The chemical parameters can be divided into water chemistry-related and surface modification-related parameters. Both of them are associated with particle-particle interaction (attachment). While the water chemistry parameters can be mostly interpreted mathematically by known equations and adequate measurements for electrostatic interaction, the surface modification can include additional forces such as steric interaction which is still more conceptual than mathematical due to difficulties in measurement. Regarding the steric interaction, NOM coating needs to be investigated because NOM is ubiquitous in natural waters. Once the nanoparticles are coated with NOM which is present in natural waters at 2~15 mg/L as C (Hepplewhite et al. 2004) (though values over 6 mg/L are rare), they normally become more stable due to the increased steric repulsion and additional electrostatic repulsion when the surface charge becomes more negative. The effect of NOM coating is influenced by the NOM characteristics such as the level of hydrophobicity and molecular weight, which can affect the coating layer thickness on the surface of AgNPs. For the sake of the NOM standardization (IHSS 2013), Suwannee River Humic Acid and Fulvic Acid have been

the representative NOMs used most often in the research field. Therefore, the effect of both representative NOMs on the granular media filtration of nanoparticles, especially for the particle-media interaction, is also desirable.

Under unfavorable attachment conditions, particle attachment in the secondary energy minimum could lead to reversible deposition depending on the experimental condition. Therefore, detachment (or release) of the captured nanoparticles in the filter bed can be considered as well. Further, little is known about the amount of the captured nanoparticles throughout the filter depth. Since the retention profile of AgNPs in granular media filtration could be different according to the influent concentration (Liang et al. 2013b), it is desirable to see the retention profile inside the filter bed by time and filter depth to elucidate the filter ripening in the granular media filtration of nanoparticles.

Previous studies on granular media filtration of AgNPs have been focused on ionic strength, pH (Lin et al. 2011), composition of the filter media (Tian et al. 2010), capping agents (Lin et al. 2012, Song et al. 2011), filter media size and filtration velocity (Sagee et al. 2012). These studies of granular media filtration of AgNPs have been conducted in the range of mg/L for the sake of the analytical simplicity such as the direct application of the samples to UV-vis spectroscopy. As a result, the clear difference in the influence and effluent concentrations could be obtained. However, it is necessary to investigate granular media filtration at the low concentration of AgNPs, because the existing AgNP concentration in the watershed is expected to be fairly low (e.g., in the range of μg/L). Also, as the initial AgNP concentration increases, the aggregation of AgNPs in suspension can be increased (Huynh and Chen 2011, Zhang et al. 2011) and the breakthrough can be reached early (Wang et al. 2008b). Therefore, the physical and chemical parameters such as ion type and ionic strength in the granular media filtration of the nanoparticles mentioned above are required to be done at the low concentration as

well. With the analytical techniques currently available, Ag concentration can be analyzed down to the range of µg/L using either the graphite furnace atomic absorption (GFAA) or the inductively coupled plasma-optical emission spectrometer (ICP-OES).

References

Akaighe, N., MacCuspie, R.I., Navarro, D.A., Aga, D.S., Banerjee, S., Sohn, M. and Sharma, V.K. (2011) Humic acid-induced silver nanoparticle formation under environmentally relevant conditions. Environmental Science & Technology 45(9), 3895-3901.

Bai, R.B. and Tien, C. (1999) Particle deposition under unfavorable surface interactions. Journal of Colloid and Interface Science 218(2), 488-499.

Baker, M.N. (1948) Quest for pure water: the history of water purification from the earliest records to the twentieth century, American Water Works Association, New York.

Benjamin, M.M. and Lawler, D.F. (2013) Water quality engineering: physical and chemical treatment processes, Wiley.

Bergendahl, J. and Grasso, D. (2000) Prediction of colloid detachment in a model porous media: hydrodynamics. Chemical Engineering Science 55(9), 1523-1532.

Bhattacharjee, S., Ko, C.H. and Elimelech, M. (1998) DLVO interaction between rough surfaces. Langmuir 14(12), 3365-3375.

Blaser, S.A., Scheringer, M., MacLeod, M. and Hungerbuhler, K. (2008) Estimation of cumulative aquatic exposure and risk due to silver: Contribution of nano-functionalized plastics and textiles. Science of the Total Environment 390(2-3), 396-409.

Bradford, S.A., Torkzaban, S. and Walker, S.L. (2007) Coupling of physical and chemical mechanisms of colloid straining in saturated porous media. Water Research 41(13), 3012-3024.

Carlson, C., Hussain, S.M., Schrand, A.M., Braydich-Stolle, L.K., Hess, K.L., Jones, R.L. and Schlager, J.J. (2008) Unique cellular interaction of silver nanoparticles: Size-dependent generation of reactive oxygen species. Journal of Physical Chemistry B 112(43), 13608-13619.

Chinnapongse, S.L., MacCuspie, R.I. and Hackley, V.A. (2011) Persistence of singly dispersed silver nanoparticles in natural freshwaters, synthetic seawater, and simulated estuarine waters. Science of the Total Environment 409(12), 2443-2450.

Choi, O. and Hu, Z.Q. (2008) Size dependent and reactive oxygen species related nanosilver toxicity to nitrifying bacteria. Environmental Science & Technology 42(12), 4583-4588.

Curley, R. (2010) New thinking about pollution, The Rosen Publishing Group, New York.

Darby, J.L. and Lawler, D.F. (1990) Ripening in depth filtration - Effect of particle-size on removal and head loss. Environmental Science & Technology 24(7), 1069-1079.

Debnath, D., Kim, C., Kim, S.H. and Geckeler, K.E. (2010) Solid-state synthesis of silver nanoparticles at room temperature: Poly(vinylpyrrolidone) as a tool. Macromolecular Rapid Communications 31(6), 549-553.

Delay, M., Dolt, T., Woellhaf, A., Sembritzki, R. and Frimmel, F.H. (2011) Interactions and stability of silver nanoparticles in the aqueous phase: Influence of natural organic matter (NOM) and ionic strength. Journal of Chromatography A 1218(27), 4206-4212.

El Badawy, A.M., Luxton, T.P., Silva, R.G., Scheckel, K.G., Suidan, M.T. and Tolaymat, T.M. (2010) Impact of environmental conditions (pH, ionic strength, and electrolyte type) on the surface charge and aggregation of silver nanoparticles suspensions. Environmental Science & Technology 44(4), 1260-1266.

Elimelech, M. (1990) The effect of particle size on the kinetics of deposition of Brownian particles in porous media, The Johns Hopkins University, Baltimore.

Elimelech, M. (1992) Predicting collision efficiencies of colloidal particles in porous-media. Water Research 26(1), 1-8.

Environmental_Working_Group (2014). Available at http://www.ewg.org/tap-water/whatsinyourwater/1050/CA/California/Silver-total/.

EPA (1990) Technologies for upgrading existing or designing new drinking water treatment facilities. EPA/625/4-89/023

EPA (1999) Guidance manual for compliance with the interim enhanced water treatment rule: Turbidity provisions. EPA/815/R-99/010

Espinasse, B., Hotze, E.M. and Wiesner, M.R. (2007) Transport and retention of colloidal aggregates of C_{60} in porous media: Effects of organic macromolecules, ionic composition, and preparation method. Environmental Science & Technology 41(21), 7396-7402.

Fleischer, M. (1963) Data of Geochemistry (6th ed.), U.S. Government printing office, Washington.

Foldbjerg, R., Olesen, P., Hougaard, M., Dang, D.A., Hoffmann, H.J. and Autrup, H. (2009) PVP-coated silver nanoparticles and silver ions induce reactive oxygen species, apoptosis and necrosis in THP-1 monocytes. Toxicology Letters 190(2), 156-162.

Gottschalk, F., Sonderer, T., Scholz, R.W. and Nowack, B. (2009) Modeled environmental concentrations of engineered nanomaterials (TiO_2, ZnO, Ag, CNT, fullerenes) for different regions. Environmental Science & Technology 43(24), 9216-9222.

Guzman, K.A.D., Finnegan, M.P. and Banfield, J.F. (2006) Influence of surface potential on aggregation and transport of titania nanoparticles. Environmental Science & Technology 40(24), 7688-7693.

Hahn, M.W. and O'Melia, C.R. (2004) Deposition and reentrainment of Brownian particles in porous media under unfavorable chemical conditions: Some concepts and applications. Environmental Science & Technology 38(1), 210-220.

Hepplewhite, C., Newcombe, G. and Knappe, D.R.U. (2004) NOM and MIB, who wins in the competition for activated carbon adsorption sites? Water Science and Technology 49(9), 257-265.

Hofmeister, H., Tan, G.L. and Dubiel, M. (2005) Shape and internal structure of silver nanoparticles embedded in glass. Journal of Materials Research 20(6), 1551-1562.

Hogg, R., Healy, T.W. and Fuersten, D.W. (1966) Mutual coagulation of colloidal dispersions. Transactions of the Faraday Society 62(522P), 1638-1651.

Huynh, K.A. and Chen, K.L. (2011) Aggregation kinetics of citrate and polyvinylpyrrolidone coated silver nanoparticles in monovalent and divalent electrolyte solutions. Environmental Science & Technology 45(13), 5564-5571.

IHSS (2013) Source materials for International Humic Substances Society samples. Available at http://www.humicsubstances.org/sources.html.

Jaisi, D.P., Saleh, N.B., Blake, R.E. and Elimelech, M. (2008) Transport of single-walled carbon nanotubes in porous media: Filtration mechanisms and reversibility. Environmental Science & Technology 42(22), 8317-8323.

Jaisi, D.P. and Elimelech, M. (2009) Single-walled carbon nanotubes exhibit limited transport in soil columns. Environmental Science & Technology 43(24), 9161-9166.

Johnson, W.P., Tong, M. and Li, X. (2007) On colloid retention in saturated porous media in the presence of energy barriers: The failure of alpha, and opportunities to predict eta. Water Resources Research 43(12). W12S13

Joo, S.H., Al-Abed, S.R. and Luxton, T. (2009) Influence of carboxymethyl cellulose for the transport of titanium dioxide nanoparticles in clean silica and mineral-coated sands. Environmental Science & Technology 43(13), 4954-4959.

Kaegi, R., Voegelin, A., Sinnet, B., Zuleeg, S., Hagendorfer, H., Burkhardt, M. and Siegrist, H. (2011) Behavior of metallic silver nanoparticles in a pilot wastewater treatment plant. Environmental Science & Technology 45(9), 3902-3908.

Kaegi, R., Voegelin, A., Sinnet, B., Zuleeg, S., Siegrist, H. and Burkhardt, M. (2012) Fate and behavior of silver nanoparticles in urban wastewater systems, Berlin, Germany.

Kanel, S.R., Goswami, R.R., Clement, T.P., Barnett, M.O. and Zhao, D. (2008) Two dimensional transport characteristics of surface stabilized zero-valent iron nanoparticles in porous media. Environmental Science & Technology 42(3), 896-900.

Key, F.S. and Maass, G. (2001) Ions, atoms and charged particles. Silver Colloids, 1-6.

Khanna, P.K., Singh, N., Kulkarni, D., Deshmukh, S., Charan, S. and Adhyapak, P.V. (2007) Water based simple synthesis of re-dispersible silver nano-particles. Materials Letters 61(16), 3366-3370.

Kim, B., Park, C.S., Murayama, M. and Hochella, M.F. (2010) Discovery and Characterization of silver sulfide nanoparticles in final sewage sludge products. Environmental Science & Technology 44(19), 7509-7514.

Kittler, S., Greulich, C., Diendorf, J., Koller, M. and Epple, M. (2010) Toxicity of silver nanoparticles increases during storage because of slow dissolution under release of silver ions. Chemistry of Materials 22(16), 4548-4554.

Lecoanet, H.F., Bottero, J.Y. and Wiesner, M.R. (2004) Laboratory assessment of the mobility of nanomaterials in porous media. Environmental Science & Technology 38(19), 5164-5169.

Lecoanet, H.F. and Wiesner, M.R. (2004) Velocity effects on fullerene and oxide nanoparticle deposition in porous media. Environmental Science & Technology 38(16), 4377-4382.

Levard, C., Hotze, E.M., Lowry, G.V. and Brown, G.E. (2012) Environmental transformations of silver nanoparticles: Impact on stability and toxicity. Environmental Science & Technology 46(13), 6900-6914.

Li, X. and Lenhart, J.J. (2012) Aggregation and dissolution of silver nanoparticles in natural surface water. Environmental Science & Technology 46(10), 5378-5386.

Li, Y.S., Wang, Y.G., Pennell, K.D. and Abriola, L.M. (2008) Investigation of the transport and deposition of fullerene (C_{60}) nanoparticles in quartz sands under varying flow conditions. Environmental Science & Technology 42(19), 7174-7180.

Liang, Y., Bradford, S.A., Simunek, J., Vereecken, H. and Klumpp, E. (2013b) Sensitivity of the transport and retention of stabilized silver nanoparticles to physicochemical factors. Water Research 47(7), 2572-2582.

Liau, S.Y., Read, D.C., Pugh, W.J., Furr, J.R. and Russell, A.D. (1997) Interaction of silver nitrate with readily identifiable groups: relationship to the antibacterial action of silver ions. Letters in Applied Microbiology 25(4), 279-283.

Lin, S.H., Cheng, Y.W., Bobcombe, Y., Jones, K.L., Liu, J. and Wiesner, M.R. (2011) Deposition of silver nanoparticles in geochemically heterogeneous porous media: Predicting affinity from surface composition analysis. Environmental Science & Technology 45(12), 5209-5215.

Lin, S.H., Cheng, Y.W., Liu, J. and Wiesner, M.R. (2012) Polymeric coatings on silver nanoparticles hinder autoaggregation but enhance attachment to uncoated surfaces. Langmuir 28(9), 4178-4186.

Liu, J.J., Xu, Z.H. and Masliyah, J. (2003) Studies on bitumen-silica interaction in aqueous solutions by atomic force microscopy. Langmuir 19(9), 3911-3920.

Liu, J.Y. and Hurt, R.H. (2010) Ion release kinetics and particle persistence in aqueous nano-silver colloids. Environmental Science & Technology 44(6), 2169-2175.

Long, W. and Hilpert, M. (2009) A correlation for the collector efficiency of Brownian particles in clean-bed filtration in sphere packings by a Lattice-Boltzmann method. Environmental Science & Technology 43(12), 4419-4424.

Lowry, G.V., Espinasse, B.P., Badireddy, A.R., Richardson, C.J., Reinsch, B.C., Bryant, L.D., Bone, A.J., Deonarine, A., Chae, S., Therezien, M., Colman, B.P., Hsu-Kim, H., Bernhardt, E.S., Matson, C.W. and Wiesner, M.R. (2012) Long-term transformation and fate of manufactured Ag nanoparticles in a simulated large scale freshwater emergent wetland. Environmental Science & Technology 46(13), 7027-7036.

Ma, H.L., Pedel, J., Fife, P. and Johnson, W.P. (2009) Hemispheres-in-cell geometry to predict colloid deposition in porous media. Environmental Science & Technology 43(22), 8573-8579.

Nelson, K.E. and Ginn, T.R. (2011) New collector efficiency equation for colloid filtration in both natural and engineered flow conditions. Water Resources Research 47(5), W05543.

Panyala, N.R., Pena-Mendez, E.M. and Havel, J. (2008) Silver or silver nanoparticles: a hazardous threat to the environment and human health? Journal of Applied Biomedicine 6(3), 117-129.

Pelley, A.J. and Tufenkji, N. (2008) Effect of particle size and natural organic matter on the migration of nano- and microscale latex particles in saturated porous media. Journal of Colloid and Interface Science 321(1), 74-83.

Phenrat, T., Song, J.E., Cisneros, C.M., Schoenfelder, D.P., Tilton, R.D. and Lowry, G.V. (2010) Estimating attachment of nano- and submicrometer-particles coated with organic macromolecules in porous media: Development of an Empirical Model. Environmental Science & Technology 44(12), 4531-4538.

Sagee, O., Dror, I. and Berkowitz, B. (2012) Transport of silver nanoparticles (AgNPs) in soil. Chemosphere 88(5), 670-675.

Saleh, N., Sirk, K., Liu, Y.Q., Phenrat, T., Dufour, B., Matyjaszewski, K., Tilton, R.D. and Lowry, G.V. (2007) Surface modifications enhance nanoiron transport and NAPL targeting in saturated porous media. Environmental Engineering Science 24(1), 45-57.

Saleh, N., Kim, H.J., Phenrat, T., Matyjaszewski, K., Tilton, R.D. and Lowry, G.V. (2008) Ionic strength and composition affect the mobility of surface-modified Fe-0 nanoparticles in water-saturated sand columns. Environmental Science & Technology 42(9), 3349-3355.

Schulz, C.R. and Okun, D.A. (1984) Surface water treatment for communities in developing countries, Wiley, New York.

Sloane, N.J.A. (1998) Kepler's conjecture confirmed. Nature 395(6701), 435-436.

Solomon, S.D., Bahadory, M., Jeyarajasingam, A.V., Rutkowsky, S.A., Boritz, C. and Mulfinger, L. (2007) Synthesis and study of silver nanoparticles. Journal of Chemical Education 84(2), 322-325.

Solovitch, N., Labille, J., Rose, J., Chaurand, P., Borschneck, D., Wiesner, M.R. and Bottero, J.Y. (2010) Concurrent aggregation and deposition of TiO_2 nanoparticles in a sandy porous media. Environmental Science & Technology 44(13), 4897-4902.

Song, J.E., Phenrat, T., Marinakos, S., Xiao, Y., Liu, J., Wiesner, M.R., Tilton, R.D. and Lowry, G.V. (2011) Hydrophobic interactions increase attachment of gum arabic- and PVP-coated Ag nanoparticles to hydrophobic surfaces. Environmental Science & Technology 45(14), 5988-5995.

Suresh, L. and Walz, J.Y. (1996) Effect of surface roughness on the interaction energy between a colloidal sphere and a flat plate. Journal of Colloid and Interface Science 183(1), 199-213.

Tian, Y.A., Gao, B., Silvera-Batista, C. and Ziegler, K.J. (2010) Transport of engineered nanoparticles in saturated porous media. Journal of Nanoparticle Research 12(7), 2371-2380.

Tiraferri, A. and Sethi, R. (2009) Enhanced transport of zerovalent iron nanoparticles in saturated porous media by guar gum. Journal of Nanoparticle Research 11(3), 635-645.

Tolaymat, T.M., El Badawy, A.M., Genaidy, A., Scheckel, K.G., Luxton, T.P. and Suidan, M. (2010) An evidence-based environmental perspective of manufactured silver nanoparticle in syntheses and applications: A systematic review and critical appraisal of peer-reviewed scientific papers. Science of the Total Environment 408(5), 999-1006.

Tufenkji, N. and Elimelech, M. (2004) Correlation equation for predicting single-collector efficiency in physicochemical filtration in saturated porous media. Environmental Science & Technology 38(2), 529-536.

Tufenkji, N. and Elimelech, M. (2005) Breakdown of colloid filtration theory: Role of the secondary energy minimum and surface charge heterogeneities. Langmuir 21(3), 841-852.

Vincent, B., Edwards, J., Emmett, S. and Jones, A. (1986) Depletion flocculation in dispersions of sterically-stabilized particles (soft spheres). Colloids and Surfaces 18(2-4), 261-281.

Wang, Y.G., Li, Y.S., Fortner, J.D., Hughes, J.B., Abriola, L.M. and Pennell, K.D. (2008b) Transport and retention of nanoscale C_{60} aggregates in water-saturated porous media. Environmental Science & Technology 42(10), 3588-3594.

WHO (2003) Silver in drinking-water. Available at http://www.who.int/water_sanitation_health/dwq/chemicals/silver.pdf.

Wijnhoven, S.W.P., Peijnenburg, W.J.G.M., Herberts, C.A., Hagens, W.I., Oomen, A.G., Heugens, E.H.W., Roszek, B., Bisschops, J., Gosens, I., Van de Meent, D., Dekkers, S., De Jong, W.H., Van Zijverden, M., Sips, A.J.A.M. and Geertsma, R.E. (2009) Nano-silver - a review of available data and knowledge gaps in human and environmental risk assessment. Nanotoxicology 3(2), 109-138.

Wood, C.M., Playle, R.C. and Hogstrand, C. (1999) Physiology and modeling of mechanisms of silver uptake and toxicity in fish. Environmental Toxicology and Chemistry 18(1), 71-83.

Yao, K.M., Habibian, M.M. and Omelia, C.R. (1971) Water and waste water filtration - Concepts and applications. Environmental Science & Technology 5(11), 1105-1112.

Zhang, W., Yao, Y., Li, K.G., Huang, Y. and Chen, Y.S. (2011) Influence of dissolved oxygen on aggregation kinetics of citrate-coated silver nanoparticles. Environmental Pollution 159(12), 3757-3762.

Chapter 3: NANOPARTICLE TRANSPORT IN GRANULAR MEDIA FILTRATION: COMPARISON TO COLLOIDAL FILTRATION THEORY

Abstract

For engineered nanoparticles that are being introduced into the environment, a considerable amount of research has been conducted on the transport of nanoparticles in natural and engineered systems, especially in granular media filtration. Most studies on the transport model of nanoparticles in granular media filtration have focused on numerical simulation of particle behavior; this research was designed to test the model expectations with experimental evidence. The aim of study was to evaluate the widely used colloidal filtration model using experimental results from the transport and capture of nanoparticles in granular media filtration. A series of filtration tests was conducted under varying physical parameters such as particle size, filter media size, filter depth, and filtration velocity. To scrutinize the effect of physical parameters, the chemical effect was minimized by selecting the spherical branched polyethylenimine (BPEI) capped silver nanoparticles (AgNPs) as a positively charged nanoparticle to avoid electrostatic repulsion with the negatively charged filter media. The ionic strength and pH of the test solution were controlled to prevent the aggregation of AgNPs during the filtration test period. Overall, the experimental results fit the model quite well, but some deviation from the model became apparent as the particle size decreased. This result demonstrates that the behavior of nanoparticles could be generally similar to the particles greater than nano range; however, a distinctive nature of nanoparticle transport could appear in smaller size ranges.

Keywords

3.1. Introduction

The extensive use of nanoparticles in various consumer products has caused an increasing interest in their fate and transport in the environment. As a consequence, an enormous effort has been devoted to investigate the fate and transport of nanoparticles in the past decade. Despite the plethora of research, the question remains whether the transport of nanoparticles at the relatively high filtration velocities used in water treatment is similar to that studied previously with larger particles.

Regarding the transport of nanoparticles in granular media filtration, the attachment efficiency (α) has often been estimated using the single collector contact efficiency (η_0) calculated from the colloidal filtration model. This approach to determine α has been adopted by many researchers because the colloidal filtration model has shown good agreement with experimental results for larger particles in general. However, considering the recent shift of research focus from supra-micrometer colloids to nanoparticles, it is worthwhile to determine whether the colloidal transport model properly describes nanoparticle transport. Though the colloidal filtration model has been updated by simulations of the detailed contact between nanoparticles and the filter media (Long and Hilpert 2009, Ma et al. 2009, Nelson and Ginn 2011, Tufenkji and Elimelech 2004), little effort has been made to verify the colloidal filtration model with experimental evidence at nano size under the conditions found in water treatment practice. In particular, few researchers have tested whether the effects of size within the nano range are well predicted by the existing models.

42

The objective of this study is to verify the colloidal filtration model with experimental results of the transport of nanoparticles in granular media filtration under conditions similar to those in water treatment plants. The filtration experiments were conducted in the absence of an energy barrier under various physical conditions and varying nanoparticle size. The physical parameters that were varied included the velocity, media size, and media depth. To isolate the effect of physical parameters, the chemical parameters were controlled in a way to minimize their effect on the filtration experiments. The experimental results were compared with the colloidal filtration model to evaluate the applicability of the model to nanoparticles.

3.2. Colloidal filtration model

The model of Yao et al. (1971) originally explored the single collector contact efficiency (η_0) as a sum of three particle removal mechanisms: diffusion, interception, and sedimentation. To express each mechanism mathematically, the analytical solution of the general convective-diffusion equation was obtained by simplifying the operational condition. This conceptual approach has been the backbone of modern colloidal filtration models which have been updated by several researchers in the four decades since the original publication of the Yao et al. model.

One of the major updates on the colloidal filtration model was the adoption of Happel's sphere-in-cell porous media model to solve the convective-diffusion equation numerically (Rajagopalan and Tien 1976). This concept was introduced to describe the flow pattern in the vicinity of a single collector by assuming a liquid envelope surrounding the surface of a collector. This theoretical flow pattern has been widely applied in the subsequent colloidal filtration models. Rajagopalan and Tien also

introduced the use of dimensionless numbers to characterize and generalize their findings.

Subsequently, Tufenkji and Elimelech (2004) advanced the colloidal filtration model with the further advance of the use of dimensionless parameters incorporated with the detailed forces and interactions between particles and a single collector. A combination of the dimensionless parameters was employed to delineate the three particle removal mechanisms. An equation for the single collector contact efficiency (η_0) was found as a statistical fit to a large number of results obtained by numerical solution of the convective-diffusion equation for a wide range of filtration conditions. Ever since, several updates were attempted mostly focusing on the detailed geometry of a filter bed (Long and Hilpert 2009, Ma et al. 2009). However, those updates resulted in minor modifications without altering the essential approach of the Tufenkji and Elimelech model. Therefore, the Tufenkji and Elimelech model was chosen as representative of the colloidal filtration model and compared with the experimental results in this study.

3.3. Materials and Methods

10, 50, and 100 nm spherical BPEI AgNPs were purchased from Nanocomposix (San Diego, CA). The size and surface charge of AgNPs were confirmed by transmission electron microscopy (TEM, FEI Tencai) (Figure 3.1), particle tracking analysis (LM10, Nanosight) (Figure 3.2), and dynamic light scattering (DLS, Malvern Zetasizer) (Figure 3.3). The size of BPEI AgNPs determined by TEM images was close to the size reported by the manufacturer (Table 3.1). The hydrodynamic diameter measured by Nanosight and DLS (Table 3.1) was considered to include the thickness of the capping agent (MacCuspie et al. 2011). The TEM measurements appear to indicate a more nearly

44

monodisperse particle size than was found from Nanosight and DLS, an apparent artifact of the latter systems. The surface charge of BPEI AgNPs was positive (Figure 3.4) because BPEI includes amine groups that would be protonated at the pH of these experiments (pH 7). However, the surface charge decreased as particle size decreased, probably due to decreased H^+ density on the particle surface (Barisik et al. 2014) or greater degree of hydroxylation (Chae et al. 2010). Note that the surface charge of the 10 nm particles was considerably less positive than that of the larger particles. Nevertheless, the point of zero charge of BPEI AgNPs was somewhat higher than 11 regardless of particle size, proving that the surface charge of BPEI AgNPs in the filtration test was positive. The molecular weight of the BPEI was reported by Nanocomposix, Inc. to be approximately 2500 Daltons, considered small enough that steric interactions between particles and (uncoated) filter media are assumed to be negligible.
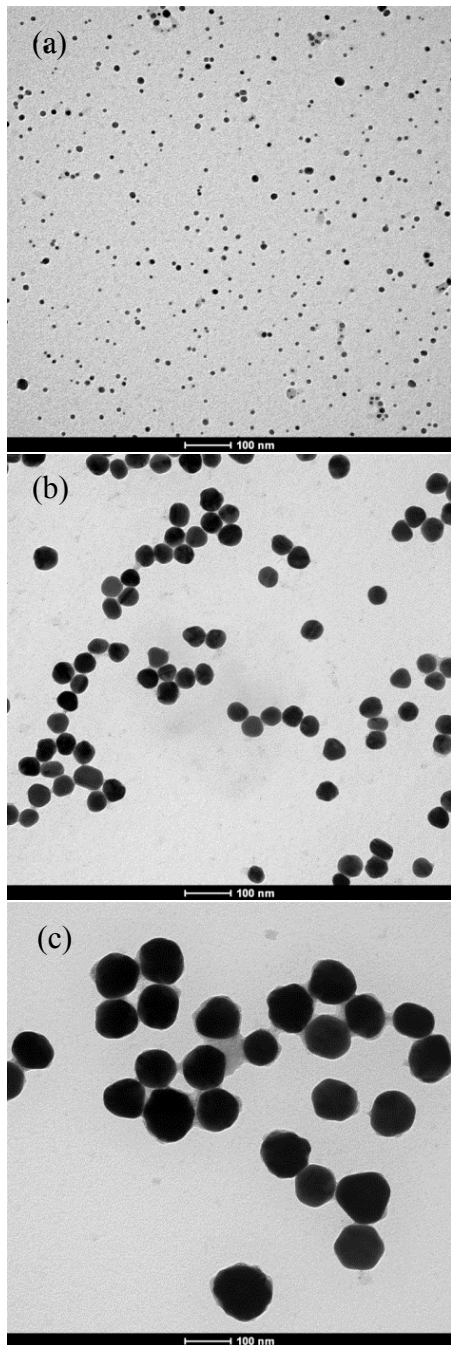
Figure 3.1: TEM images of (a) 10 nm, (b) 50 nm, and (c) 100 nm BPEI AgNPs. (The scale bar is 100 nm is all cases.)
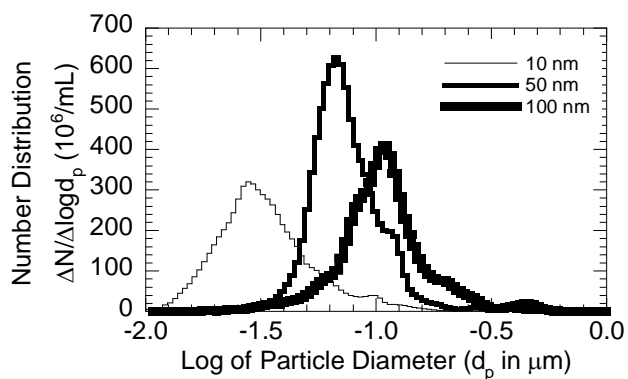
Figure 3.2:   Particle size distribution of 10 nm, 50 nm, and 100 nm BPEI AgNPs by Nanosight.
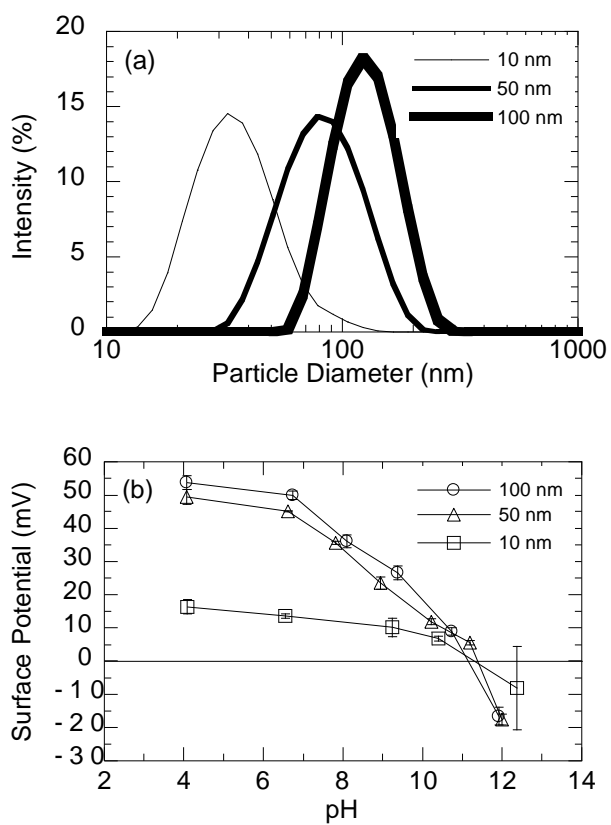
Figure 3.3:   (a) Particle size distributions and (b) surface potentials of 10 nm, 50 nm, and 100 nm BPEI AgNPs by DLS.

47

Table 3.1: BPEI AgNP properties used for filtration tests.

| Manufactured size | Mean diameter[a] (nm) | Hydrodynamic diameter (nm) | | Surface charge[b] (mV) | pH_{pzc} |
		Nanosight	DLS		
10 nm	8.28±2.57	33.31±21.34	38.01±16.69	12.98	11.30
50 nm	44.95±3.96	83.56±35.40	87.57±33.12	42.00	11.39
100 nm	93.35±9.77	119.01±66.65	130.24±38.63	47.30	11.15

[a]determined by TEM images (details in Appendix E), [b]at I=1 mM of $NaNO_3$ and pH 7
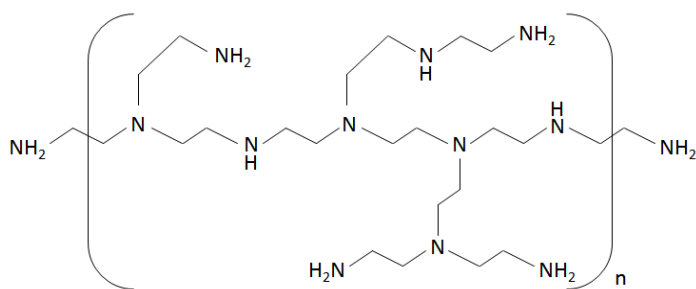
Figure 3.4: Chemical structure of BPEI

Spherical glass beads with diameters in the range of 300~355, 425~500, and 710~850 μm were purchased from MO-SCI (St. Louis, MO) for use as the filter media. The chemical composition of the glass beads is shown in Table 3.2. Each group of beads was sieved on a pair of US sieves corresponding to the designated size range (#45 (354 μm) and #50 (297 μm), #35 (500 μm) and #40 (425 μm), #20 (841 μm) and #25 (710 μm), respectively). Prior to use, the beads were washed by the following cleaning process: Rinsing with DI water 10 times, sonication in 1M HNO_3 solution overnight followed by rinsing with DI water 10 times, sonication in DI water for 10 min followed by rinsing with DI water 20 times, and complete drying in 105˚C oven.

Table 3.2: Chemical composition of glass beads.

Compound	Content (by weight)
SiO_2	60-75%
Al_2O_3	0-5%
CaO	6-15%
MgO	1-5%
Na_2O	10-20%
Fe_2O_3	$< 0.8\%$

The energy of interaction was calculated using the sum of the repulsive energy (V_R) and attractive energy (V_A) according to Equations 3-1 and 3-2; all variables in the following equations are defined in Appendix B.

$$V_R = \pi \varepsilon_0 \varepsilon_r a_p \left(2\psi_{d_f}\psi_{d_p} \ln\left[\frac{1+\exp(-\kappa s)}{1-\exp(-\kappa s)}\right] + \left(\psi_{d_f}{}^2 + \psi_{d_p}{}^2\right)\ln\left[1-\exp(-2\kappa s)\right] \right) \quad (3\text{-}1)$$

$$V_A = \frac{Aa_p}{6s}\left(1+\frac{14s}{\lambda}\right)^{-1} \quad (3\text{-}2)$$

The calculations (shown in Figure 3.5) indicate that favorable attachment conditions exist between BEPI AgNPs and the filter media for all particle sizes; that is, no repulsive energy barrier occurs at any separation distance. The attachment efficiency (α) was, therefore, assumed to be 1. With that assumption, the single collector contact efficiency (η_0) was directly calculated from Equation 3-3 using the removal efficiency from each filtration test.

$$\ln \frac{N}{N_0} = -\frac{3}{2}(1-\varepsilon)\eta_0\left(\frac{L}{d_c}\right) \quad (3\text{-}3)$$
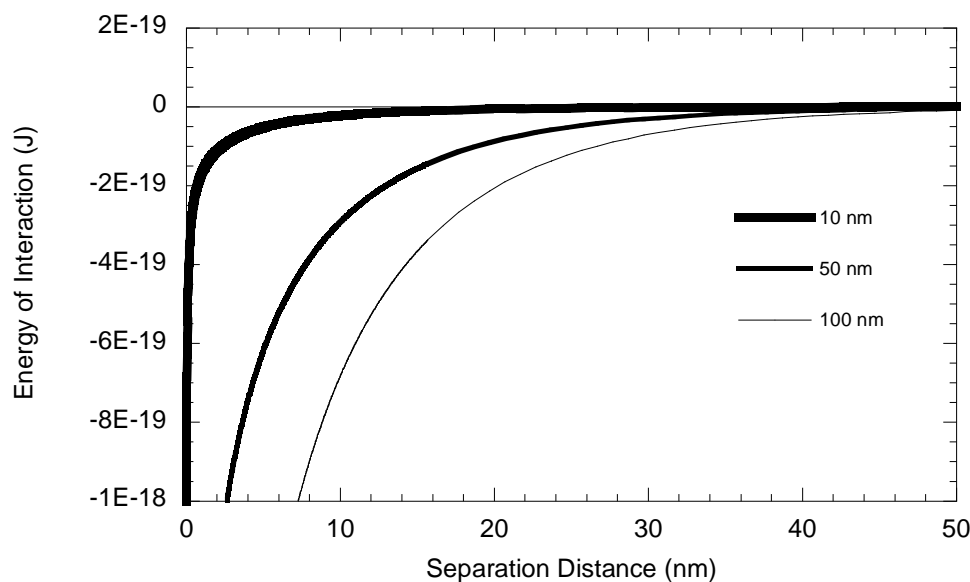
Figure 3.5:   Energy of interaction with 10 nm, 50 nm, and 100 nm BPEI AgNPs (I=1 mM of $NaNO_3$ at pH 7).

A cylindrical column with a 3.81 cm inner diameter was employed for the filtration tests. The filtration test system was designed to separate the AgNP suspension and the background solution until the two solutions were mixed immediately before the filter entrance (Figure 3.6). The flow rate of each solution was controlled to achieve the designated filtration velocity (2, 4, or 8 m/hr) and influent AgNP concentration (100 µg/L). A series of filtration tests was conducted under varying filter depth, filtration velocity, particle size, and filter media size (Table 3.3). Each filtration test consisted of two phases; 45 pore volumes of filtration with AgNPs followed by 45 pore volumes of filtration without AgNPs. The main purpose of each test was to obtain the removal efficiency, that is, a plateau in relative concentration according to the test condition, to compare with model predictions. Ionic strength was fixed at 1 mM of $NaNO_3$ and pH was controlled at 7 using 0.025 mM bicarbonate buffer. The influent and effluent samples were acidified in 3% trace metal grade HNO_3 solution, and Ag concentration was

analyzed using a Varian 710 (Agilent, Santa Clara, CA) inductively coupled plasma-optical emission spectroscopy (ICP-OES).
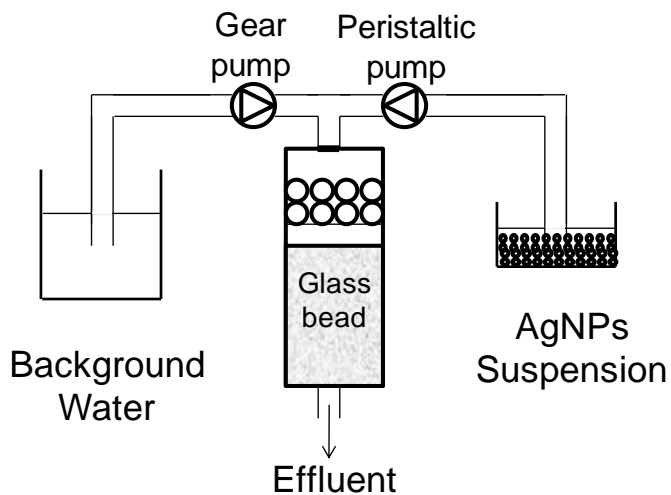
Figure 3.6:   Schematic figure of the granular media filtration system.

Table 3.3: Summary of the filtration tests.

Experiment #[a]	Particle size (nm)	Filter media size (µm)	Filter depth (cm)	Filtration velocity (m/hr)
B10-M325-L4-V2	10	325	4	2
B10-M325-L4-V4	10	325	4	4
B10-M325-L4-V8	10	325	4	8
B10-M325-L2-V4	10	325	2	4
B10-M325-L8-V4	10	325	8	4
B10-M463-L4-V4	10	463	4	4
B10-M776-L4-V4	10	776	4	4
B50-M325-L4-V2	50	325	4	2
B50-M325-L4-V4	50	325	4	4
B50-M325-L4-V8	50	325	4	8
B50-M325-L2-V4	50	325	2	4
B50-M325-L8-V4	50	325	8	4
B50-M463-L4-V4	50	463	4	4
B50-M776-L4-V4	50	776	4	4
B100-M325-L4-V2	100	325	4	2
B100-M325-L4-V4	100	325	4	4
B100-M325-L4-V8	100	325	4	8
B100-M325-L2-V4	100	325	2	4
B100-M325-L8-V4	100	325	8	4
B100-M463-L4-V4	100	463	4	4
B100-M776-L4-V4	100	776	4	4

[a] Details of experiment case name conventions are in Appendix F.

3.4. Results and Discussion

Particle aggregation. Aggregation of BPEI AgNPs was negligible at I=1 mM of NaNO$_3$ and pH 7 (Figure 3.7). This result was consistent with previous reports that the stability of BPEI AgNP would be greatest near pH 7 (El Badawy et al. 2010) and the aggregation of BPEI AgNP would be insignificant even at I=1000 mM (El Badawy et al. 2012). Therefore, the stability of BPEI AgNPs was assured in the filtration condition.
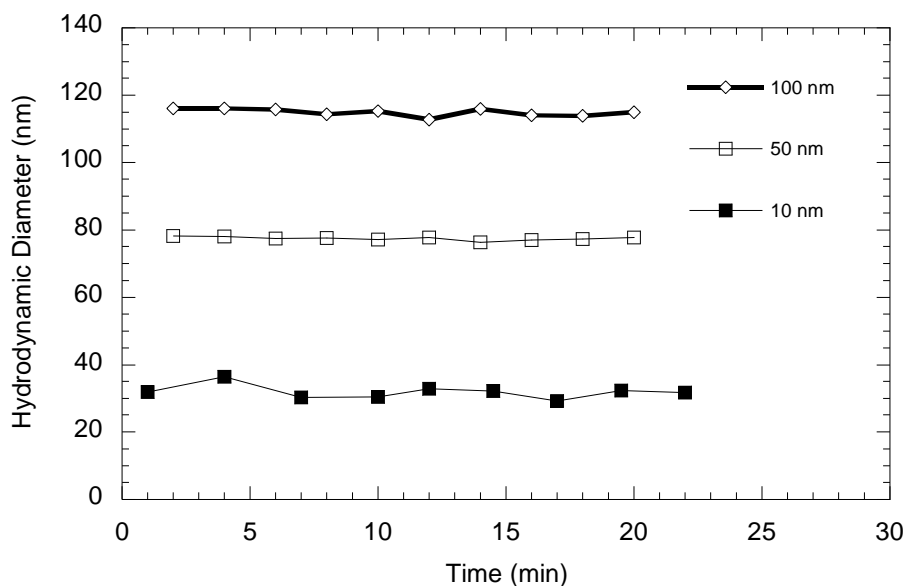
Figure 3.7:   Time-resolved aggregation results of 10 nm, 50 nm, and 100 nm BPEI AgNPs (I=1 mM of NaNO$_3$ at pH 7).

Electrostatic effect on transport of BPEI AgNPs. As a supplemental study, the transport of BPEI AgNPs was examined under different pH values or ionic strengths (Figure 3.8). The breakthrough curves were almost identical even with the change in pH (Figure 3.8a) or ionic strength (Figure 3.8b&c). These results suggest that the electrostatic (or steric) interactions between BPEI AgNPs are unimportant relative to the favorable electrostatic interaction between the nanoparticles and the filter media.

53
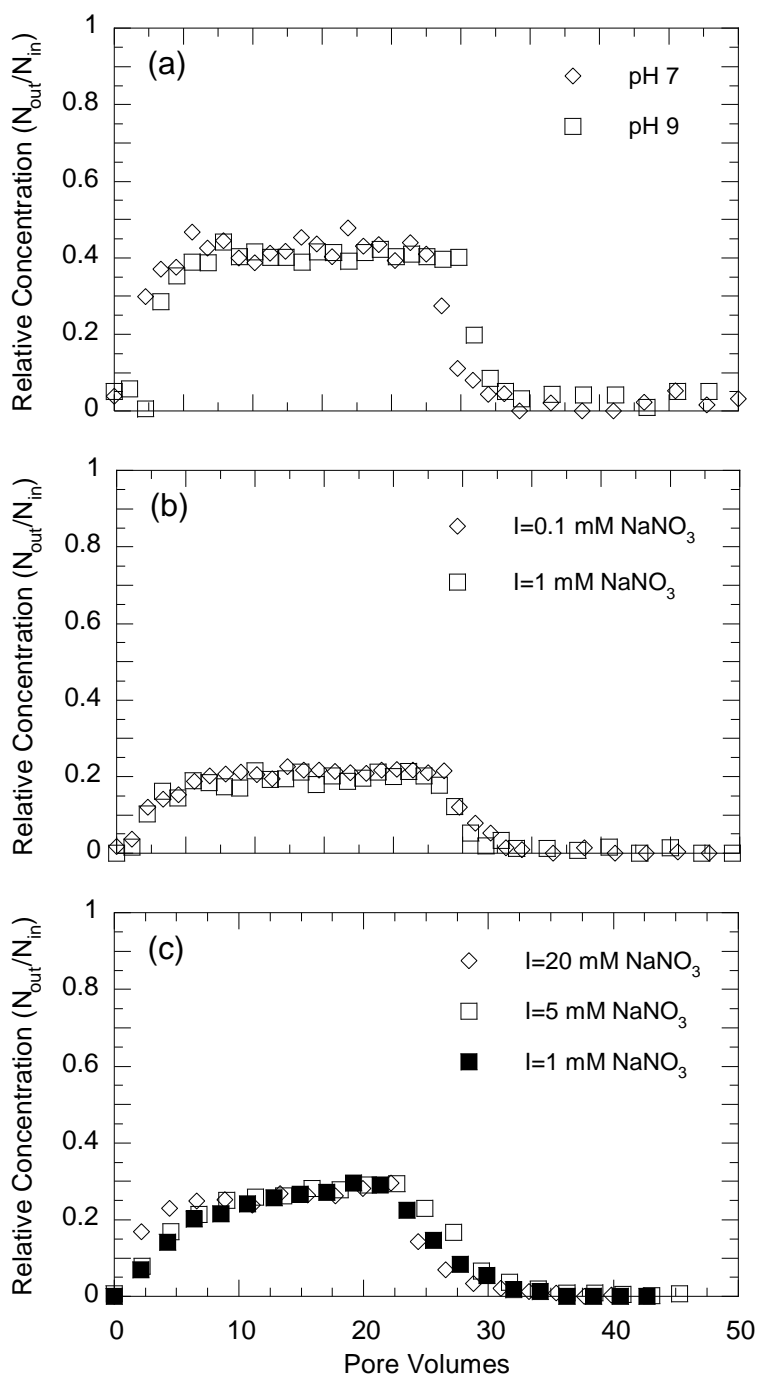
Figure 3.8: (a) Effect of pH on 10 nm BPEI AgNPs at I=1 mM of $NaNO_3$, (b) Effect of ionic strength on 10 nm BPEI AgNPs at pH 7, and (c) Effect of ionic strength on 50 nm BPEI AgNPs at pH 7.

Effect of filter depth. For the contact efficiency (η_0) estimation from the experimental results, the stabilized relative concentrations of 10, 50, and 100 nm BPEI AgNPs were examined at three different filter depths (2, 4, and 8 cm) with 4 m/hr filtration velocity and 325 µm filter media size. The overall result qualitatively followed the general expectation that deeper filter depth results in greater particle deposition (Figure 3.9). The time to reach a stabilized relative concentration was slightly increased as the filter depth became shallower. The removal trend as a function of particle size indicates the greater AgNP capture of smaller AgNPs due to their more vigorous Brownian motion. Note that the relative concentration was nearly constant after a short period. Even though the tests were conducted at the low range of the ratio of filter depth to filter media size (L/d_c) (62, at the lowest), a constant level of AgNP deposition was maintained for a sufficient period to obtain an apparent steady state relative concentration. This result might be due to slow ripening as a consequence of low influent AgNP concentration.
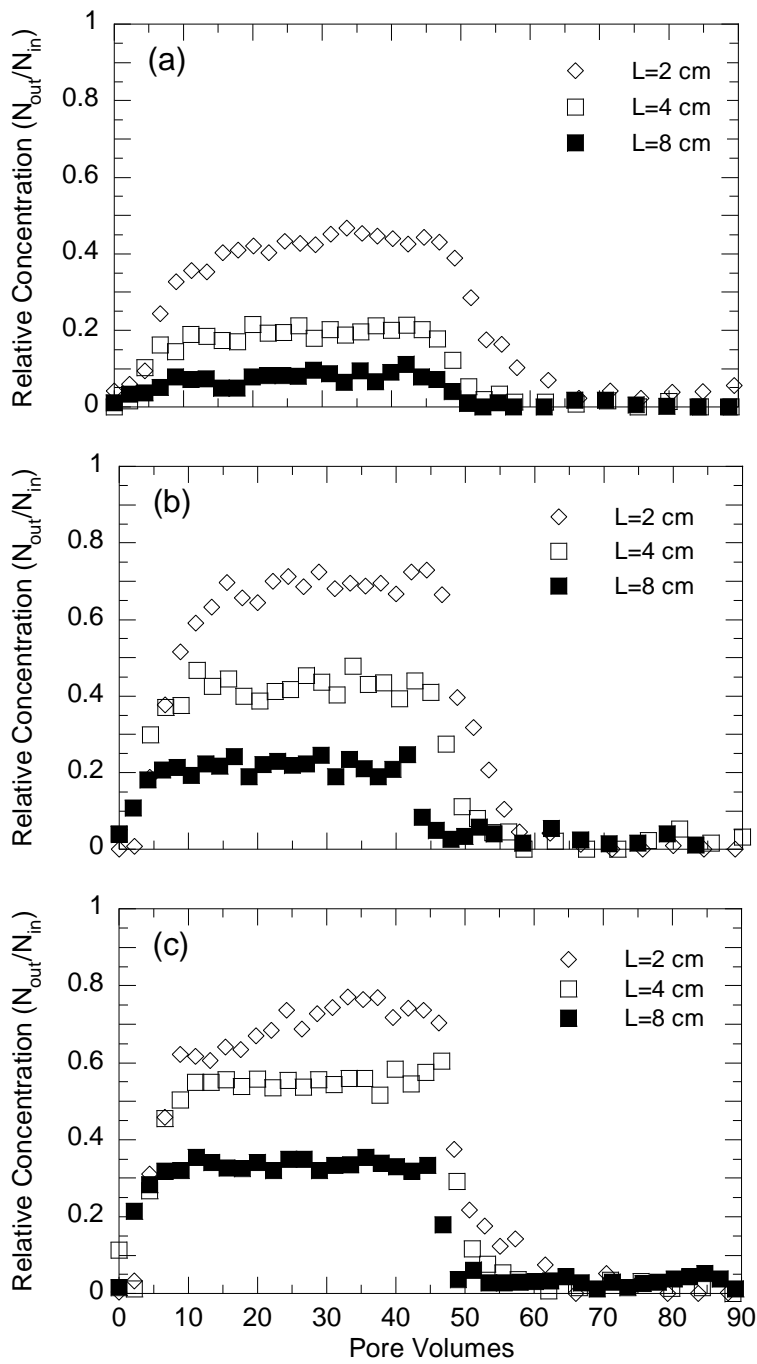
Figure 3.9:   Effect of filter depth on the transport of (a) 10 nm, (b) 50 nm, and (c) 100
nm BPEI AgNPs (v_0=4 m/hr and d_c=325 μm).

Effect of filtration velocity. To investigate the effect of filtration velocity, three filtration velocities (2, 4, and 8 m/hr) were applied to the filtration of 10, 50, and 100 nm BPEI AgNPs with 4 cm filter depth and 325 μm filter media size. Particles have less time to contact the filter media with increased filtration velocity, leading to less particle deposition. The effect of increased velocity on deposition is expected to be greater for particles whose capture is by sedimentation than for particles captured by Brownian motion. Although Ag has a relatively high density (10.49 g/cm^3), sedimentation of these small nanoparticles onto the filter media was calculated to be negligible in comparison to deposition by Brownian motion. The velocity effect was apparent in all particle sizes tested (Figure 3.10). The results from these experiments show a moderate change in AgNP deposition caused by the velocity variation (i.e., approximately 30% increase in the fraction remaining with a four-fold increase in filtration velocity).
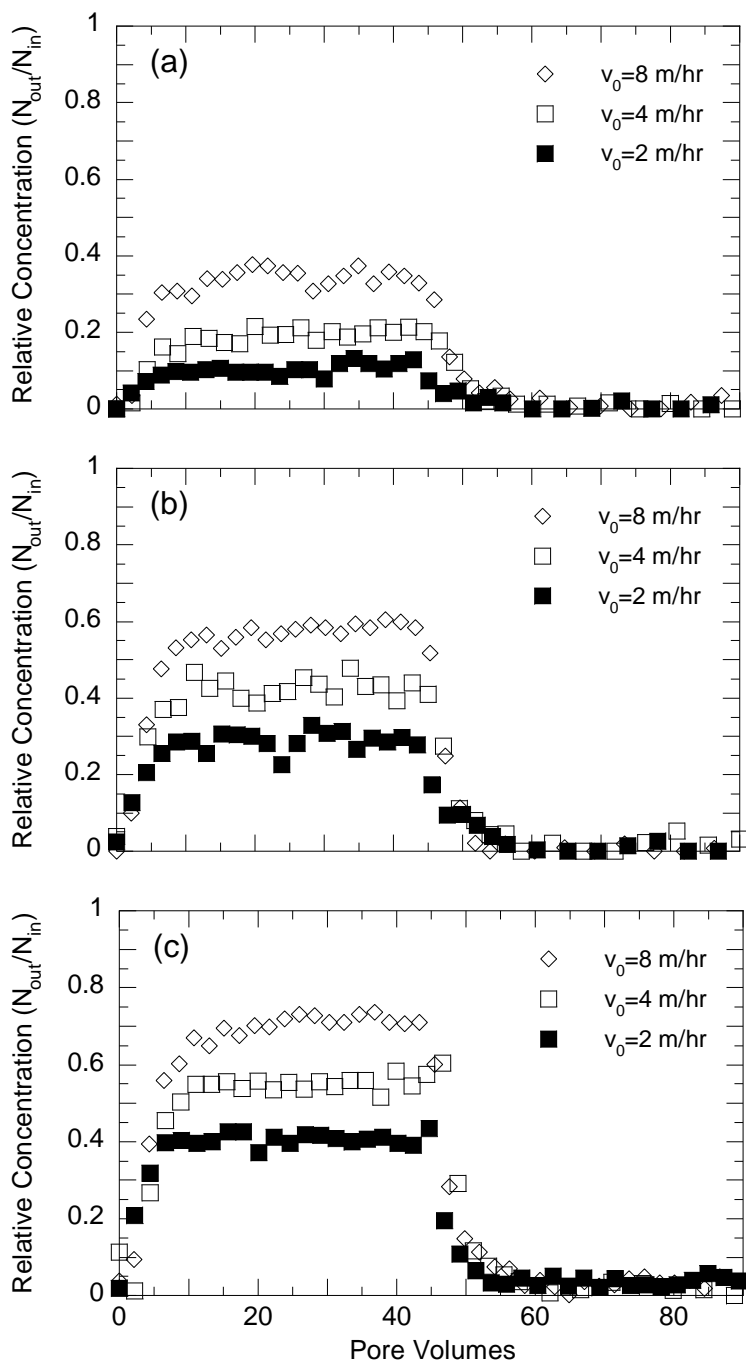
Figure 3.10: Effect of filtration velocity on the transport of (a) 10 nm, (b) 50 nm, and (c) 100 nm BPEI AgNPs (L=4 cm and d_c=325 µm).

Effect of filter media size. Three different filter media sizes (325, 463, and 776 µm) were employed to study the effect of filter media size on the filtration of 10, 50, and 100 nm BPEI AgNPs. The filtration tests were conducted with 4 cm filter depth and 4 m/hr filtration velocity. With regard to the three sizes of AgNPs, the AgNP deposition was elevated as filter media size decreased (Figure 3.11) due to the decreased pore sizes, the increased number of media layers for the same depth, and the increased surface area of the filter media. As the size of AgNPs increased from 10 nm to 100 nm, the AgNP deposition decreased for all filter media sizes. Specifically, when the filter media size was decreased from 776 to 325 µm, the fraction remaining for 10, 50, and 100 nm was decreased 65.1%, 46.5%, and 37.6%, respectively. Especially, 100 nm AgNPs were rarely captured in 776 µm filter media even under favorable attachment conditions. If nanoparticles are to be removed using granular media filtration, decreasing filter media size could be considered an important option.
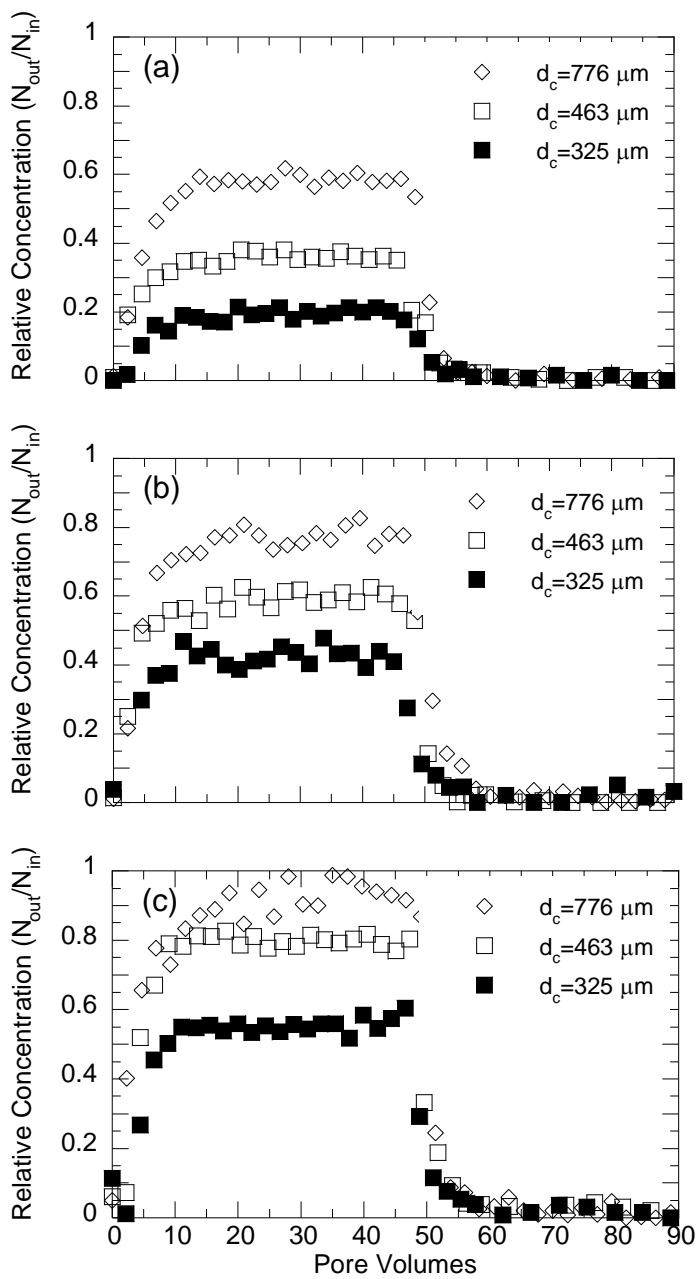
Figure 3.11: Effect of filter media size on the transport of (a) 10 nm, (b) 50 nm, and (c) 100 nm BPEI AgNPs (L=4 cm and v_0=4 m/hr).

Effect of particle size. All of the tests followed the general knowledge that the filtration efficiency is lowered at less filter depth, higher velocity, and greater media size,

60

but the objective in this research was to test whether these trends fit the predictions of the Tufenkji and Elimelech model. In Figure 3.12, the model predictions and the experimental results are compared, using both the mean diameter and the hydrodynamic diameter determined by TEM and DLS, respectively, in the model predictions. Recall from Table 3.1 that these two values for each particle size were substantially different, with the hydrodynamic diameter being 30 to 40 nm larger than the mean diameter. The hydrodynamic diameter includes the solvent and macromolecules that adhere to particle surface in a liquid medium; using this measure in the predictions accounts for the fact that the added layer on the core particle impacts the diffusivity of the particle. In virtually all cases shown in Figure 3.12, the two sets of model predictions bracket the experimental results, but in some cases, one of the predictions fits much better.

Considering the predictions using the mean (TEM) diameter, the experimental results were quite consistent with the colloidal filtration model expectation in the case of the 50 and 100 nm BPEI AgNPs (parts (d) to (i) of Figure 3.12). Of the 18 experiments shown for these two types of particles, only three have results that were closer to the model predictions using the hydrodynamic diameter, and several results were predicted quite precisely by using the mean diameter. However, the removal efficiency of 10 nm BPEI AgNPs (parts (a) to (c) of Figure 3.12) was approximately 20~30% less than the model prediction using the mean diameter for the model particle size, and most of the results were predicted somewhat better (but not precisely) using the hydrodynamic diameter. Taken together, these results suggest that the colloidal filtration model is generally quite valid, but the effect of particle size is not accounted for quite properly.
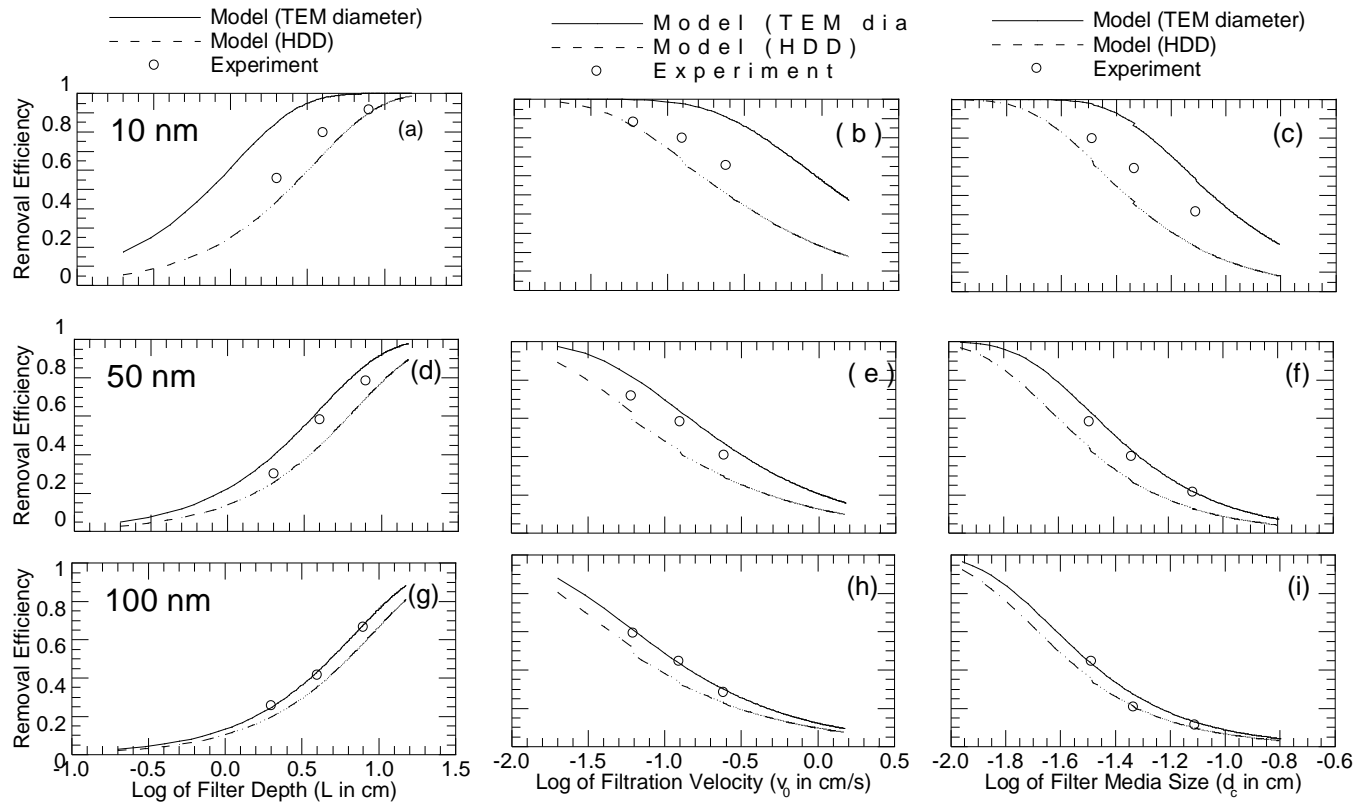
Figure 3.12: Comparison of experimental results and model predictions for all parameters studied.   (Particle size varies from top (10 nm) to bottom (100 nm) and each column represents the variation of a different physical parameter (depth, velocity, and media size from left to right.)   .

As far as diffusion is concerned, hydrodynamic diameter has a preference over core diameter because the adsorbed layer on the particle surface is also considered as a part of particle. Therefore, the entire particle diameter including the added layer is generally considered to affect the diffusivity of a particle.

However, considering a 30-40 nm discrepancy between the mean diameter and the hydrodynamic diameter in this study, the hydrodynamic diameter could be overestimated due to the artifact of the analytical method. In fact, the data processing in DLS could provide inevitable error which leads to overestimation (Khlebtsov and Khlebtsov 2011). Therefore, the true hydrodynamic diameter is likely to be between the diameters determined by TEM and DLS, and such a trend would result in a better fit of the experimental results to the model.

Nevertheless, smaller AgNPs showed a different degree of deviation between the experimental results and the model predictions, suggesting a possible alteration of nanoparticle properties as the size gets smaller than 50 nm. Others have suggested that the size dependent property is more likely to appear below 10 nm (Bian et al. 2011), but, little is known about the details.

Regarding the size dependent property, the vigorous Brownian motion of nanoparticles especially at extremely small size could cause a change in the deposition of nanoparticles. Either increased or decreased removal can be anticipated by an increased number of collisions with filter media as well as the slippery movement of particles in vicinity of filter media. A drastic increase in the diffusion coefficient of nanoparticles less than 10 nm (Bhatt et al. 2013) supports the greater kinetic energy of such a small nanoparticle. The rebounding nature of nanoparticles below 10 nm was proposed in aerosol filtration studies since early 1990's (Wang and Kasper 1991), but this phenomenon is far less likely in water where the   mean free path is far smaller than in

air. In case of particle transport in a liquid medium, the decreased deposition (relative to model predictions) could be a result of lesser friction between particles. Thus, this scenario suggests that the attachment efficiency (α) of a very small nanoparticle might be less than 1 even under favorable attachment conditions. To elucidate the change in diffusion as a function of nanoparticle size, the transport of nanoparticles can be investigated under conditions that vary the viscosity of the background solutions (e.g., applying deuterium oxide (D_2O) or methanol instead of water).

Also, smaller particles such as 10 nm in size could display more hydrophilic nature because the curvature becomes greater as particle size becomes smaller leading to more bound water molecules on the surface. For example, as fullerene nanoparticle size becomes smaller, less fullerene deposition onto silica surfaces was reported due to more hydrophilic nature of smaller nanoparticles which led to greater charge stabilization (Chae et al. 2010). Also, considering a smaller nanoparticle in the transition stage from molecule to particle, the deposition of nanoparticles onto filter media could be undermined in terms of hydrophobic interaction.

Another possible reason for variation in removal efficiency of smaller nanoparticles than predicted by the model is the stronger steric stabilization by the capping agent. More organic molecules can adsorb on smaller particles which have greater abundance of the edge and corner sites (Grassian 2008), so that smaller BPEI AgNPs are likely to have a denser capping layer compared to the larger particles. Further estimation of the adsorbed layer thickness on AgNPs is required to support this argument.

3.5. Conclusions

The effect of physical parameters on the transport of BPEI AgNPs in granular media filtration was experimentally evaluated under favorable attachment conditions. A stable relative concentration of the effluent was obtainable during the test period due to low influent AgNP concentration which retarded ripening and prevented aggregation in the suspension. Brownian motion was dominant in the experimental conditions tested in this study. Deeper filter depth, lower filtration velocity, and smaller filter media size led to more AgNP deposition as expected. With regard to the physical variables and their values tested in this study, the removal efficiency for all particle sizes was significantly enhanced by decreasing filter media size from 776 to 325 µm. This result suggests that the selection of filter media size could be a decisive factor for nanoparticle removal using granular media filtration. When using the mean (TEM) diameter for the model predictions, the transport of 100 nm BPEI AgNPs in granular media filtration showed good agreement with the expectations from the colloidal filtration model of Tufenkji and Elimelech (2004), proving the validity of the model. However, as the particles decreased to 50 and 10 nm, the experimental results tended to move toward the predictions using the (larger) hydrodynamic diameter. These results imply a variation in nanoparticle property as particles get smaller. Since size-dependent nanoparticle transport is not well understood, more experimental evidence with different types of nanoparticles is required to support the conceivable arguments in favor of such an effect.

Further investigation on the transport of the smaller-sized nanoparticles is required to obtain sufficient experimental data to update the colloidal filtration model especially in the size range less than 50 nm. The updated colloidal filtration model would be beneficial for predicting contact efficiency (η_0) in such a small particle size range,

which then could lead to an accurate estimation of the attachment efficiency (α) under unfavorable attachment conditions.
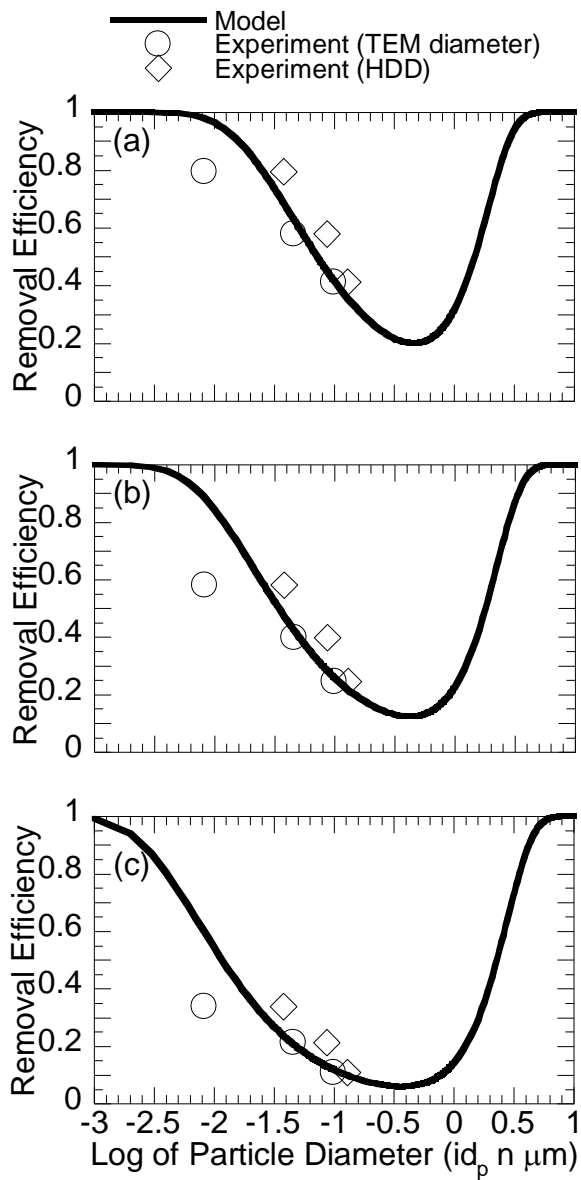
Figure 3.13: Comparison of experimental results and model predictions: (a) d_c=325 µm, L=4 cm, v_0=4 m/hr, (b) d_c=463 µm, L=4 cm, v_0=4 m/hr, (c) d_c=776 µm, L=4 cm, v_0=4 m/hr.
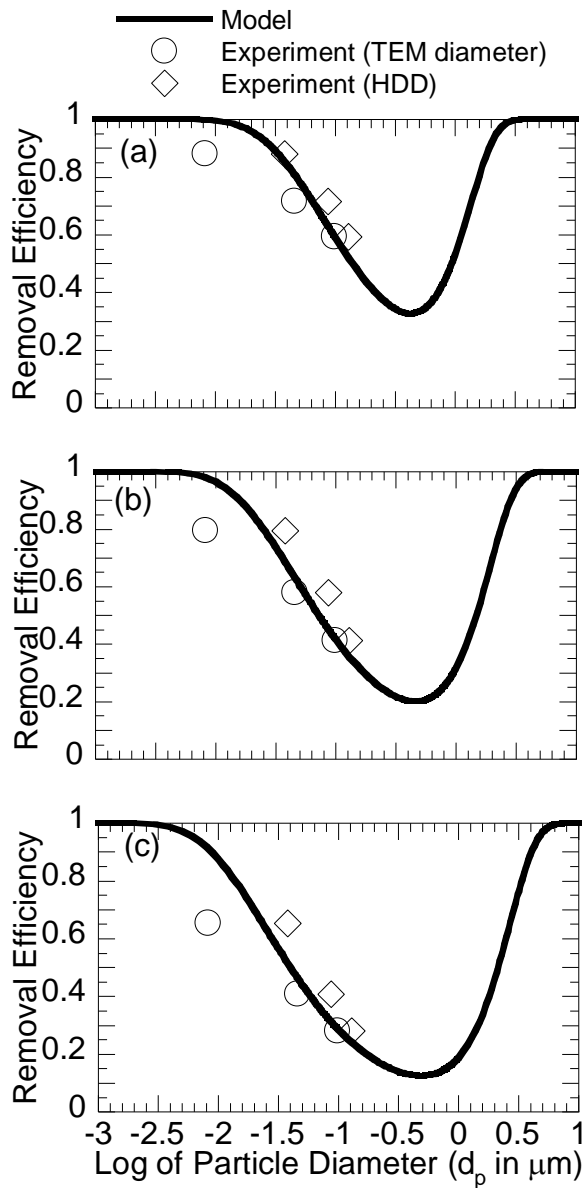
Figure 3.14: Comparison of experimental results and model predictions: (a) d_c=325 µm, L=4 cm, v_0=2 m/hr, (b) d_c=325 µm, L=4 cm, v_0=4 m/hr, (c) d_c=325 µm, L=4 cm, v_0=8 m/hr.
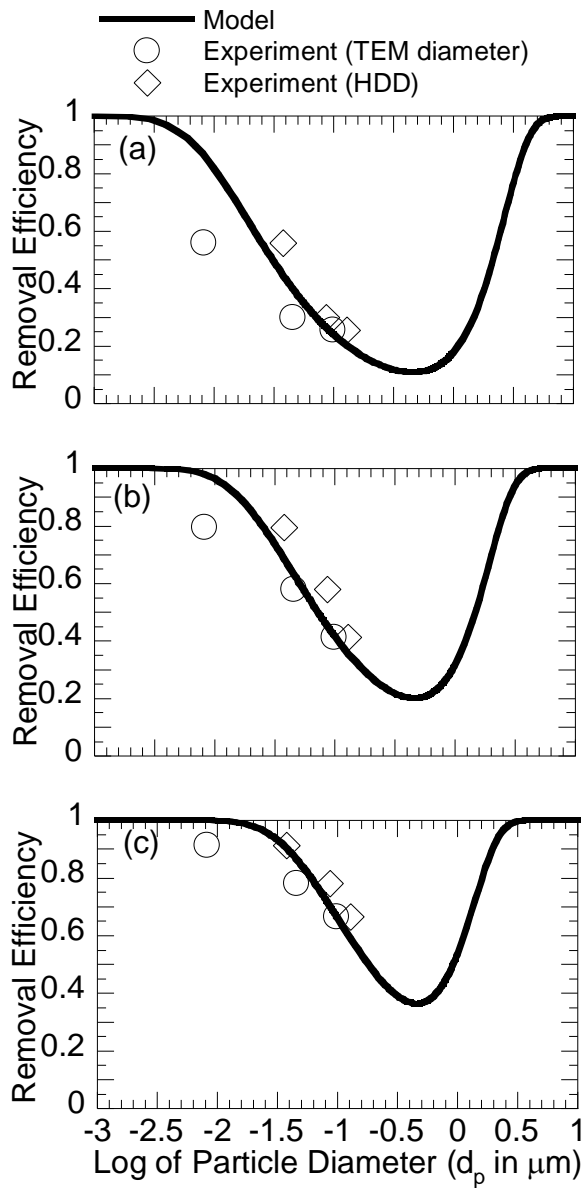
Figure 3.15: Comparison of experimental results and model predictions: (a) d_c=325 µm, L=2 cm, v_0=4 m/hr, (b) d_c=325 µm, L=4 cm, v_0=4 m/hr, (c) d_c=325 µm, L=8 cm, v_0=4 m/hr.

References

Barisik, M., Atalay, S., Beskok, A. and Qian, S.Z. (2014) Size dependent surface charge properties of silica nanoparticles. Journal of Physical Chemistry C 118(4), 1836-1842.

Bhatt, P.A., Pratap, A. and Jha, P.K. (2013) Size and dimension dependent diffusion coefficients of SnO_2 nanoparticles. International Conference on Recent Trends in Applied Physics and Material Science 1536, 237-238.

Bian, S.W., Mudunkotuwa, I.A., Rupasinghe, T. and Grassian, V.H. (2011) Aggregation and dissolution of 4 nm ZnO nanoparticles in aqueous environments: Influence of pH, ionic strength, size, and adsorption of humic acid. Langmuir 27(10), 6059-6068.

Chae, S.R., Badireddy, A.R., Budarz, J.F., Lin, S.H., Xiao, Y., Therezien, M. and Wiesner, M.R. (2010) Heterogeneities in fullerene nanoparticle aggregates affecting reactivity, bioactivity, and transport. ACS Nano 4(9), 5011-5018.

El Badawy, A.M., Luxton, T.P., Silva, R.G., Scheckel, K.G., Suidan, M.T. and Tolaymat, T.M. (2010) Impact of environmental conditions (pH, ionic strength, and electrolyte type) on the surface charge and aggregation of silver nanoparticles suspensions. Environmental Science & Technology 44(4), 1260-1266.

El Badawy, A.M., Scheckel, K.G., Suidan, M. and Tolaymat, T. (2012) The impact of stabilization mechanism on the aggregation kinetics of silver nanoparticles. Science of the Total Environment 429, 325-331.

Grassian, V.H. (2008) When size really matters: size-dependent properties and surface chemistry of metal and metal oxide nanoparticles in gas and liquid phase environments. Journal of Physical Chemistry C 112(47), 18303-18313.

Khlebtsov, B.N., Klebtsov, N.G. (2011) On the measurement of gold nanoparticle sizes by the dynamic light scattering method. Colloid Journal 73(1), 118-127.

Long, W. and Hilpert, M. (2009) A correlation for the collector efficiency of Brownian particles in clean-bed filtration in sphere packings by a Lattice-Boltzmann method. Environmental Science & Technology 43(12), 4419-4424.

Ma, H.L., Pedel, J., Fife, P. and Johnson, W.P. (2009) Hemispheres-in-cell geometry to predict colloid deposition in porous media. Environmental Science & Technology 43(22), 8573-8579.

MacCuspie, R.I., Rogers, K., Patra, M., Suo, Z.Y., Allen, A.J., Martin, M.N. and Hackley, V.A. (2011) Challenges for physical characterization of silver nanoparticles under pristine and environmentally relevant conditions. Journal of Environmental Monitoring 13(5), 1212-1226.

Nelson, K.E. and Ginn, T.R. (2011) New collector efficiency equation for colloid filtration in both natural and engineered flow conditions. Water Resources Research 47(5), W05543.

Rajagopalan, R. and Tien, C. (1976) Trajectory analysis of deep-bed filtration with sphere-in-cell porous-media model. AICHE Journal 22(3), 523-533.

Tufenkji, N. and Elimelech, M. (2004) Correlation equation for predicting single-collector efficiency in physicochemical filtration in saturated porous media. Environmental Science & Technology 38(2), 529-536.

Wang, H.C. and Kasper, G. (1991) Filtration efficiency of nanometer-size aerosol-particles. Journal of Aerosol Science 22(1), 31-41.

Yao, K.M., Habibian, M.M. and Omelia, C.R. (1971) Water and waste water filtration - Concepts and applications. Environmental Science & Technology 5(11), 1105-1112.

Chapter 4: EFFECT OF IONIC STRENGTH AND ION TYPE ON ATTACHMENT OF SILVER NANOPARTICLES IN GRANULAR MEDIA FILTRATION

Abstract

The increasing use of silver nanoparticles (AgNPs) has raised concerns about their impact on the environment. Therefore, it is desirable to examine the transport of AgNPs in both natural and engineered systems. Since many researchers focused on a relatively high concentration of nanoparticles in their transport study, this study focuses on the transport of low concentrations of AgNPs in granular media filtration at velocities used in water treatment. Experiments with different ionic strengths, ion types, and AgNP capping agents (citrate and PVP) were conducted. Attachment of citrate AgNPs was enhanced with high ionic strength and divalent ions (Ca and Mg ions), in accordance with classical electrostatic destabilization. It was found that either a lower energy barrier or a suppressed double layer contributed to yield less electrostatic repulsion. The retention profile (captured particles as a function of filter depth) showed relatively uniform AgNP deposition throughout the filter depth when aggregation was impeded. On the other hand, under conditions at which aggregation was likely to occur, the deposition was greatest near the entrance to the filter bed and decreased hyper-exponentially with greater depth. Due to the low AgNP concentration, more than 90% of AgNPs could be recovered using the simplified AgNP dissolution method. PVP capped AgNPs showed stronger stabilizing effects than citrate-capping due to the minimized electrostatic effect.

Keywords

Ionic strength, ion type, capping agent, attachment, retention profile

4.1. Introduction

Silver nanoparticles (AgNPs) are the most frequently reported additions to nanotechnology-based consumer products (Rejeski et al. 2014). As the use of AgNPs increases, their discharge and transport from terrestrial regions into water bodies is expected to increase (Gottschalk et al. 2009, Kaegi et al. 2011, Lowry et al. 2012). The toxicity of AgNPs to microorganisms (Laban et al. 2010, Wood et al. 1999) and to humans (Panyala et al. 2008) is well known. Further, the reported silver concentration in selected waters (Wen et al. 2002) is already close to the quantity of AgNPs that have demonstrated a negative impact on bacteria (Choi and Hu 2008) and daphnia (Griffitt et al. 2008). It is therefore advantageous to study the fate and transport of AgNPs in the environment to evaluate realistic toxicity risks and determine how they might be mitigated.

The transport of AgNPs into the environment could lead to encounters with other particles such as soil or filter media. As a research tool of particle-particle interactions, water saturated granular media filters have been used to study attachment between filter media and various nanoparticles such as TiO_2 (Guzman et al. 2006, Joo et al. 2009, Petosa et al. 2012, Solovitch et al. 2010), fullerene (Espinasse et al. 2007, Lecoanet and Wiesner 2004, Wang et al. 2008b), carbon nanotubes (Jaisi et al. 2008, Liu et al. 2009a), and Fe^0 (Phenrat et al. 2009, Saleh et al. 2008, Tiraferri and Sethi 2009). Previous studies report that nanoparticles are highly affected by the electrostatic (Tosco et al. 2012) and steric (Jones and Su 2012) interactions of their stabilizing organic coatings ("caps"), an indication that chemical attachment is the main removal mechanism rather than physical straining.

Several studies have specifically looked at the transport of AgNPs in granular media filtration. They have shown that the stability of the particles is affected by a host of

factors such as ionic strength, pH (Lin et al. 2011), composition of the filter media (Tian et al. 2010), capping agents (Lin et al. 2012, Song et al. 2011), filter media size, and filtration velocity (Sagee et al. 2012). However, those studies were conducted at mg/L levels of silver for the sake of analytical convenience (Fabrega et al. 2011). To assess the actual transport of AgNPs within granular media filters, it is necessary to perform experiments at environmentally relevant concentrations (µg/L). High concentrations of nanoparticles produce unrealistic conditions such as inhibition of further attachment by early coverage of the available deposition sites (Bradford et al. 2007, Wang et al. 2012a), more likely aggregation prior to deposition, or higher electrostatic repulsion from the deposited nanoparticles (Chowdhury et al. 2011).

Generally, particles suspended in water possess a negative charge under relevant pH conditions. This means the interaction between the nanoparticles and filter media is energetically unfavorable. Nevertheless, the capacity to capture nanoparticles in a filter bed can be enhanced through varying physical and chemical conditions, and complete deposition of the nanoparticles has been observed (Petosa et al. 2010).

In this study, a low AgNP concentration was applied to a granular media filter to investigate the effect of different ionic strengths, ion types, and capping agents on the AgNP attachment. The energy of interaction was introduced on the basis of the surface charges of AgNPs and the filter media to interpret the electrostatic interaction. In addition, the amount of AgNPs captured in the filter bed was quantified at different filter depths to examine the AgNP attachment throughout the entire filter depth.

4.2. Materials and Methods

4.2.1. AgNP suspensions

Citrate and PVP capped AgNPs were purchased from NanoComposix (San Diego, CA). Citrate and PVP were chosen because they are the two most commonly used capping agents in AgNPs synthesis (Tolaymat et al. 2010). The stock AgNP suspension was 1 mg/mL with an average particle size of 50 nm. The monodispersed size distribution and spherical shape for the citrate- and PVP-capped particles were confirmed by transmission electron microscopy (TEM, FEI Tencai) and dynamic light scattering (DLS, Malvern) as shown in Figure 4.1. The surface charge of the particles was analyzed by dynamic light scattering (DLS, Malvern).

The mean diameter measured from TEM images was close to the diameter reported by manufacturer. However, a greater particle size (expressed as hydrodynamic diameter) was obtained by DLS (Table 4.1). DLS estimates the diffusivity of particles from the wavelength of scattered light and utilizes the Stokes-Einstein equation to determine particle size as hydrodynamic diameter (Boyd et al. 2011). Since the hydrodynamic diameter includes the adsorbed molecules on the particle surface, a greater particle size is expected from DLS than TEM. Considering the greater molecular weight of PVP compared to citrate, it is conceivable to have a greater hydrodynamic diameter with PVP capping. Assuming more reliability on direct observation (Domingos et al. 2009), the TEM mean diameter was used in the calculations of the following sections. Note that the standard deviations of the diameters for both types of particles were far greater for the hydrodynamic diameter than for the TEM measurements; the TEM images in Figure 4.1 seem to confirm that the distribution was much tighter than suggested by the DLS measurements.

The stock suspension was diluted in DI water to obtain the desired concentration for the filtration experiments. The stock suspension was stored at 4°C protected from light. This study focused on the transport of AgNPs, preventing the change of particle property such as dissolution (Liu and Hurt 2010), aggregation (Li and Lenhart 2012), or sulfidation (Kim et al. 2010, Levard et al. 2011) during the experiment.
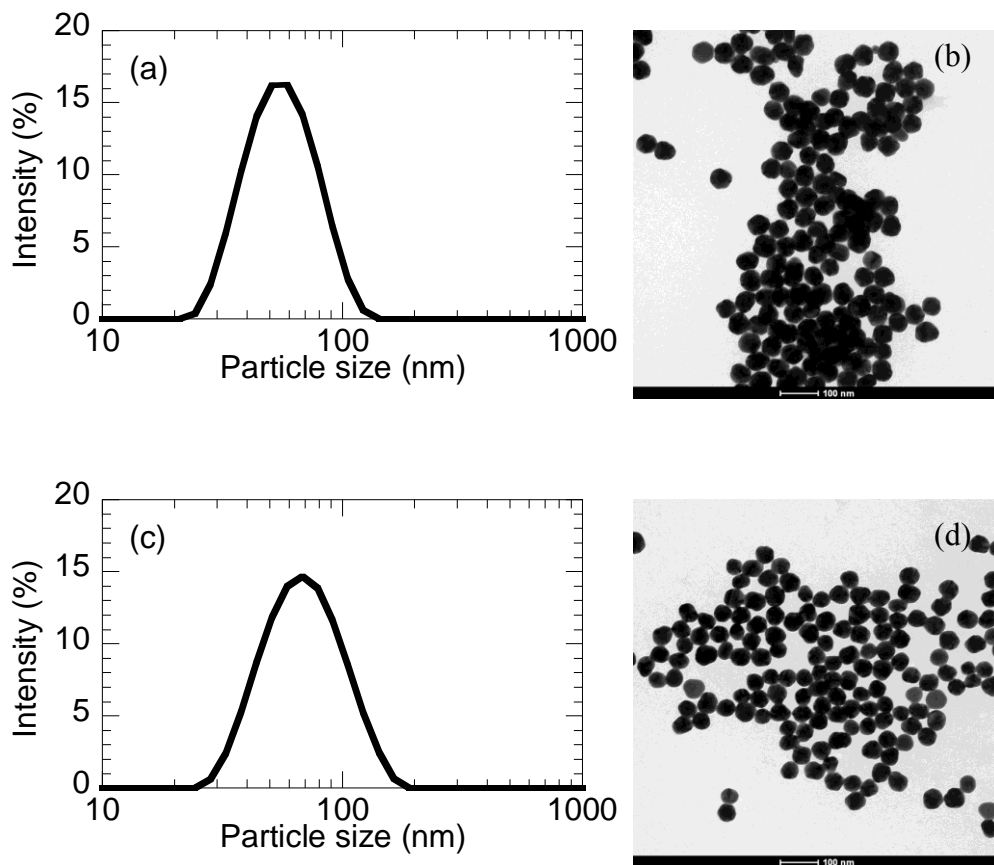
Figure 4.1: (a) Citrate AgNP size distribution by DLS and (b) TEM image of citrate AgNPs. (c) PVP AgNP size distribution by DLS and (d) TEM image of PVP AgNPs. (The scale bar is 100 nm in (b) and (d).)

Table 4.1: Citrate- and PVP-capped AgNP properties used for filtration tests.

Capping agent	Mean diameter[a] (nm)	Mean diameter[b] (nm)	Mean hydrodynamic diameter[c] (nm)	Surface charge[d] (mV)
Citrate	53.5±4.4	54.30±2.52	58.05±19.12	-43.37
PVP	49.9±4.6	45.86±5.06	72.59±26.78	-28.32

[a]reported by manufacturer (details in Appendix D), [b]determined by TEM images (details in Appendix E), [c]determined by DLS, [d]at I=10 mM of $NaNO_3$ and pH 7

4.2.2. Granular media

Spherical glass beads with diameters in the range of 300~355 μm were purchased from MO-SCI (St. Louis, MO) and used to pack the granular media bed. The spherical shape and monodisperse size distribution was confirmed by the scanning electron microscopy (SEM, Zeiss) as shown in Figure 4.2. Prior to use, the beads were screened using US sieves #45 (354 μm) and #50 (297 μm). After each filtration test, the beads were washed by an overnight sonication in 1M HNO_3 solution as well as a standard cleaning process (Tobiason 1987) to ensure that the surface of the beads was clean. The surface charge of the beads was measured by DLS after grinding particles (El Badawy et al. 2013, Liang et al. 2013b).

200 µm   EHT = 5.00 kV   Signal A = SE2   Date :3 Mar 2014
WD = 16.4 mm   Mag = 61 X
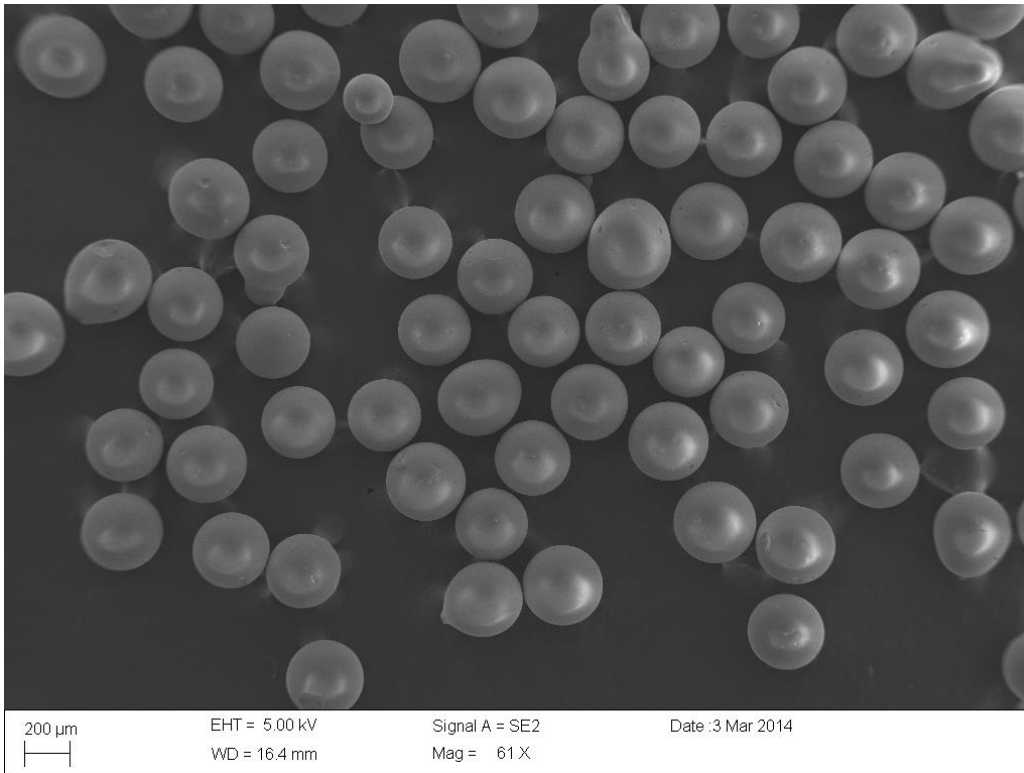
Figure 4.2:   SEM image of the 300~355 µm spherical glass beads.

4.2.3. Filtration experiments

A laboratory-scale acrylic cylindrical column (3.81 cm inner diameter) was used for the experiments. Eight Teflon spherical balls were placed above the filter bed to produce an evenly distributed influent flow across the top of the filter bed. The glass beads were packed to a 10 cm depth inside the column. The porosity of the packed bed was determined gravimetrically to be 0.42. The AgNP suspension and background water were separately prepared (Figure 4.3) to prevent physical/chemical changes in the AgNPs prior to the filtration test. The two influents (AgNP suspension and background water) were pumped via a gear pump (Micropump, Cole Parmer) and a peristaltic pump (Easy-load II, Masterflex), respectively, and mixed immediately before the column entrance. The flow ratio of the AgNP suspension to the background water was kept at 1:20 to

maintain an influent AgNP concentration less than 100 µg/L. The total flow rate was kept at 40 mL/min in a down-flow configuration, yielding a superficial velocity of 2 m/h, a value that is within the range of filtration velocities used in conventional drinking water treatment plants. These conditions are calculated to yield a Reynolds number of 0.2 and are therefore thought to reflect laminar flow.
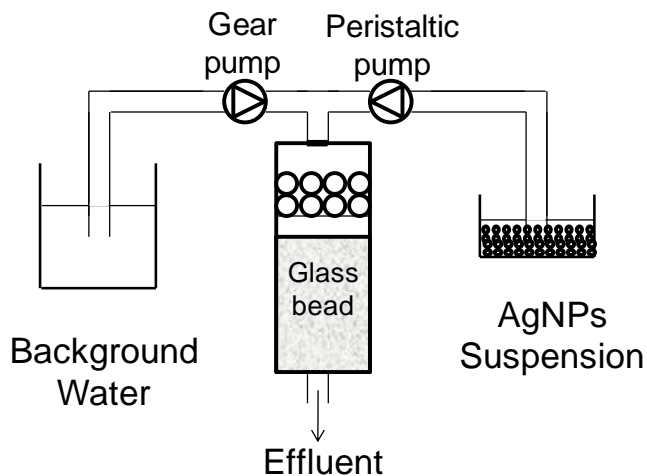
Figure 4.3:   Schematic figure of the granular media filtration system.

Ionic strength was held to 1 to 100 mM by varying the amount of $Ca(NO_3)_2$, $Mg(NO_3)_2$, or $NaNO_3$ added to the background water; the specific chemical conditions for each test are summarized in Table 4.2. The pH of the background water was maintained at 7.0 with 0.025 mM bicarbonate buffer to prevent any significant change of the surface charge. No natural organic matter (NOM) was included in this study. The media was flushed at least for 30 pore volumes by the background water used in the subsequent test. Each filtration test included the following steps: 1) 25 pore volumes (30 minutes) of filtration with AgNPs and 2) 25 pore volumes (30 minutes) of filtration without AgNPs. Samples were collected every 1 to 2 min during the filtration period. All

79

glassware used in the experiments was cleaned in a 10% nitric acid (v/v) bath overnight and rinsed with DI water at least seven times followed by complete drying before use.

After each filtration test was completed, the filter bed was cut into five sections after draining. To obtain five sections from the entire filter bed, the filter bed was gently pushed out of the column using a rod in the vertical downward direction until approximately 2 cm filter depth was collected in a container. Once the container was fully filled with filter media, the sectioned filter bed was acidified with 3% nitric acid solution to achieve a complete dissolution of AgNPs from the filter bed. This process was repeated five times until the entire filter bed was sectioned.

Table 4.2: Summary of the filtration tests with different ionic strengths, ion types, and capping agents.

Experiment #[a]	Capping agent	Ionic strength (and source)
C50-I1-Ca	Citrate	1 mM $Ca(NO_3)_2$
C50-I5-Ca	Citrate	5 mM $Ca(NO_3)_2$
C50-I10-Ca	Citrate	10 mM $Ca(NO_3)_2$
C50-I10-Na	Citrate	10 mM $NaNO_3$
C50-I100-Na	Citrate	100 mM $NaNO_3$
C50-I10-Mg	Citrate	10 mM $Mg(NO_3)_2$
P50-I1-Ca	PVP	1 mM $Ca(NO_3)_2$
P50-I5-Ca	PVP	5 mM $Ca(NO_3)_2$
P50-I10-Ca	PVP	10 mM $Ca(NO_3)_2$
P50-I10-Na	PVP	10 mM $NaNO_3$
P50-I100-Na	PVP	100 mM $NaNO_3$
P50-I10-Mg	PVP	10 mM $Mg(NO_3)_2$

[a] C or P refers to citrate or PVP, 50 is for 50 nm size, the I value is the ionic strength (mM), and the chemical name is the source of the ionic strength.

4.2.4. Energy of interaction

DLVO theory was adopted to calculate the energy of interaction between AgNPs and the filter media. Assuming the interaction between a flat plate and a spherical particle, the repulsive energy (V_R), attractive energy (V_A), and Born repulsive energy

(V_B) were calculated according to Equations 4-1, 4-2, and 4-3, respectively. The sum of the energy values was used to express the energy of interaction.

$$V_R = \pi \varepsilon_0 \varepsilon_r a_p \left(2\psi_{d_f} \psi_{d_p} \ln\left[\frac{1+\exp(-\kappa s)}{1-\exp(-\kappa s)}\right] + \left(\psi_{d_f}^{\,2} + \psi_{d_p}^{\,2}\right)\ln\left[1-\exp(-2\kappa s)\right]\right) \quad (4\text{-}1)$$

$$V_A = \frac{Aa_p}{6s}\left(1+\frac{14s}{\lambda}\right)^{-1} \quad (4\text{-}2)$$

$$V_B = \frac{A\sigma_c^6}{7560}\left(\frac{8a_p+s}{(2a_p+s)^7} + \frac{6a_p-s}{s^7}\right) \quad (4\text{-}3)$$

where a_p : Particle radius (nm)

ε_0 : Permittivity in vacuum (8.854×10^{-12} C^2/J-m)

ε_r : Relative permittivity of water (78.5 at 298K)

ψ_{df} : Surface potential of filter media (V)

ψ_{dp} : Surface potential of AgNP (V)

κ : Inverse characteristic length of diffuse layer (nm^{-1})

s : Separation distance (nm)

A : Hamaker constant (generally assumed 2.75×10^{-20} J (El Badawy et al. 2013))

λ : Characteristic wavelength (generally assumed as 100 nm (Anandarajah and Chen 1995))

σ_c : Collision diameter (generally assumed as 0.5 nm (Elimelech et al. 1998))

The inverse characteristic length of the diffuse layer was simply calculated as in Equation 4-4 (Hunter 1981)

$$\kappa = 3.288\sqrt{I} \quad (4\text{-}4)$$

where I : Ionic strength (M).

Note the energy of interaction is highly dependent on surface potentials. However, these did not vary significantly around pH 7 which was used in the experiment. Surface potentials were calculated from zeta potential using Equation 4-5 (z is taken to be 5 Å) (Vanoss et al. 1990).

$$\psi = \zeta\left(1 + \frac{z}{a}\right)e^{\kappa z} \tag{4-5}$$

where ψ : Surface potential (V)

ζ : Zeta potential (V)

a : Particle radius (nm)

z : Distance from the particle surface to the slipping plane (nm)

4.2.5. Sample analysis

AgNP samples of the filter effluent were immediately acidified with trace metal grade HNO_3 to a final acid concentration of 3% (v/v) (sample pH < 0.5), which promotes virtually complete dissolution of AgNPs (Elzey and Grassian 2010). The samples were stored acidified at least six hours at 4˚C. Ag concentration was analyzed using a Varian 710 (Aglient) inductively coupled plasma-optical emission spectroscopy (ICP-OES) with 1 μg/L Ag instrument detection limit.

4.3. Results and Discussion

During the first 25 pore volumes of the filtration, the breakthrough curve was rapidly developed and approached a steady-state value, indicating the AgNPs removal was consistent. As soon as AgNP injection was stopped and the rinsing period started at 25 pore volumes, the relative concentration of AgNPs started to drop to zero approaching another steady-state. In this period, it was considered that the uncaptured AgNPs were flushed out of the filter.

Effect of ionic strength and ion type. Figure 4.4 shows the effect of ionic strength and ion type on the granular media filtration of citrate AgNPs. As shown in parts (a) and (b) of the figure, increasing the ionic strength as $Ca(NO_3)_2$ or $NaNO_3$ resulted in higher attachment between AgNPs and filter media, caused by the decreasing

electrostatic repulsive forces by reducing the thickness of the diffuse layer surrounding the AgNPs. Note that dramatic difference in the effect of changing ionic strength in these citrate experiments than in the BPEI experiments shown in Chapter 3; for BPEI substantial changes in $NaNO_3$ concentration made little or no difference (Figure 3.8c), but for citrate capped AgNPs, the difference was dramatic (Figure 4.4b). As explained in Chapter 3, removal of particles was essentially independent of the solution conditions in the BPEI experiments because of the favorable electrostatic interaction between the positively charged AgNPs and the negatively charged media surface. For these citrate capped AgNPs, both the particles and the media were negative, so that the solution conditions became important.

Figure 4.4(c) indicates the attachment of AgNPs surrounded by $Ca(NO_3)_2$ or $Mg(NO_3)_2$ was dramatically enhanced in comparison to those with $NaNO_3$ at the same ionic strength (10 mM). This difference is considered to be a result of Ca-citrate or Mg-citrate complexation. Since Ca and Mg ions have higher affinity to citrate than Na ion (Walser 1961) and the adsorption of positively charged ions such as Ca^{2+} and Mg^{2+} onto the particle surface leads to charge neutralization, Ca- or Mg-citrate complex reduces the electrostatic repulsion. Also, the dissociation constants calculated at pH 7 indicate slightly stronger complex with Mg^{2+} than Ca^{2+} (Equations 4-6, 4-7, and 4-8), and the results in Figure 4.4(c) indicate better destabilization by Mg^{2+} than by Ca^{2+}.

$$NaC_6H_5O_8^{2-} \rightarrow Na^+ + C_6H_5O_8^{3-} \quad K_{NaC_6H_5O_8^{2-}} = 7.58 \times 10^{-2} \quad (4\text{-}6)$$

$$CaC_6H_5O_8^{2-} \rightarrow Ca^{2+} + C_6H_5O_8^{3-} \quad K_{CaC_6H_5O_8^{2-}} = 4.67 \times 10^{-5} \quad (4\text{-}7)$$

$$MgC_6H_5O_8^{2-} \rightarrow Mg^{2+} + C_6H_5O_8^{3-} \quad K_{MgC_6H_5O_8^{2-}} = 4.46 \times 10^{-5} \quad (4\text{-}8)$$
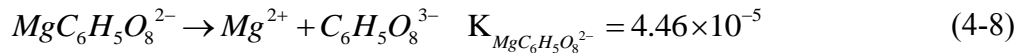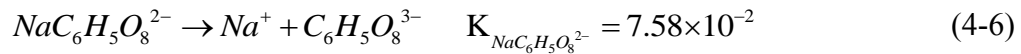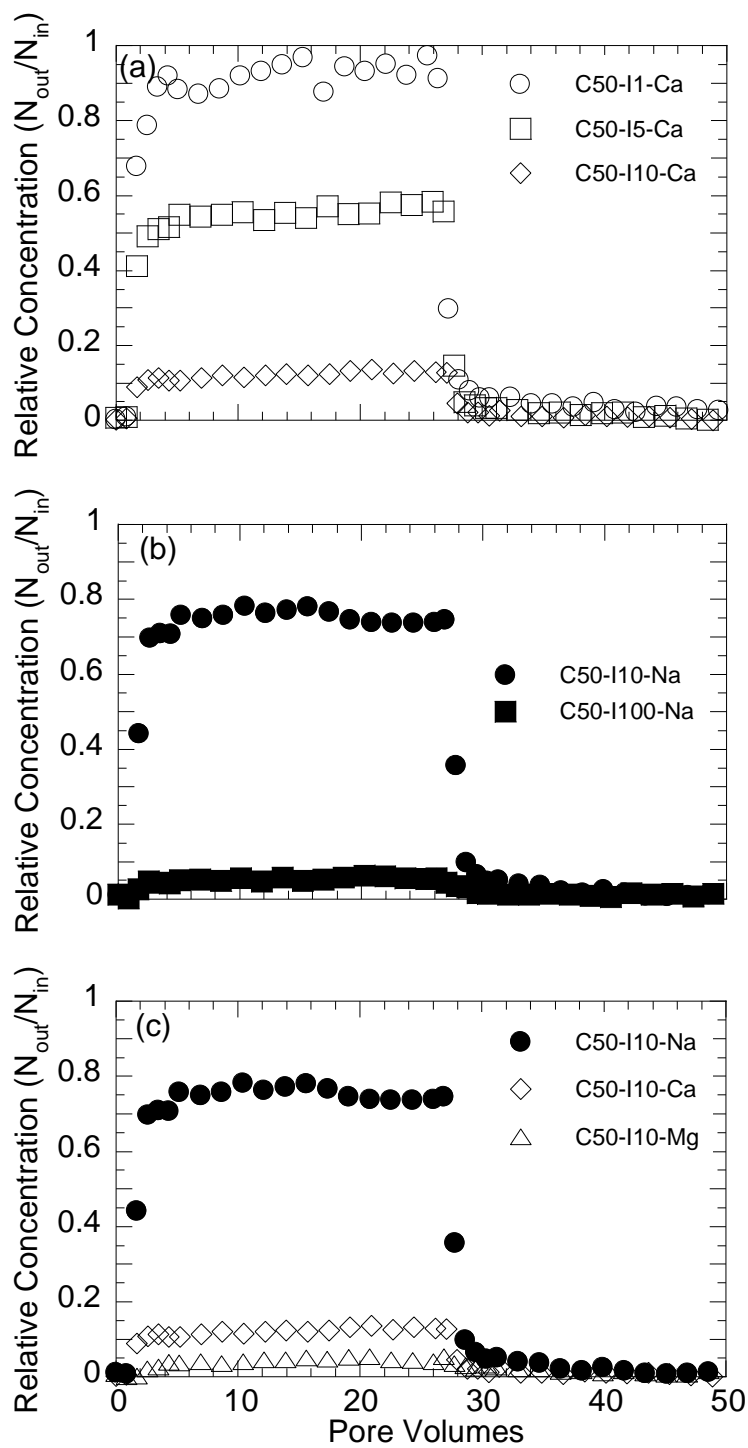
Figure 4.4: Breakthrough curves of citrate AgNPs with different (a) ionic strength of Ca(NO$_3$)$_2$, (b) ionic strength of NaNO$_3$ and (c) ion type (at pH 7).

The different levels of citrate AgNP deposition is clearly shown in terms of attachment efficiency (α) which was calculated by the following equation (Tufenkji and Elimelech 2004).

$$\alpha = -\frac{2}{3}\frac{d_c}{(1-\varepsilon)L\eta_0}\ln\left(\frac{C}{C_0}\right) \tag{4-9}$$

where d_c: Filter media diameter (cm)

ε: Porosity

L: Filter depth (cm)

η_0: Contact efficiency (Tufenkji and Elimelech 2004)

Figure 4.5 shows the attachment efficiency (α) calculated from each test condition. Because all physical conditions and the particles themselves were identical in this set of experiments, the α value qualitatively followed the inverse of the fraction remaining in the breakthrough curves. This result also demonstrates the significant attachment caused by ionic strength increase or greater complexation of the citrate-capped surface by the background ions. However, the experimental conditions in this study were not sufficient to reach α=1, which represents favorable attachment (no electrostatic repulsion). α can be an indicator to compare the overall attachment degree among different test conditions. However, this calculation is based on the equal deposition rate throughout a full filter since the contact efficiency is assumed to be the same throughout the filter bed. Therefore, it is desirable to examine the retention profile whether the deposition rate is different at different filter depths.

86
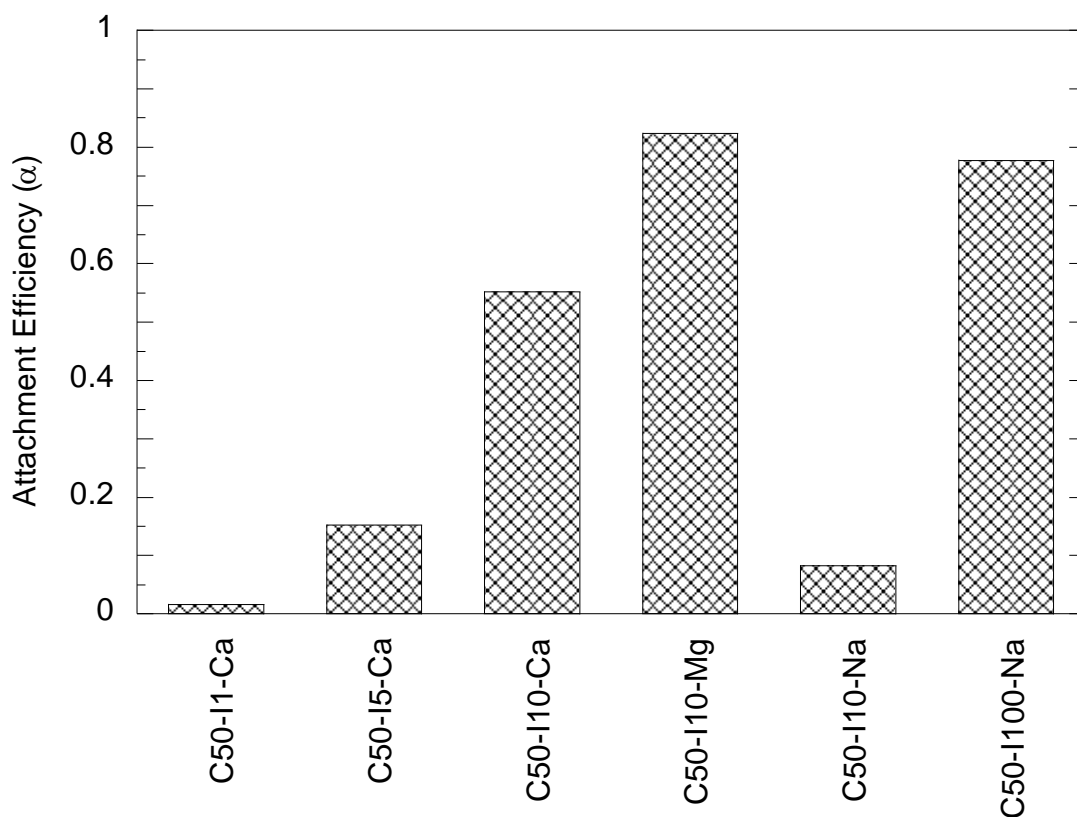
Figure 4.5:   Attachment efficiency of citrate AgNPs according to different ionic strength and ion types.

Retention profile. In the tests with citrate AgNPs at I=1 mM Ca(NO$_3$)$_2$ or I=10 mM NaNO$_3$, a nearly vertical line was obtained for the retention profile (Figure 4.6), indicating that the attachment occurred evenly throughout the filter depth. This result suggests that AgNPs can travel through the pore spaces and deposit onto any filter media. For particles greater than nano-scale, it is generally found that the upper filter bed can attract more particles because the particle concentration in the suspension decreases with depth. However, AgNPs seem to be distributed fairly equally throughout the filter, perhaps due to their tiny size and vigorous (Brownian) movement which enable AgNPs to move everywhere and even to the primary energy minimum. On the other hand, since

AgNP deposition onto the filter media is more likely to happen at higher ionic strength such as I=10 mM Ca(NO$_3$)$_2$, those with the hyperexponential curve are considered to have ripening at the top of the filter bed, resulting in a possible AgNP aggregation on the filter media surface; that is, AgNPs that were captured early in the filter run helped to capture more particles later in the run.
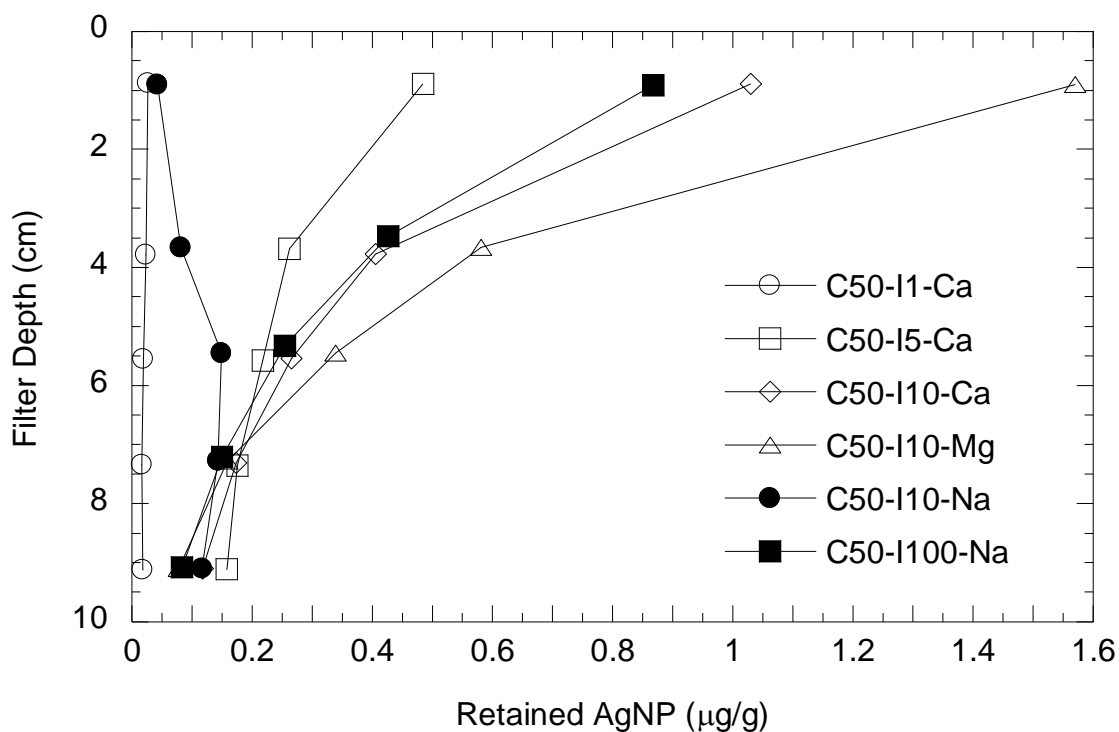
Figure 4.6:   Retention profile of citrate AgNPs after filtration test.

Mass balance. Figure 4.7 shows the portion of attached, not attached, and lost citrate AgNPs by mass. More than 90% of the injected AgNP was recovered in all tests. This result indicates that the simplified analytical method (AgNP dissolution in 3% nitric acid) was successful to analyze the dissolved AgNPs using ICP-OES with a low AgNP concentration.
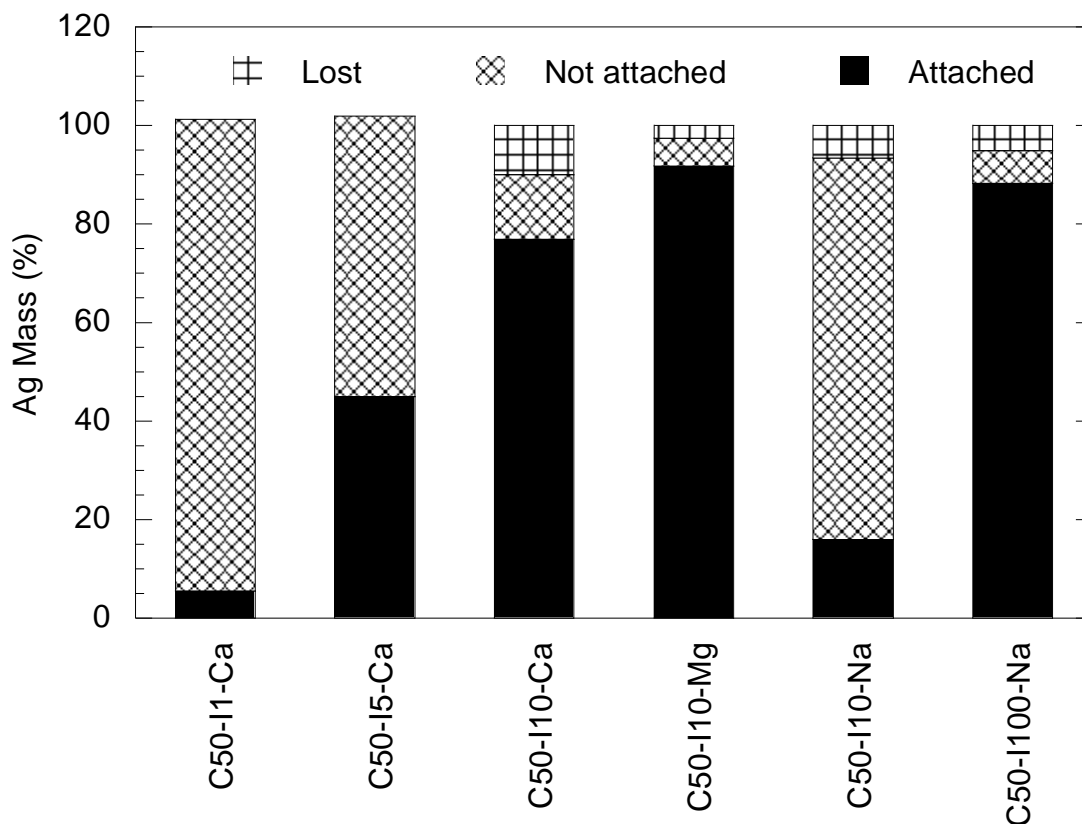
Figure 4.7:   Mass balance of citrate AgNPs in the filtration tests.

Electrostatic interactions. The surface charges of citrate AgNPs and glass beads at different ionic strengths and ion types (Figure 4.8) were employed to investigate electrostatic interaction. In the neutral pH range (pH 7) at which the filtration tests were conducted, the greatest (negative) surface charge was shown with Na ion at I=10 mM, while the surface charge with Ca or Mg ion was less negative. This result supports the idea that more complexation of citrate occurred with Mg and Ca ions than with Na ions in this study. In addition, the surface charge of citrate AgNPs with Ca ions was almost identical regardless of ionic strength, suggesting that the surface potential of citrate

89

AgNPs was neutralized even at the lowest ionic strength. According to DLVO theory, the double layer thickness is the same for monovalent and divalent ions at the same ionic strength. Overall, the magnitude of the negative surface potential value was greater for glass beads than for citrate AgNPs, which could be additional evidence of charge neutralization by Ca-citrate complexation. Interestingly, the surface charge of glass beads with I=10 mM of $NaNO_3$ was substantially more negative compared to other conditions. Considering the fact that there was no citrate on the surface of glass beads, the charge neutralization of glass beads occurred differently from that of citrate AgNPs. It is considered that negatively charged glass beads would interact with cations such as Ca^{2+}, Mg^{2+}, and Na^+. Therefore, the level of neutralization could depend on the concentration and the valence of cations in background solution. Also, since the surface charge was calculated from the zeta potential measured by DLS, the suppressed double layer by Ca^{2+}, Mg^{2+}, or high concentration of Na^+ might exhibit higher surface potential compared to less suppressed one.

In terms of the calculated height of energy barrier (Figure 4.9), the case with I=10 mM of $NaNO_3$ was supposed to yield the least attachment. However, the AgNP removal was the least with I=1 mM $Ca(NO_3)_2$, a condition which was calculated to have a lower but wider energy barrier. It is plausible that electrostatic repulsion could be interpreted by not only the height but also the width of the energy barrier.
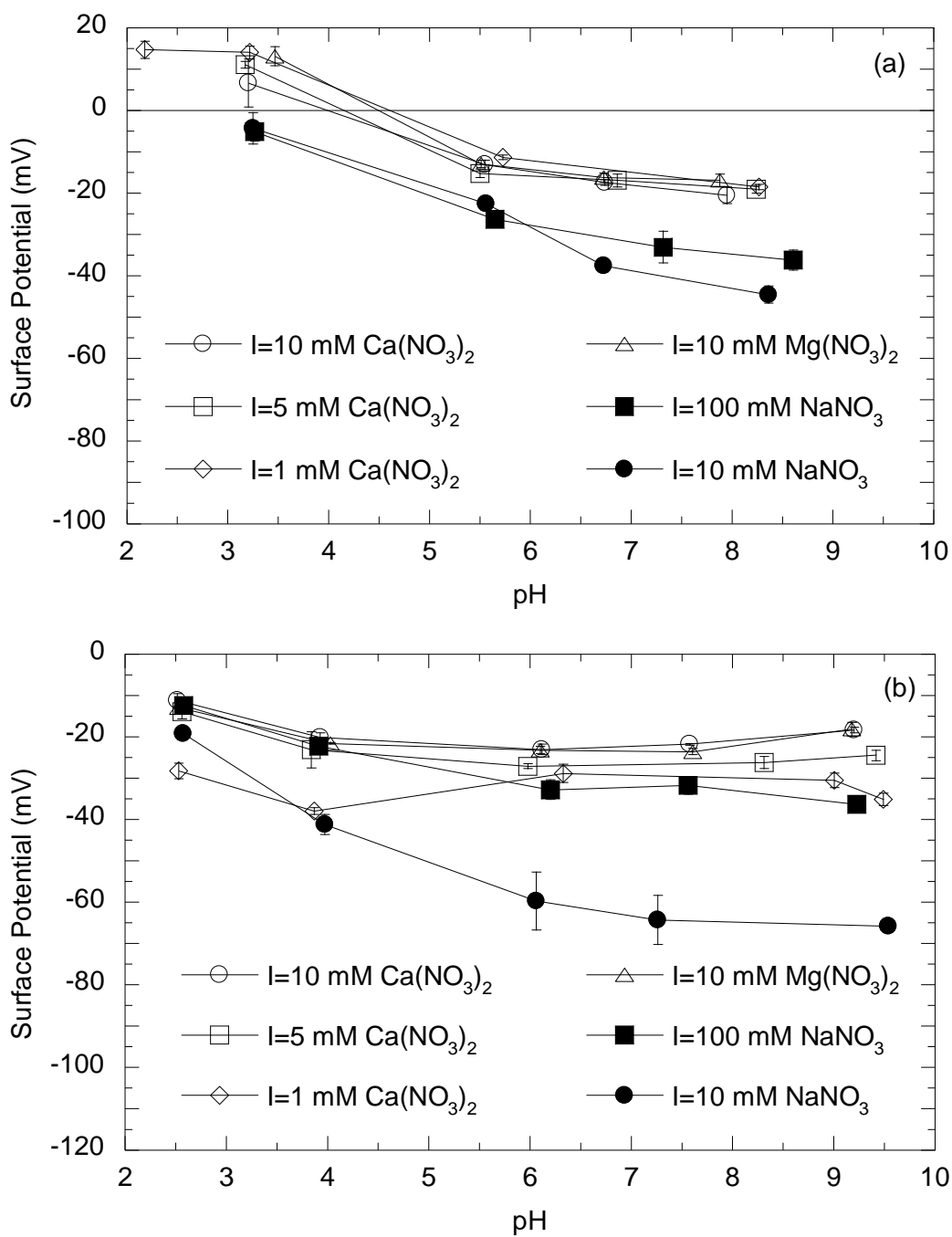
Figure 4.8: Surface potentials of (a) citrate AgNPs and (b) glass beads at different ionic strengths and ion types.
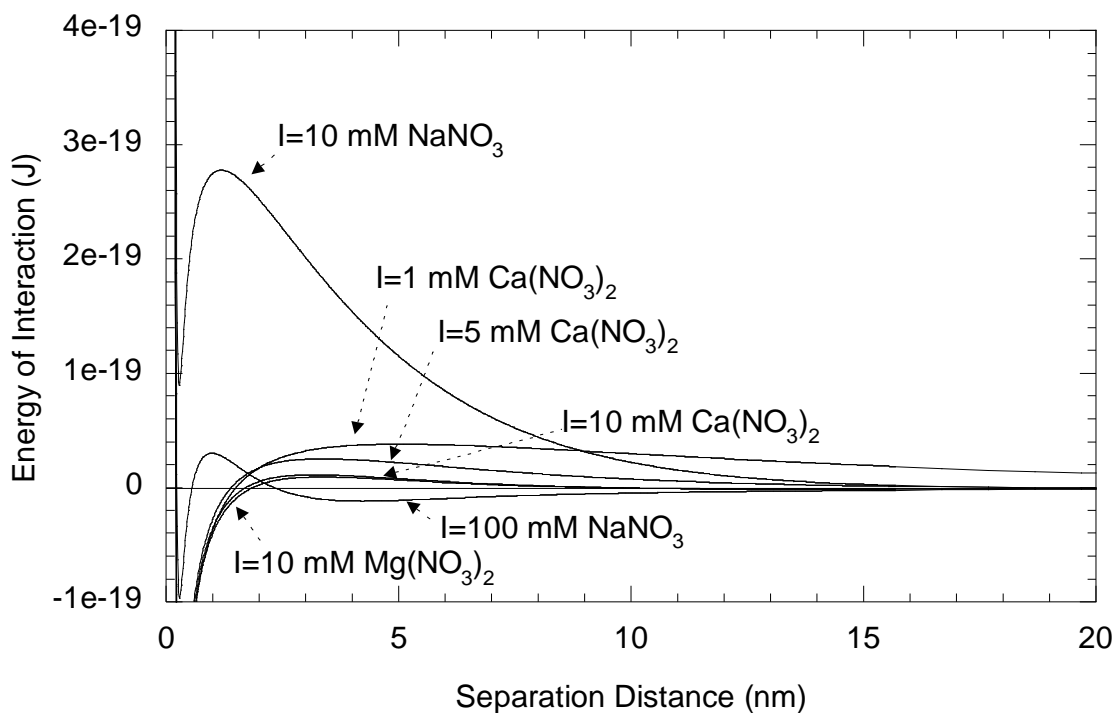
Figure 4.9:   Energy of interaction between citrate AgNPs and filter media (pH=7).

PVP capped AgNPs. With PVP AgNPs, the impact of electrostatic interaction was minimal (Figure 4.10), with nearly identical breakthrough curves regardless of ionic strength and ion type. The change of electric charge and the associated effect on double layer was insignificant with PVP coating in the tested range of ionic strength. Also, the tailing effect in the rinsing period (especially 30-40 pore volumes) was obvious suggesting detachment or re-entrainment of the loosely captured AgNPs; note that the decline to near zero concentration in this period was much slower than in the citrate experiments (Figure 4.4).

These results support the idea that PVP is a steric stabilizer while citrate is an electrostatic stabilizer (Tejamaya et al. 2012). Although both citrate and PVP can be adsorbed on AgNPs as ligands (Sun and Xia 2002, Wagener et al. 2012), PVP can be

strongly bound to AgNPs via hydrogen bonds (Malynych et al. 2002). Also, PVP is a macromolecule with aromaticity which can yield greater steric effect (Gondikas et al. 2012) in comparison to the smaller, lower molecular weight citrate. The molecular weight of PVP as a AgNP capping agent could be as high as 40,000 g/mol (Song et al. 2014), whereas the molecular weight of citrate is 192 g/mol.
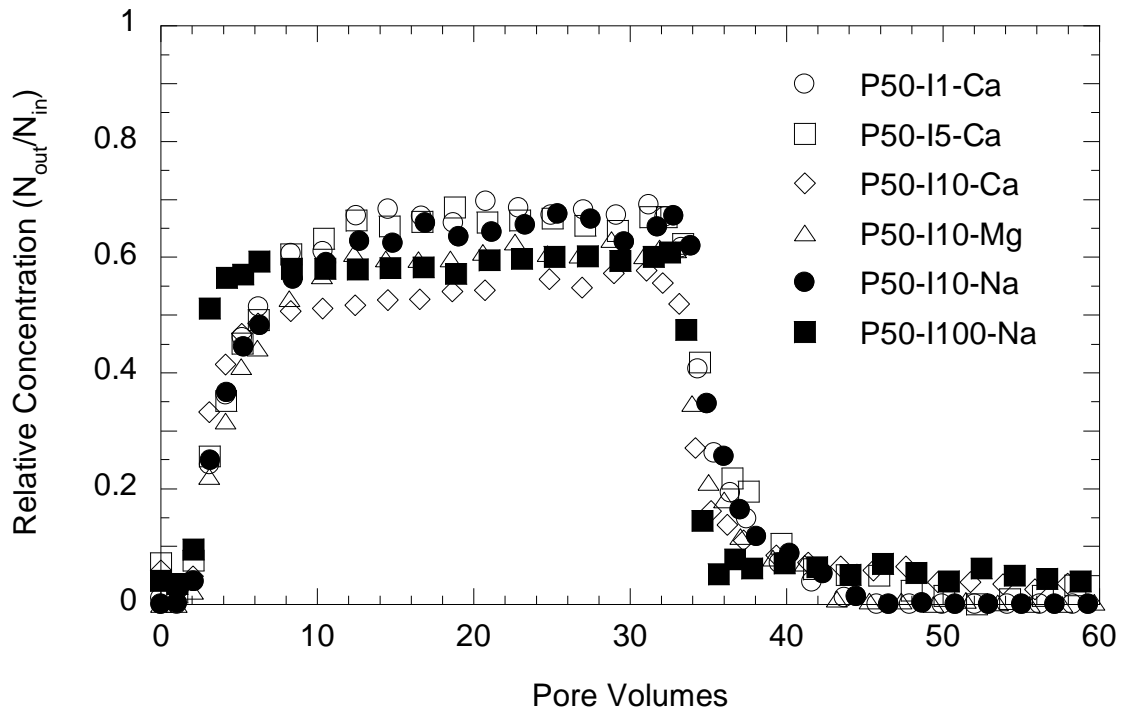
Figure 4.10: Breakthrough curves of PVP AgNPs with different ionic strength and ion type (at pH 7).

4.4. Conclusions

A low AgNP concentration was successfully applied to study the attachment of AgNPs in granular media filtration. The removal of the citrate-capped AgNPs varied

significantly depending on the ionic strength and/or ion type, while the removal of PVP-capped AgNPs showed very little variation. This result means that, during the design of new technologies incorporating AgNPs, the capping agent might play a large role in determining the environmental fate of AgNPs.

Ca or Mg ions lowered the energy barrier by complexation with citrate which caused charge neutralization, probably allowing more citrate AgNPs to approach the primary energy minimum. However, a low but, wide repulsive energy barrier could yield a force sufficient to prevent the deposition. In the tests that showed the even distribution of the remaining AgNPs throughout the filter depth, AgNP aggregation was unlikely to occur and the filter was expected to be fully contacted by AgNPs. This result suggests that one of the limiting factors for nanoparticle transport would be the environmental conditions that cause the aggregation of nanoparticles.

Further chemical parameters such as natural organic matter or physical parameters such as filtration velocity would be worth studying to elucidate their role in the transport of nanoparticles in granular media filtration.

References

Anandarajah, A. and Chen, J. (1995) Single correction function for computing retarded van der Waals attraction. Journal of Colloid and Interface Science 176(2), 293-300.

Boyd, R.D., Pichaimuthu, S.K. and Cuenat, A. (2011) New approach to inter-technique comparisons for nanoparticle size measurements; using atomic force microscopy, nanoparticle tracking analysis and dynamic light scattering. Colloids and Surfaces A: Physicochemical and Engineering Aspects 387(1), 35-42.

Bradford, S.A., Torkzaban, S. and Walker, S.L. (2007) Coupling of physical and chemical mechanisms of colloid straining in saturated porous media. Water Research 41(13), 3012-3024.

Choi, O. and Hu, Z.Q. (2008) Size dependent and reactive oxygen species related nanosilver toxicity to nitrifying bacteria. Environmental Science & Technology 42(12), 4583-4588.

Chowdhury, I., Hong, Y., Honda, R.J. and Walker, S.L. (2011) Mechanisms of TiO_2 nanoparticle transport in porous media: Role of solution chemistry, nanoparticle concentration, and flowrate. Journal of Colloid and Interface Science 360(2), 548-555.

Domingos, R.F., Baalousha, M.A., Ju-Nam, Y., Reid, M.M., Tufenkji, N., Lead, J.R., Leppard, G.G. and Wilkinson, K.J. (2009) Characterizing manufactured nanoparticles in the environment: multimethod determination of particle sizes. Environmental Science & Technology 43(19), 7277-7284.

El Badawy, A.M., Hassan, A.A., Scheckel, K.G., Suidan, M.T. and Tolaymat, T.M. (2013) Key factors controlling the transport of silver nanoparticles in porous media. Environmental Science & Technology 47(9), 4039-4045.

Elimelech, M., Jia, X., Gregory, J. and Williams, R. (1998) Particle deposition & aggregation: Measurement, Modeling and Simulation, Butterworth-Heinemann.

Elzey, S. and Grassian, V.H. (2010) Agglomeration, isolation and dissolution of commercially manufactured silver nanoparticles in aqueous environments. Journal of Nanoparticle Research 12(5), 1945-1958.

Espinasse, B., Hotze, E.M. and Wiesner, M.R. (2007) Transport and retention of colloidal aggregates of C_{60} in porous media: Effects of organic macromolecules, ionic composition, and preparation method. Environmental Science & Technology 41(21), 7396-7402.

Fabrega, J., Luoma, S.N., Tyler, C.R., Galloway, T.S. and Lead, J.R. (2011) Silver nanoparticles: Behaviour and effects in the aquatic environment. Environment International 37(2), 517-531.

Gondikas, A.P., Morris, A., Reinsch, B.C., Marinakos, S.M., Lowry, G.V. and Hsu-Kim, H. (2012) Cysteine-induced modifications of zero-valent silver nanomaterials: implications for particle surface chemistry, aggregation, dissolution, and silver speciation. Environmental Science & Technology 46(13), 7037-7045.

Gottschalk, F., Sonderer, T., Scholz, R.W. and Nowack, B. (2009) Modeled environmental concentrations of engineered nanomaterials (TiO_2, ZnO, Ag, CNT, fullerenes) for different regions. Environmental Science & Technology 43(24), 9216-9222.

Griffitt, R.J., Luo, J., Gao, J., Bonzongo, J.C. and Barber, D.S. (2008) Effects of particle composition and species on toxicity of metallic nanomaterials in aquatic organisms. Environmental Toxicology and Chemistry 27(9), 1972-1978.

Guzman, K.A.D., Finnegan, M.P. and Banfield, J.F. (2006) Influence of surface potential on aggregation and transport of titania nanoparticles. Environmental Science & Technology 40(24), 7688-7693.

Hunter, R.J. (1981) Zeta potential in colloid science, Academic Press, New York.

Jaisi, D.P., Saleh, N.B., Blake, R.E. and Elimelech, M. (2008) Transport of single-walled carbon nanotubes in porous media: Filtration mechanisms and reversibility. Environmental Science & Technology 42(22), 8317-8323.

Jones, E.H. and Su, C.M. (2012) Fate and transport of elemental copper (Cu-0) nanoparticles through saturated porous media in the presence of organic materials. Water Research 46(7), 2445-2456.

Joo, S.H., Al-Abed, S.R. and Luxton, T. (2009) Influence of carboxymethyl cellulose for the transport of titanium dioxide nanoparticles in clean silica and mineral-coated sands. Environmental Science & Technology 43(13), 4954-4959.

Kaegi, R., Voegelin, A., Sinnet, B., Zuleeg, S., Hagendorfer, H., Burkhardt, M. and Siegrist, H. (2011) Behavior of metallic silver nanoparticles in a pilot wastewater treatment plant. Environmental Science & Technology 45(9), 3902-3908.

Kim, B., Park, C.S., Murayama, M. and Hochella, M.F. (2010) Discovery and characterization of silver sulfide nanoparticles in final sewage sludge products. Environmental Science & Technology 44(19), 7509-7514.

Laban, G., Nies, L.F., Turco, R.F., Bickham, J.W. and Sepulveda, M.S. (2010) The effects of silver nanoparticles on fathead minnow (*Pimephales promelas*) embryos. Ecotoxicology 19(1), 185-195.

Lecoanet, H.F. and Wiesner, M.R. (2004) Velocity effects on fullerene and oxide nanoparticle deposition in porous media. Environmental Science & Technology 38(16), 4377-4382.

Levard, C., Reinsch, B.C., Michel, F.M., Oumahi, C., Lowry, G.V. and Brown, G.E. (2011) Sulfidation processes of PVP-coated silver nanoparticles in aqueous solution: impact on dissolution rate. Environmental Science & Technology 45(12), 5260-5266.

Li, X. and Lenhart, J.J. (2012) Aggregation and dissolution of silver nanoparticles in natural surface water. Environmental Science & Technology 46(10), 5378-5386.

Liang, Y., Bradford, S.A., Simunek, J., Vereecken, H. and Klumpp, E. (2013b) Sensitivity of the transport and retention of stabilized silver nanoparticles to physicochemical factors. Water Research 47(7), 2572-2582.

Lin, S.H., Cheng, Y.W., Bobcombe, Y., Jones, K.L., Liu, J. and Wiesner, M.R. (2011) Deposition of silver nanoparticles in geochemically heterogeneous porous media: Predicting affinity from surface composition analysis. Environmental Science & Technology 45(12), 5209-5215.

Lin, S.H., Cheng, Y.W., Liu, J. and Wiesner, M.R. (2012) Polymeric coatings on silver nanoparticles hinder autoaggregation but enhance attachment to uncoated surfaces. Langmuir 28(9), 4178-4186.

Liu, J.Y. and Hurt, R.H. (2010) Ion release kinetics and particle persistence in aqueous nano-silver colloids. Environmental Science & Technology 44(6), 2169-2175.

Liu, X.Y., O'Carroll, D.M., Petersen, E.J., Huang, Q.G. and Anderson, C.L. (2009a) Mobility of multiwalled carbon nanotubes in porous media. Environmental Science & Technology 43(21), 8153-8158.

Lowry, G.V., Espinasse, B.P., Badireddy, A.R., Richardson, C.J., Reinsch, B.C., Bryant, L.D., Bone, A.J., Deonarine, A., Chae, S., Therezien, M., Colman, B.P., Hsu-Kim, H., Bernhardt, E.S., Matson, C.W. and Wiesner, M.R. (2012) Long-term transformation and fate of manufactured Ag nanoparticles in a simulated large scale freshwater emergent wetland. Environmental Science & Technology 46(13), 7027-7036.

Malynych, S., Luzinov, I. and Chumanov, G. (2002) Poly(vinyl pyridine) as a universal surface modifier for immobilization of nanoparticles. Journal of Physical Chemistry B 106(6), 1280-1285.

Panyala, N.R., Pena-Mendez, E.M. and Havel, J. (2008) Silver or silver nanoparticles: a hazardous threat to the environment and human health? Journal of Applied Biomedicine 6(3), 117-129.

Petosa, A.R., Jaisi, D.P., Quevedo, I.R., Elimelech, M. and Tufenkji, N. (2010) Aggregation and deposition of engineered nanomaterials in aquatic environments: Role of physicochemical interactions. Environmental Science & Technology 44(17), 6532-6549.

Petosa, A.R., Brennan, S.J., Rajput, F. and Tufenkji, N. (2012) Transport of two metal oxide nanoparticles in saturated granular porous media: Role of water chemistry and particle coating. Water Research 46(4), 1273-1285.

Phenrat, T., Kim, H.J., Fagerlund, F., Illangasekare, T., Tilton, R.D. and Lowry, G.V. (2009) Particle size distribution, concentration, and magnetic attraction affect transport of polymer-modified Fe-0 nanoparticles in sand columns. Environmental Science & Technology 43(13), 5079-5085.

Rejeski, D., Kulken, T., Pollschuk, P. and Pauwels, E. (2014) The project on emerging nanotechnologies.

Sagee, O., Dror, I. and Berkowitz, B. (2012) Transport of silver nanoparticles (AgNPs) in soil. Chemosphere 88(5), 670-675.

Saleh, N., Kim, H.J., Phenrat, T., Matyjaszewski, K., Tilton, R.D. and Lowry, G.V. (2008) Ionic strength and composition affect the mobility of surface-modified Fe-0 nanoparticles in water-saturated sand columns. Environmental Science & Technology 42(9), 3349-3355.

Solovitch, N., Labille, J., Rose, J., Chaurand, P., Borschneck, D., Wiesner, M.R. and Bottero, J.Y. (2010) Concurrent aggregation and deposition of TiO_2 nanoparticles in a sandy porous media. Environmental Science & Technology 44(13), 4897-4902.

Song, J.E., Phenrat, T., Marinakos, S., Xiao, Y., Liu, J., Wiesner, M.R., Tilton, R.D. and Lowry, G.V. (2011) Hydrophobic interactions increase attachment of gum arabic- and PVP-coated Ag nanoparticles to hydrophobic surfaces. Environmental Science & Technology 45(14), 5988-5995.

Song, Y.J., Wang, M.L., Zhang, X.Y., Wu, J.Y. and Zhang, T. (2014) Investigation on the role of the molecular weight of polyvinyl pyrrolidone in the shape control of high-yield silver nanospheres and nanowires. Nanoscale Research Letters 9(1), 17.

Sun, Y.G. and Xia, Y.N. (2002) Shape-controlled synthesis of gold and silver nanoparticles. Science 298(5601), 2176-2179.

Tejamaya, M., Romer, I., Merrifield, R.C. and Lead, J.R. (2012) Stability of citrate, PVP, and PEG coated silver nanoparticles in ecotoxicology media. Environmental Science & Technology 46(13), 7011-7017.

Tian, Y.A., Gao, B., Silvera-Batista, C. and Ziegler, K.J. (2010) Transport of engineered nanoparticles in saturated porous media. Journal of Nanoparticle Research 12(7), 2371-2380.

Tiraferri, A. and Sethi, R. (2009) Enhanced transport of zerovalent iron nanoparticles in saturated porous media by guar gum. Journal of Nanoparticle Research 11(3), 635-645.

Tobiason, J.E. (1987) Physicochemical aspects of particle deposition in porous media, Johns Hopkins University, Baltimore, MD.

Tolaymat, T.M., El Badawy, A.M., Genaidy, A., Scheckel, K.G., Luxton, T.P. and Suidan, M. (2010) An evidence-based environmental perspective of manufactured silver nanoparticle in syntheses and applications: A systematic review and critical appraisal of peer-reviewed scientific papers. Science of the Total Environment 408(5), 999-1006.

Tosco, T., Bosch, J., Meckenstock, R.U. and Sethi, R. (2012) Transport of ferrihydrite nanoparticles in saturated porous media: Role of ionic strength and flow rate. Environmental Science & Technology 46(7), 4008-4015.

Tufenkji, N. and Elimelech, M. (2004) Correlation equation for predicting single-collector efficiency in physicochemical filtration in saturated porous media. Environmental Science & Technology 38(2), 529-536.

Vanoss, C.J., Giese, R.F. and Costanzo, P.M. (1990) DLVO and Non-DLVO interactions in hectorite. Clays and Clay Minerals 38(2), 151-159.

Wagener, P., Schwenke, A. and Barcikowski, S. (2012) How citrate ligands affect nanoparticle adsorption to microparticle supports. Langmuir 28(14), 6132-6140.

Walser, M. (1961) Ion association .5. Dissociation constants for complexes of citrate with sodium, potassium, calcium, and magnesium ions. Journal of Physical Chemistry 65(1), 159-161.

Wang, C., Bobba, A.D., Attinti, R., Shen, C.Y., Lazouskaya, V., Wang, L.P. and Jin, Y. (2012a) Retention and transport of silica nanoparticles in saturated porous media: Effect of concentration and particle size. Environmental Science & Technology 46(13), 7151-7158.

Wang, Y.G., Li, Y.S., Fortner, J.D., Hughes, J.B., Abriola, L.M. and Pennell, K.D. (2008b) Transport and retention of nanoscale C_{60} aggregates in water-saturated porous media. Environmental Science & Technology 42(10), 3588-3594.

Wen, L.S., Santschi, P.H., Gill, G.A. and Tang, D.G. (2002) Silver concentrations in Colorado, USA, watersheds using improved methodology. Environmental Toxicology and Chemistry 21(10), 2040-2051.

Wood, C.M., Playle, R.C. and Hogstrand, C. (1999) Physiology and modeling of mechanisms of silver uptake and toxicity in fish. Environmental Toxicology and Chemistry 18(1), 71-83.

Chapter 5: EFFECT OF NATURAL ORGANIC MATTER ON ATTACHMENT OF NANOPARTICLES

Abstract

Natural organic matter (NOM) is ubiquitous and likely to coat the surface of nanoparticles in natural and engineered systems, affecting the fate and transport of nanoparticles. The aim of this study was to investigate the effect of NOM coating on the attachment of citrate or PVP capped silver nanoparticles (AgNPs) in granular media filtration. Attachment of the AgNPs in the presence or absence of NOM was examined with I=10 mM of $Ca(NO_3)_2$ at pH 7 or 9. Suwannee River Humic and Fulvic acids were chosen as representative examples of NOM. When AgNPs were coated by NOM, there was no significant aggregation of the AgNPs, as indicated by the lack of change in the particle size distribution. The surface charge of the NOM-coated AgNPs showed more negativity, indicating the adsorption of NOM and increasing the electrostatic repulsion of particle-particle and particle-media interactions. However, the addition of Ca ions (I=10 mM) neutralized the surface charge at both pH values tested, eliminating the added electrostatic repulsion by NOM coating. Consequently, steric effects were considered as the sole reason for limited AgNP deposition with NOMs. When the AgNPs were coated with NOM, the surface charge of AgNPs was similar regardless of the original capping agent, implying the assimilated surface property by NOM coating. Overall, the deposition of the NOM-coated AgNPs was limited compared to the AgNPs without NOM. Nevertheless, the deposition of citrate AgNP was less with humic acid than fulvic acid, probably due to the greater molecular weight of humic acid. Thus, greater molecular weight of NOM can lead to a greater steric effect by keeping a greater distance between AgNPs and filter media.

Keywords

Natural organic matter, silver nanoparticles, steric effect, granular media filtration

5.1. Introduction

Natural organic matter (NOM) is ubiquitous in the environment, with sources that are considered to be unlimited. Various sources of NOM have been studied for their impact on the fate and transport of pollutants in the environment and on their removal in engineered treatment systems. The NOM concentration (measured in terms of organic carbon) is generally higher in surface water than in groundwater, but it occurs in both. NOM is known to be a precursor of trihalomethanes (THMs), haloacetic acids (HAAs), and other disinfection by-products (DBPs) in drinking water treatment when a chlorine-based disinfectant is used. Many researchers have investigated the fate and role of NOM in drinking water treatment processes such as coagulation (Sharp et al. 2006) and membrane filtration (Zularisam et al. 2006). Also, NOM is often removed from the water sources to prevent the formation of harmful byproducts (Edzwald and Tobiason 1999, Roalson et al. 2003, Siddiqui et al. 1997).

The interaction between NOM and a wide variety of pollutants seems inevitable in the environment. When it comes to particulate pollutants, NOM normally coats and stabilizes the particles, resulting in less removal efficiency in the water treatment process. Once nanoparticles are coated with NOM, they can persist longer in the water environment. Although a substantial amount of research has been done to understand the transport of nanoparticles in porous media emulating groundwater flow, few have been done in the presence of NOM. In addition, little is known about the interaction between different NOM types and surface coatings of nanoparticles. Therefore, it is necessary to

study the transport of NOM-coated nanoparticles with a combination of different sources of NOM and surface coatings of nanoparticles.

A common process in drinking water treatment is granular media filtration. Several studies on transport of nanoparticles in granular media were done at groundwater flow velocities. Assuming the granular media filtration would encounter the NOM-coated nanoparticles, it is desirable to study the transport of the NOM-coated nanoparticles under conditions that are representative of filtration in drinking water treatment.

In this study, two different types of NOM (humic and fulvic acids) and two different silver nanoparticles (citrate and PVP capped AgNPs) were chosen to examine the effect of NOM coating on the transport of AgNPs in granular media filtration. The surface property of AgNPs in the presence or absence of NOM coating was investigated to evaluate the resultant electrostatic effect.

5.2. Materials and Methods

Citrate and PVP capped AgNPs were purchased from NanoComposix (San Diego, CA). Citrate and PVP were chosen because they are among the most commonly used capping agents in AgNPs synthesis (Tolaymat et al. 2010). The spherical particle shape and monodispersed size distribution were confirmed by transmission electron microscopy (TEM, FEI Tencai) and dynamic light scattering (DLS, Malvern) (refer to Section 4.2.1 for the details of the particle size determination). In addition, the particle size distribution was analyzed by nanoparticle tracking analysis (LM 10, Nanosight) in the presence or absence of NOM. The surface charge of the particles was analyzed by dynamic light scattering (DLS, Malvern).

As commonly used reference examples of NOM, Suwannee River Humic and Fulvic Standard II (International Humic Substances Society, MN) were purchased. The carbon content of the NOM samples was quantified by a TOC Analyzer (Aurora 1030, O.I.Analytical). The detailed chemical properties of the NOM sources are available at http://www.humicsubstances.org/elements.html.

Filtration tests were conducted using a cylindrical acrylic column (3.81 cm inner diameter) filled with 10 cm depth of 300~350 µm spherical glass beads (MO-SCI, St. Louis). Background solution of I=10 mM $Ca(NO_3)_2$ was prepared at pH 7 or 9 using bicarbonate or borate buffer, respectively. The AgNP suspension was separately prepared in DI water without ionic strength to prevent any property changes prior to the test. For the filtration tests with NOM, the background solution was prepared with NOM at 3.5 mg TOC/L to emulate surface water. The glass beads were preconditioned by soaking in the NOM-containing background solution for 24 hrs. AgNPs were also mixed with NOM solution (3.5 mg TOC/L in DI water) for 24 hrs. During the 24-hr mixing period, the zeta potential of AgNPs was monitored using DLS to ensure that a steady-state value was obtained, and it was assumed that steady state conditions meant that the adsorption had reached equilibrium. During the filtration test period, the NOM concentration in the filtration effluent was monitored by UV-VIS spectrophotomoter (Agilent Technologies) to examine additional NOM adsorption onto or desorption from the glass beads.

As mentioned in Chapter 4, filtration tests started with flushing the filter bed for 30 pore volumes followed by two steps: 25 pore volumes of filtration with AgNPs and 25 pore volumes of filtration without AgNPs. The sampling and analytical methods were the same as introduced in Chapter 4.

Table 5.1:   Summary of the filtration tests.

Experiment #[a]	Capping agent	NOM coating	pH
C50-I10-Ca	Citrate	No	7
C50-I10-Ca-HA	Citrate	Humic acid	7
C50-I10-Ca-FA	Citrate	Fulvic acid	7
C50-I10-Ca-pH9	Citrate	No	9
C50-I10-Ca-HA-pH9	Citrate	Humic acid	9
P50-I10-Ca-pH9	PVP	No	9
P50-I10-Ca-HA-pH9	PVP	Humic acid	9

[a] C or P refers to citrate or PVP, 50 is for 50 nm size, the I value is the ionic strength (mM), the chemical name is the source of the ionic strength, HA or FA refers to humic acid or fulvic acid coating, and pH9 refers to the cases tested at pH 9.

5.3. Results and Discussion

The NOM coating on AgNPs caused no measurable change in AgNP size. The particle size distribution of AgNPs measured by the Nanosight instrument was almost identical regardless of NOM coating (Figure 5.1) for both types of particles. Although most NOM is considered to be around 1.5 nm in diameter (Lead et al. 2000), the additional layer of NOM coating on the AgNP surface caused no apparent change in the particle size.

105
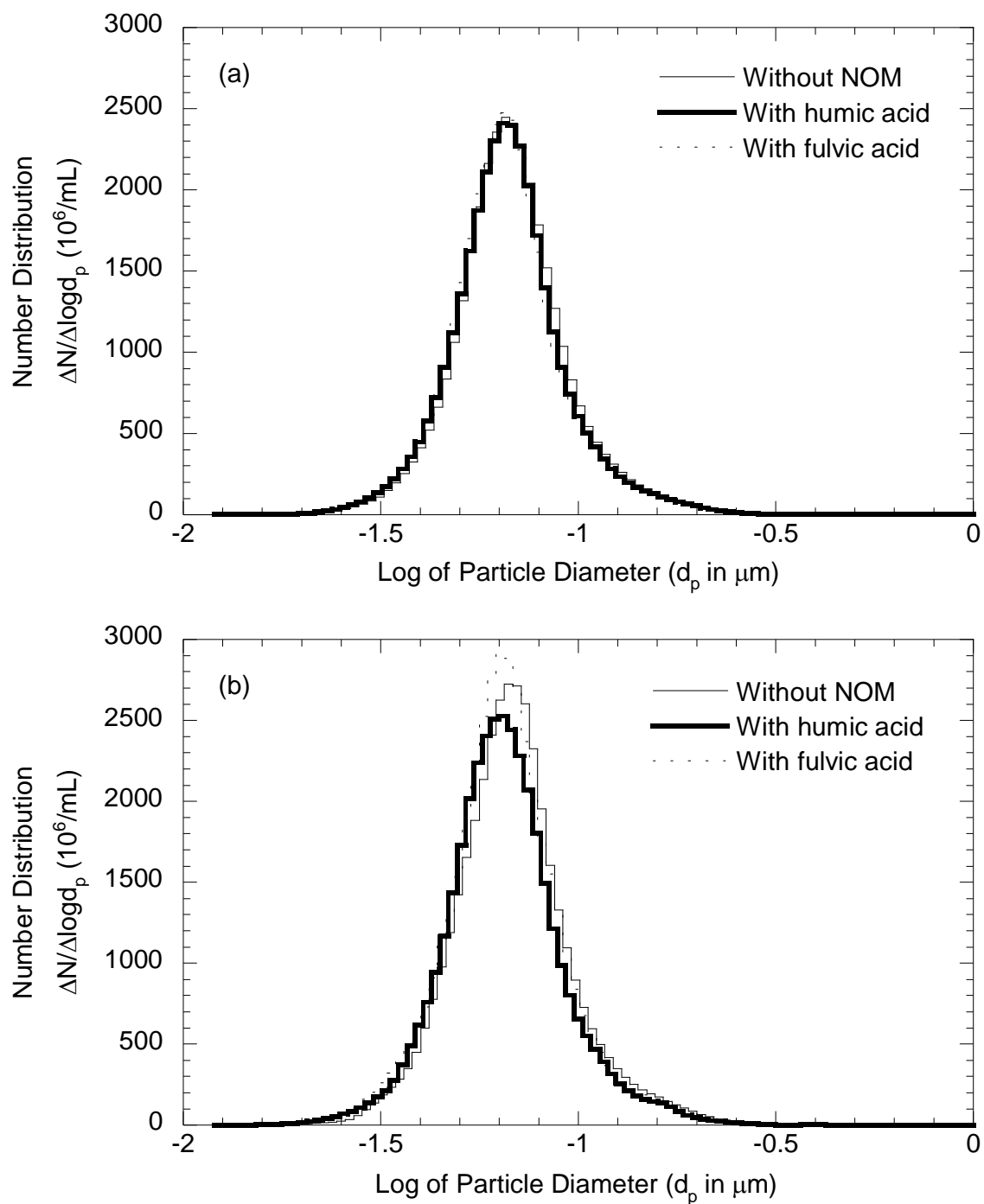
Figure 5.1: Particle size distribution of (a) citrate and (b) PVP AgNPs with and without NOM.

Compared to the case without NOM coating, the surface charge was decreased (i.e., became more negative) with both types of NOM coating (Figure 5.2). Considering intrinsic nature of steric effect provided by NOM coating, this result supports so-called electrosteric effect which has been introduced by many previous investigators (Joo et al. 2009, Phenrat et al. 2009, Saleh et al. 2008, Tiraferri and Sethi 2009). However, the addition of Ca ions (I=10 mM) reduced the magnitude of surface charge to a constant value in the -10~-20 mV range in the entire measured pH range, regardless of the type of capping agent and type of NOM. This constancy might be due to charge neutralization by Ca ions (called a shielding effect by some investigators) which results from the adsorption of Ca ions onto surface carboxylic groups (Yang et al. 2013). The adsorption of Ca ions to citrate is anticipated since citrate contains carboxylic groups; however, it is questionable whether Ca ions can bind with PVP which has no carboxylic group (Figure 5.3). Nevertheless, once AgNPs are coated with either humic acid or fulvic acid, there would be carboxylic groups on the surface (DePaolis and Kukkonen 1997). Consequently, the surface charge control by NOM coating and Ca ions seemed almost identical regardless of the original capping agent. Because the different surface properties by various capping agents on nanoparticles were equalized in the presence of NOM (also found by Stankus et al. 2011), it seems that the NOM coating is potent enough to eliminate or override the original surface property of nanoparticles. Note that the surface potential of citrate AgNPs with Ca ions (I=10 mM) was almost identical regardless of the presence of NOM in neutral pH range. This result indicates that the adsorption of Ca ions onto either citrate or NOM could be similar.
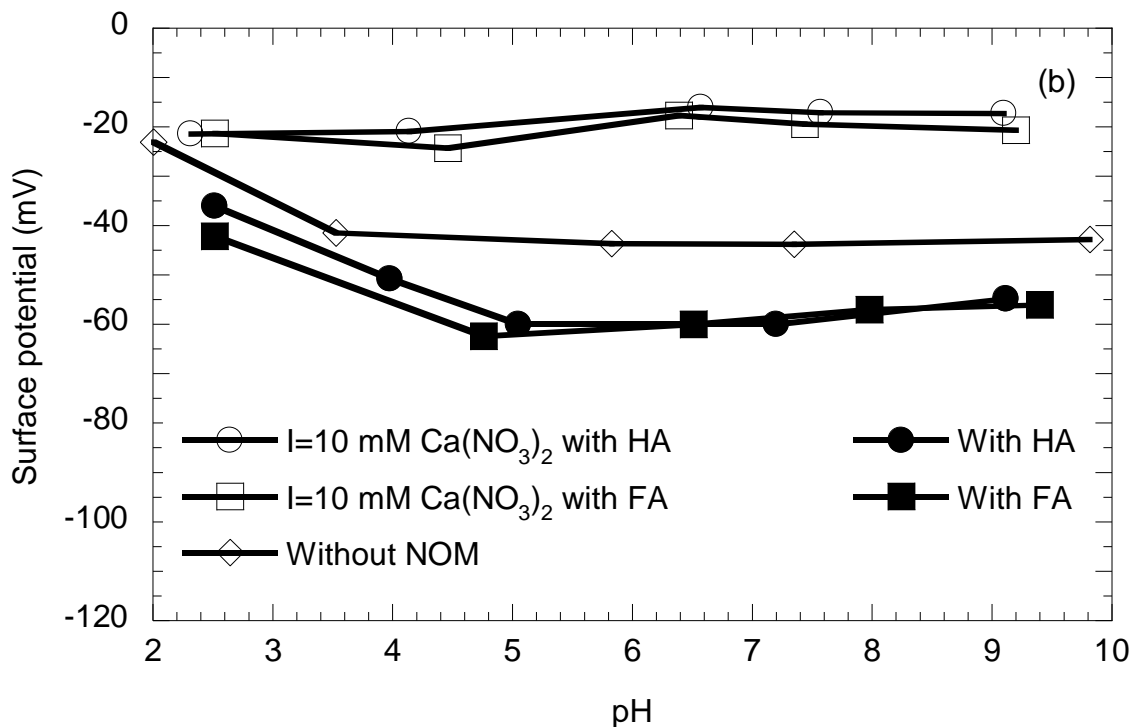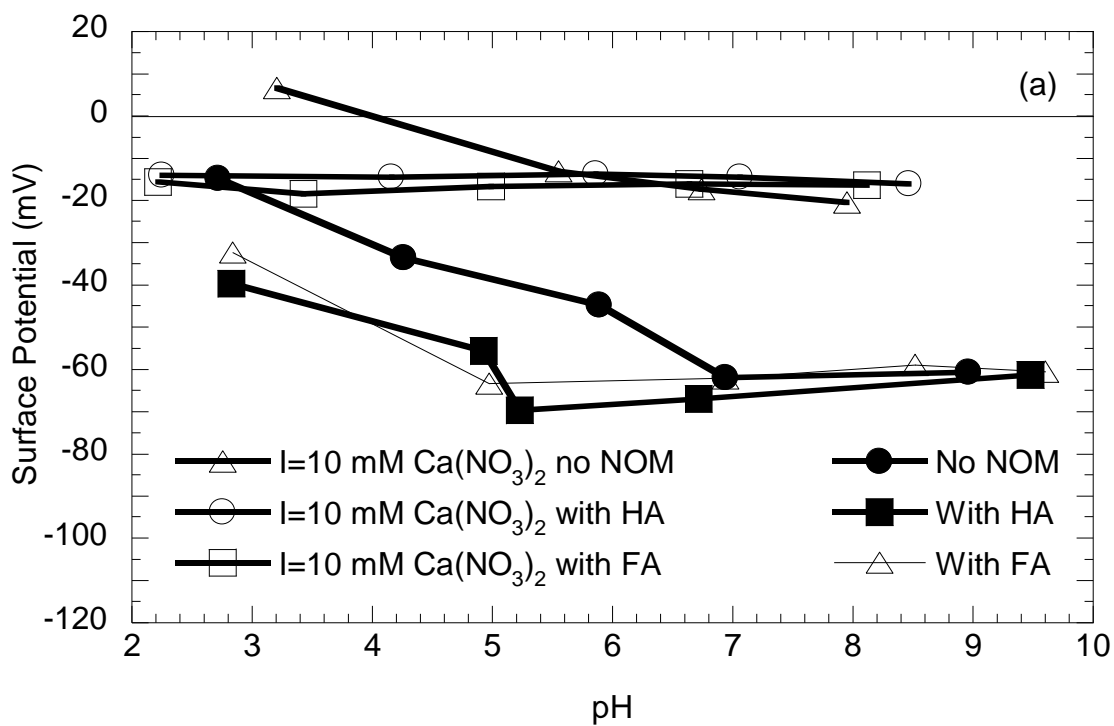
Figure 5.2: Surface potentials of (a) citrate and (b) PVP AgNPs in the presence or absence of NOM.
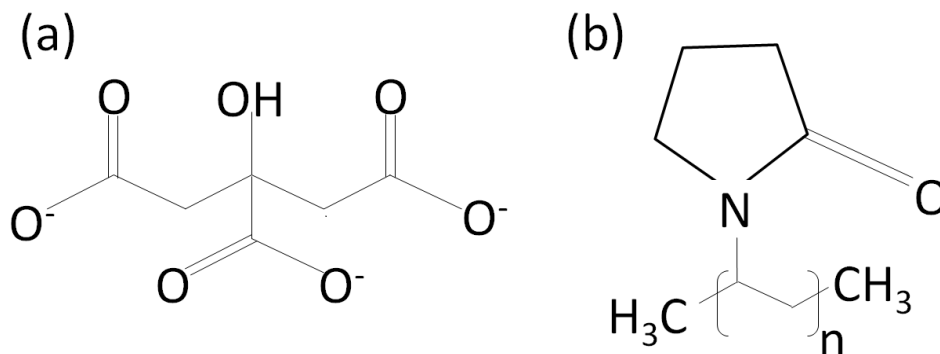
Figure 5.3: Molecular structures of (a) citrate and (b) PVP.

The AgNPs were simply mixed with NOM in DI water for 24 hrs to complete the NOM coating on AgNPs. The surface charge was monitored during the NOM coating process, and it became consistent within a few minutes (Figure 5.4) at a value lower (more negative) than the original surface charge of AgNPs without NOMs. This result implies that the NOM adsorption could be completed quite rapidly. This result supports the idea that the interaction between PVP capped AgNPs and humic acid was instantaneous (Yang et al. 2014), and a rapid interaction with fulvic acid could also be anticipated.

The glass beads were soaked in the background solution containing NOM of 3.5 mg TOC/L for 24 hrs. The complete NOM coating on the glass beads was indirectly assured by monitoring the NOM concentration in the filter effluents. The relative NOM concentration (the ratio of the effluent to influent NOM concentration) was very nearly 1.0 during the AgNP injection period (not shown), implying a complete NOM coating without additional adsorption or desorption of NOM from the glass beads.
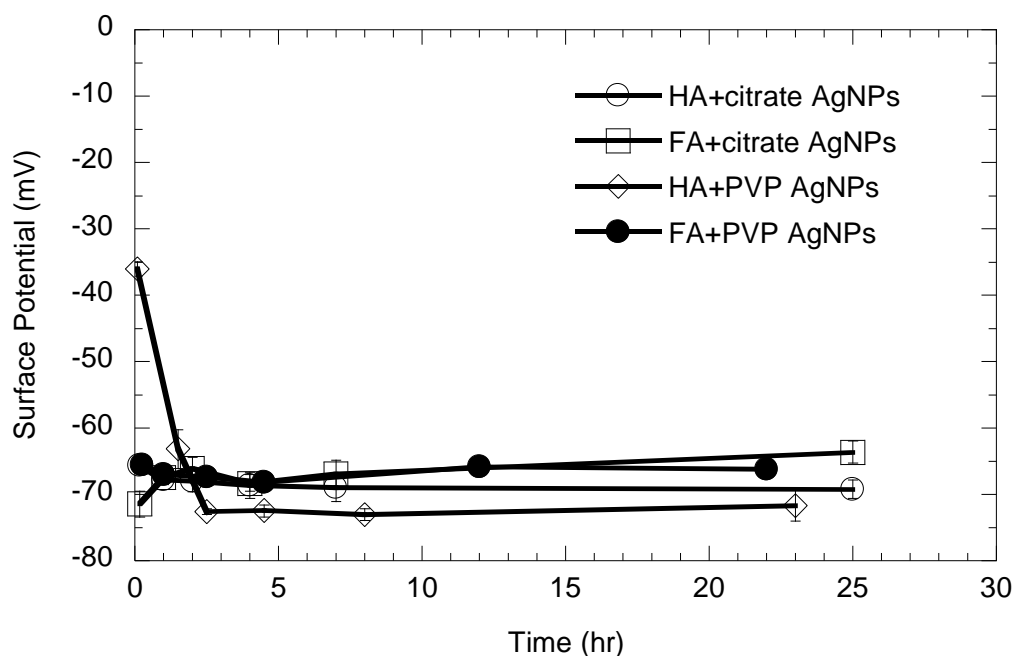
Figure 5.4: Surface potential monitoring in the process of the NOM coating on AgNPs at pH 7.0.

The effect of different types of NOM coatings on AgNP deposition is shown in Figure 5.5. Note that all tests were done at I=10 mM $Ca(NO_3)_2$ and pH 7. While the AgNPs were almost completely removed in the absence of NOM, the AgNP removal was drastically decreased in the presence of NOM. Therefore, it is considered that the bridging between the NOM coatings on the AgNPs and the filter media (Wang et al. 2008b) was unlikely to take place. Since both the AgNPs and filter media were pretreated with NOM of 3.5 mg TOC/L and the surface charge was partially neutralized by Ca ions, it is conceivable that the primary interaction between the NOM-coated AgNPs and filter media was steric stabilization (Lin et al. 2012). Interestingly, the AgNP deposition was interrupted more by humic acid than fulvic acid. Humic acid is known to have a greater molecular weight than fulvic acid (Beckett et al. 1987, Gueguen and Cuss 2011). Therefore, a greater distance imparted by humic acid coating between the AgNP and

filter media is likely to occur, leading to more extensive repulsion (Hassett and Anderson 1979). Furthermore, since the binding affinity to hydrophobic compounds is greater with humic acid than fulvic acid (DePaolis and Kukkonen 1997), a denser and thicker coating layer on both AgNPs and filter media could be expected by humic acid adsorption.
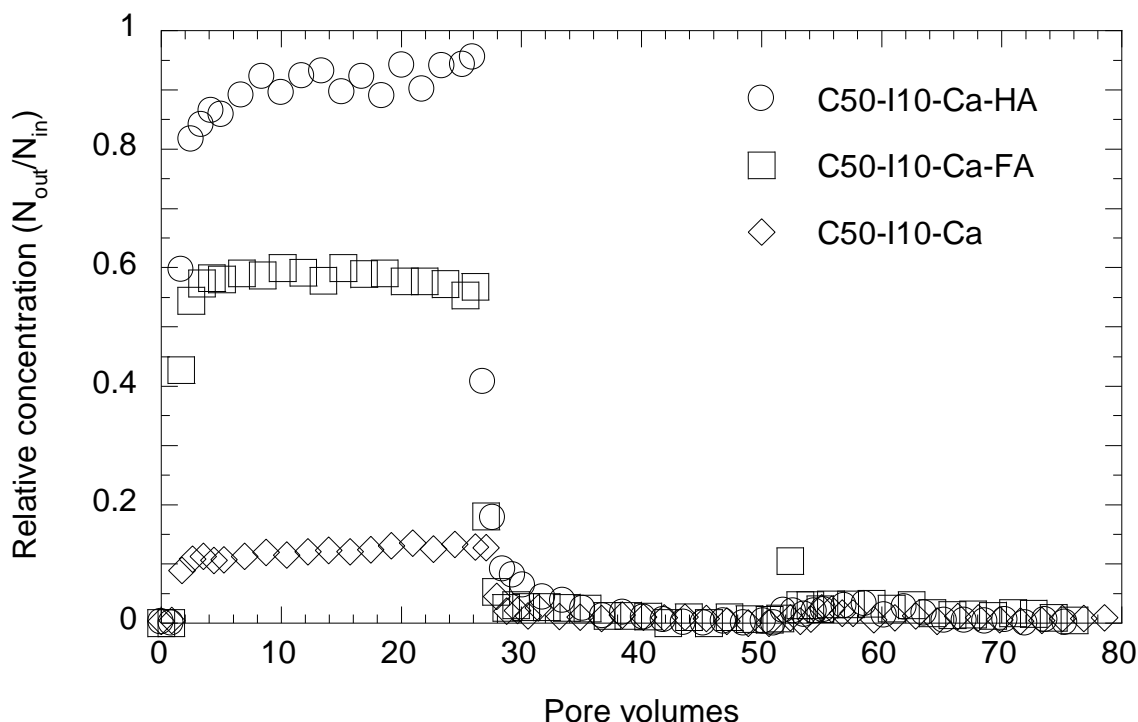
Figure 5.5:   Breakthrough curves of citrate AgNPs with different NOM coatings (at pH 7).

The effect of a humic acid coating on the AgNP deposition was obvious for citrate, but less for PVP at I=10 mM of Ca(NO$_3$)$_2$ and pH 9 (Figure 5.6); it is believed that the overall attachment of PVP AgNPs was limited by the strong steric hindrance of PVP capping. The relative decrease in attachment efficiency (α) between non-NOM and NOM coating at pH 9 was 93.4% and 57.1% for citrate and PVP, respectively. However, the level of AgNP deposition in the presence of humic acid was similar regardless of the capping agent of AgNPs, probably because the surface charge (Figure 5.2a&b) is similar

111

between the two types of particles. This similarity in surface potential supports the idea of displacement of capping agents by NOM (Lau et al. 2013) and/or a complete coverage of NOM over the capping agent followed by the adsorption of Ca ions. Also, the filtration results of citrate AgNPs in the presence or absence of humic acid was qualitatively the same at pH 7 and 9, indicating a prevalent property of humic acid coating on AgNP deposition.
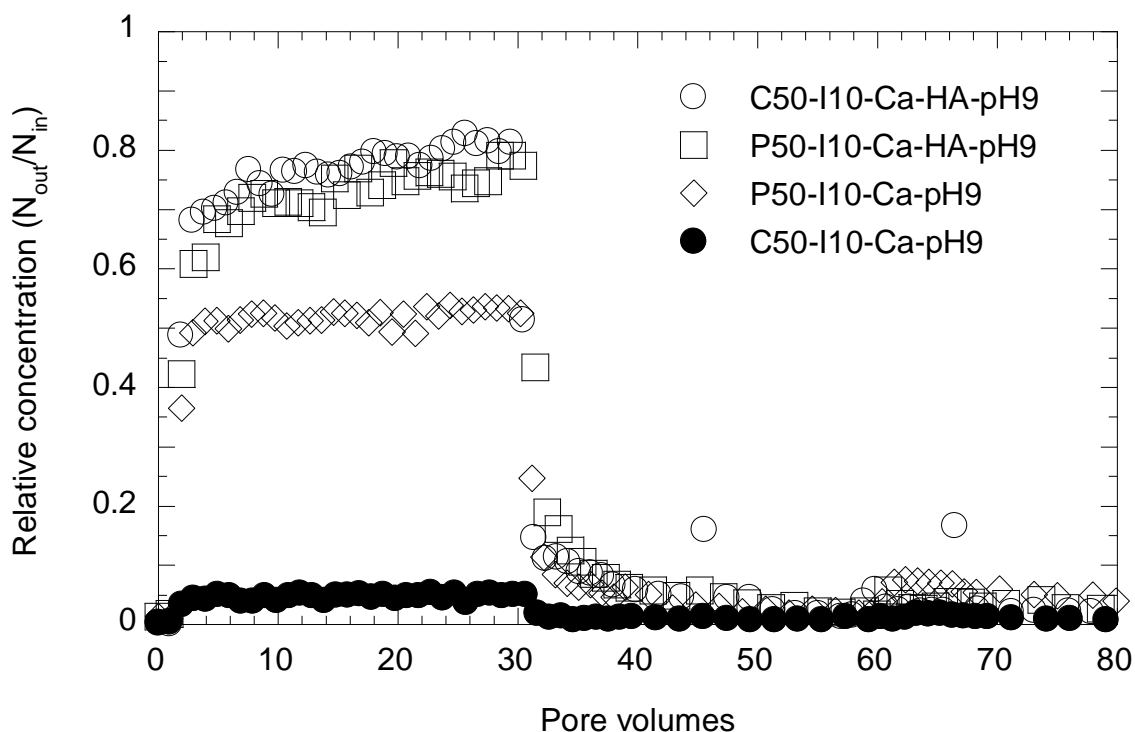
Figure 5.6: Breakthrough curves of citrate and PVP AgNPs with humic acid coating (at pH 9).

In Figure 5.6, a sharp increase and decrease are evident for both citrate and PVP AgNPs. This result directly corresponds to the experimental procedure; however, a tailing effect was observed after 30 min for the citrate AgNPs with humic acid and the PVP AgNPs. Similar tailing was found for other PVP experiments without NOM (Figure

4.10), however, little tailing was evident in the citrate experiments without NOM (Figure 4.5). This tailing suggests that advective forces might be dragging the AgNPs along with the bulk flow. These trends indicate that the attachment between humic acid coated citrate AgNPs or PVP AgNPs and the filter media is not as strong as for other cases of citrate AgNPs, meaning reversible attachment is more likely in those conditions. Again, this could be further evidence of the assimilated surface property by NOM coating. Given the similarity in tailing in the NOM experiments (for both citrate and PVP AgNPs) and the difference in tailing for the citrate experiments without NOM, it is reasonable to conclude that tailing is associated with steric effects on particle deposition.

The curves for the energy of interaction (Figure 5.7) showed no clear relationship between NOM coating and the height of energy barrier. On the contrary, the height of the energy barrier was reduced by NOM coating at pH 7. Therefore, the effect of NOM coating on the filtration results was likely caused by steric stabilization rather than electrostatic repulsion in this study. Since the surface charge was almost constant through the entire measured pH range with $I=10$ mM of $Ca(NO_3)_2$, there was little difference in the energy of interaction between pH 7 (Figure 5.7a) and pH 9 (Figure 5.7b).
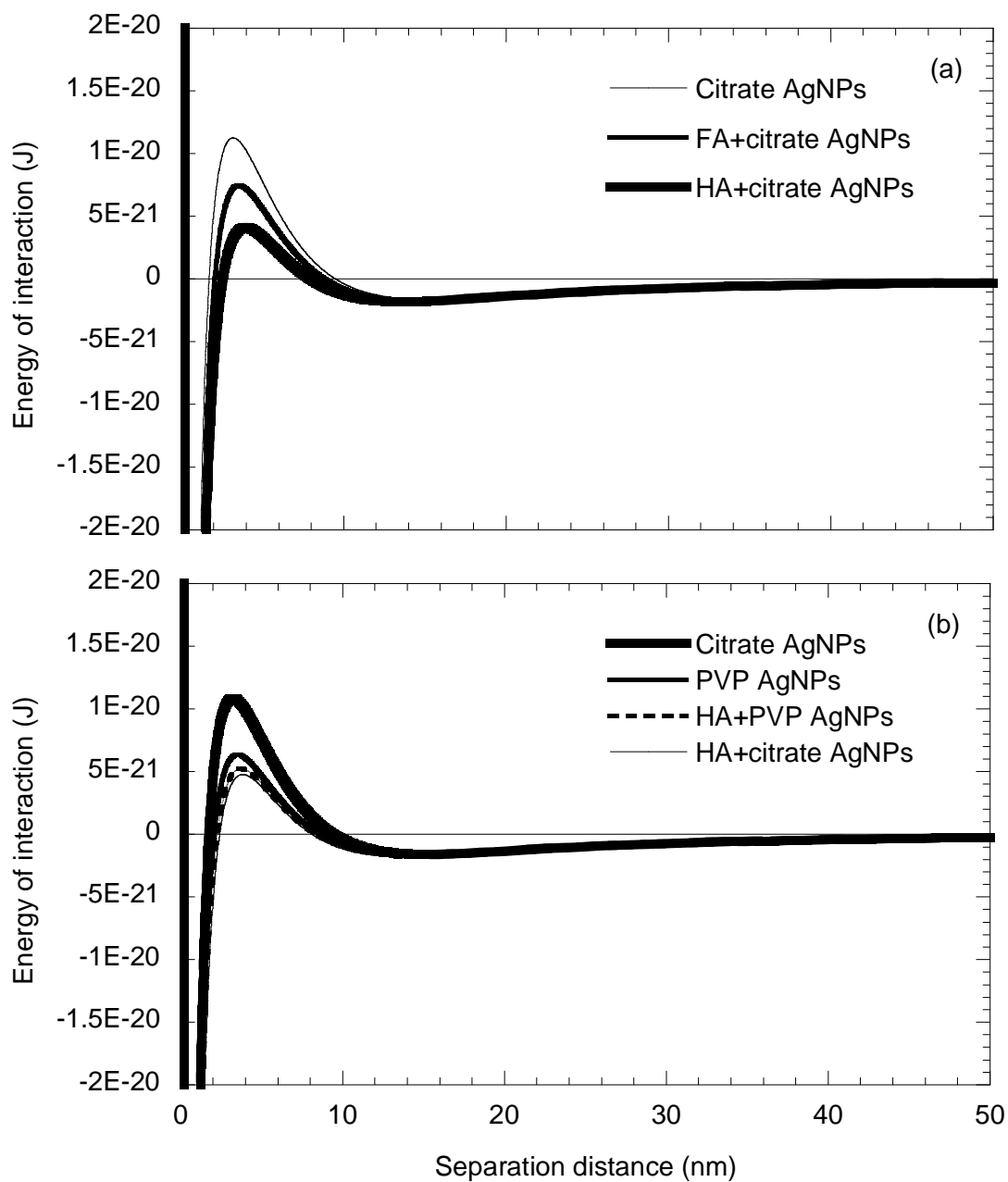
Figure 5.7:   Energy of interactions with I=10 mM of $Ca(NO_3)_2$ at (a) pH 7 and (b) pH 9.

Aggregation was unlikely to occur with a NOM coating at I=10 mM of $Ca(NO_3)_2$ (Lawler et al. 2013). As shown in the retention profiles (Figure 5.8), the vertical line indicates a uniform deposition throughout the filter depth, indicating no significant

114

aggregation of AgNPs. Therefore, this result could be evidence that the retention profile tends to be a vertical line (i.e., retention in the filter is constant over the depth) regardless of the amount of AgNP deposition as long as there is no or little aggregation of AgNPs either in the suspension or by attachment of a particle in suspension to a previously collected particle on the filter surface.
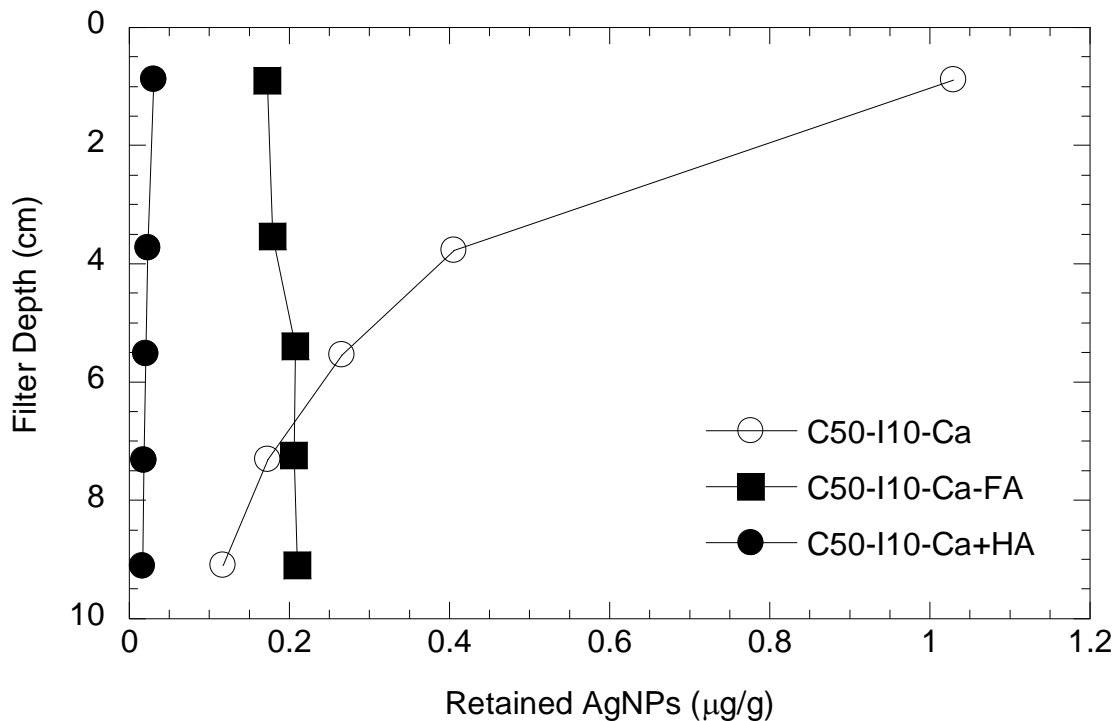
Figure 5.8:   Retention profiles of citrate AgNPs at pH 7.

5.4. Conclusions

In this study, the steric effect by NOM coating was exclusively featured because the addition of Ca ions in the background water reduced the magnitude of surface charge dramatically and eliminated the differences between different types of AgNPs. The greater steric effect of humic acid than fulvic acid was apparently caused by the greater

115

molecular weight of the humic acid, leading to a greater separation distance between two particles. Furthermore, the humic acid-coated AgNPs showed a similar deposition regardless of the capping agent, implying the possible displacement of the capping agent and/or the complete coverage by humic acid. This result is in direct contrast to the experiments without NOM, in which the removal of citrate capped AgNPs was drastically affected by solution characteristics (ionic strength and the specific cations) but the removal of PVP capped AgNPs were not.

NOM coating on nanoparticles, which occurs universally in the environment, could increase the stability and therefore the transport of nanoparticles, making the NOM-coated nanoparticles more likely to be found ubiquitously in the environment. In addition, the NOM coating tends to change the surface property of nanoparticles beyond the original surface chemistry. Though PVP is known to be a more stable capping agent than citrate, the role of the capping agent was minimized by NOM coating. Therefore, the role of NOM should be emphasized in the fate and transport of nanoparticles in natural and engineered systems.

Further study on the interaction of NOM and nanoparticle is required to elucidate the role of NOM on the surface of nanoparticles in terms of a quantitative evaluation of steric hindrance as well as organic surface groups. Recent advances in analytic methods such as nuclear magnetic resonance and raman spectroscopy would facilitate exploration of the surface chemistry in detail. The behavior of nanoparticles is expected to be different according to the type and amount of NOM, further warranting a more complete understanding of NOM adsorption.

References

Beckett, R., Jue, Z. and Giddings, J.C. (1987) Determination of molecular-weight distributions of fulvic and humic acids using flow field-Flow fractionation. Environmental Science & Technology 21(3), 289-295.

DePaolis, F. and Kukkonen, J. (1997) Binding of organic pollutants to humic and fulvic acids: Influence of pH and the structure of humic material. Chemosphere 34(8), 1693-1704.

Edzwald, J.K. and Tobiason, J.E. (1999) Enhanced coagulation: US requirements and a broader view. Water Science and Technology 40(9), 63-70.

Gueguen, C. and Cuss, C.W. (2011) Characterization of aquatic dissolved organic matter by asymmetrical flow field-flow fractionation coupled to UV-Visible diode array and excitation emission matrix fluorescence. Journal of Chromatography A 1218(27), 4188-4198.

Hassett, J.P. and Anderson, M.A. (1979) Association of hydrophobic organic-compounds with dissolved organic-matter in aquatic Systems. Environmental Science & Technology 13(12), 1526-1529.

Joo, S.H., Al-Abed, S.R. and Luxton, T. (2009) Influence of carboxymethyl cellulose for the transport of titanium dioxide nanoparticles in clean silica and mineral-coated sands. Environmental Science & Technology 43(13), 4954-4959.

Lau, B.L.T., Hockaday, W.C., Ikuma, K., Furman, O. and Decho, A.W. (2013) A preliminary assessment of the interactions between the capping agents of silver nanoparticles and environmental organics. Colloids and Surfaces A-Physicochemical and Engineering Aspects 435, 22-27.

Lawler, D.F., Mikelonis, A.M., Kim, I., Lau, B.L.T. and Youn, S. (2013) Silver nanoparticle removal from drinking water: flocculation/sedimentation or filtration? Water Science and Technology: Water Supply 13(5), 1181-1187.

Lead, J.R., Wilkinson, K.J., Balnois, E., Cutak, B.J., Larive, C.K., Assemi, S. and Beckett, R. (2000) Diffusion coefficients and polydispersities of the Suwannee River fulvic acid: Comparison of fluorescence correlation spectroscopy, pulsed-field gradient nuclear magnetic resonance, and flow field-flow fractionation. Environmental Science & Technology 34(16), 3508-3513.

Lin, S.H., Cheng, Y.W., Liu, J. and Wiesner, M.R. (2012) Polymeric coatings on silver nanoparticles hinder autoaggregation but enhance attachment to uncoated surfaces. Langmuir 28(9), 4178-4186.

117

Phenrat, T., Kim, H.J., Fagerlund, F., Illangasekare, T., Tilton, R.D. and Lowry, G.V. (2009) Particle size distribution, concentration, and magnetic attraction affect transport of polymer-modified Fe-0 nanoparticles in sand columns. Environmental Science & Technology 43(13), 5079-5085.

Roalson, S.R., Kweon, J., Lawler, D.F. and Speitel, G.E. (2003) Enhanced softening: Effects of lime dose and chemical additions. Journal American Water Works Association 95(11), 97.

Saleh, N., Kim, H.J., Phenrat, T., Matyjaszewski, K., Tilton, R.D. and Lowry, G.V. (2008) Ionic strength and composition affect the mobility of surface-modified Fe-0 nanoparticles in water-saturated sand columns. Environmental Science & Technology 42(9), 3349-3355.

Sharp, E.L., Parsons, S.A. and Jefferson, B. (2006) Seasonal variations in natural organic matter and its impact on coagulation in water treatment. Science of the Total Environment 363(1-3), 183-194.

Siddiqui, M.S., Amy, G.L. and Murphy, B.D. (1997) Ozone enhanced removal of natural organic matter from drinking water sources. Water Research 31(12), 3098-3106.

Stankus, D.P., Lohse, S.E., Hutchison, J.E. and Nason, J.A. (2011) Interactions between natural organic matter and gold nanoparticles stabilized with different organic capping agents. Environmental Science & Technology 45(8), 3238-3244.

Tiraferri, A. and Sethi, R. (2009) Enhanced transport of zerovalent iron nanoparticles in saturated porous media by guar gum. Journal of Nanoparticle Research 11(3), 635-645.

Tolaymat, T.M., El Badawy, A.M., Genaidy, A., Scheckel, K.G., Luxton, T.P. and Suidan, M. (2010) An evidence-based environmental perspective of manufactured silver nanoparticle in syntheses and applications: A systematic review and critical appraisal of peer-reviewed scientific papers. Science of the Total Environment 408(5), 999-1006.

Wang, Y.G., Li, Y.S., Fortner, J.D., Hughes, J.B., Abriola, L.M. and Pennell, K.D. (2008b) Transport and retention of nanoscale C_{60} aggregates in water-saturated porous media. Environmental Science & Technology 42(10), 3588-3594.

Yang, J., Bitter, J.L., Smith, B.A., Fairbrother, D.H. and Ball, W.P. (2013) Transport of oxidized multi-walled carbon nanotubes through silica based porous media: Influences of aquatic chemistry, surface chemistry, and natural organic matter. Environmental Science & Technology 47(24), 14034-14043.

118

Yang, X.Y., Lin, S.H. and Wiesner, M.R. (2014) Influence of natural organic matter on transport and retention of polymer coated silver nanoparticles in porous media. Journal of Hazardous Materials 264, 161-168.

Zularisam, A.W., Ismail, A.F. and Salim, R. (2006) Behaviours of natural organic matter in membrane filtration for surface water treatment - a review. Desalination 194(1-3), 211-231.

Chapter 6: DETACHMENT OF NANOPARTICLES IN GRANULAR MEDIA FILTRATION

Abstract

An understanding of particle-particle interactions in filtration requires studying the detachment as well as the attachment of nanoparticles. Nanoparticles captured in a granular media filter can be released by changing the physicochemical factors. In this study, the detachment of captured silver nanoparticles (AgNPs) in granular media filtration was examined under different ionic strengths, ion type, and the presence or absence of natural organic matter (NOM). Filtration velocity and ionic strength were chosen as the physical and chemical factors to cause the detachment. Increasing filtration velocity caused a negligible amount of AgNP detachment. On the other hand, lowering ionic strength showed different release amounts depending on the background ions, implying a population of loosely captured particles inside the filter bed. Overall detachment was affected by ionic strength and ion type, and to a lesser degree by NOM coating which resulted in slightly more detachment (in otherwise identical conditions) than in the absence of that coating, possibly by steric effects. The secondary energy minimum with Na ions was deeper and wider than with Ca ions, probably due to the lack of complexation with citrate and charge neutralization that would be caused by Ca ions. This result implies that the change in chemical force by reducing ionic strength of Na ions could significantly enhance the detachment compared to that caused by a change in physical force, due to a weak electrostatic deposition between nanoparticles and filter media. A modification of the 1-D filtration model to incorporate a detachment term showed good agreement with experimental data; estimating the detachment coefficients for that model suggested that the detachment rate could be similar regardless of the amount of previously captured AgNPs.

120

Keywords

Detachment, secondary energy minimum, granular media filtration model

6.1. Introduction

The use of nanoparticles has increased in various areas such as medical (Farokhzad and Langer 2009), material (Zhu et al. 2004), cosmetics (Mu and Sprando 2010), and energy applications (Serrano et al. 2009) and is expected to grow further in the near future (Project on Emerging Nanotechnologies 2014). Consequently, the release of nanoparticles to the environment from industrial sources or households can be anticipated (Benn et al. 2010, Nowack and Bucheli 2007). Concerns about the potential harm from nanoparticles to humans and the environment are growing as the likelihood of exposure to nanoparticles becomes evident.

So far, the primary focus has been on the beneficial uses of nanoparticles, which has contributed to the growth of nanotechnology. Though public perception of nanotechnology has been positive, it should be noted that the knowledge about nanoparticles has been limited (Cobb and Macoubrie 2004). This lack of knowledge about nanoparticles has made risk assessment and decision-making difficult. Therefore, a balanced evaluation of nanoparticles is required.

Predicting human and environmental exposure to nanoparticles requires research on the transport of nanoparticles. A considerable amount of research has been conducted on the transport of nanoparticles in granular media filtration (Petosa et al. 2010). Since granular media filtration can mimic the soil or groundwater environment, it has been used to understand the migration of nanoparticles in such environments. Less attention has been given to the study of nanoparticle removal in granular media filtration at conditions reflecting drinking water and wastewater treatment.

Nanoparticle-filter media interaction can be divided into two sections; attachment and detachment. Most previous studies have focused on attachment. The effects of various particle characteristics (Lecoanet et al. 2004), solution chemistries (Solovitch et al. 2010), and operational conditions (Lecoanet and Wiesner 2004) on attachment have been investigated. Despite their tiny size, nanoparticles can be captured in granular media filter by controlling environmental conditions. However, the release of captured nanoparticles was reported when operational conditions changed chemically (e.g., ionic strength reduction (Franchi and O'Melia 2003), pH rise (Ryan and Elimelech 1996), and cation exchange (Shen et al. 2012)). For particles larger than 2 μm, detachment also occurred by an increase in filtration velocity (Bergendahl and Grasso 2000).

Generally, attachment and detachment are highly affected by electrostatic forces produced by the surface charges of particles. Detachment was believed to occur when attractive forces are weak in terms of electrostatic interaction, that is, when particles stay in the secondary energy minimum (Hahn and O'Melia 2004). However, this belief was challenged by a recent study (Shen et al. 2012) which suggested a possible detachment from the primary energy minimum. All things considered, the exact mechanism is still unclear as to how nanoparticles are captured reversibly in granular media filters. Since detachment of nanoparticles in granular media filtration has not received much attention, detachment of nanoparticles under varying environmental conditions needs to be investigated.

This study selected silver nanoparticles (AgNPs) as the target compound because they are the most widely used nanoparticles in consumer products. The objective of this study was to investigate the effect of physical and chemical forces on the detachment of AgNPs in granular media filtration. A series of laboratory scale granular media filtration tests was conducted under varying filtration velocities, ionic strengths, ion types, and the

presence or absence of NOM to quantify the amounts of AgNPs captured and subsequently released when a physical or chemical condition was changed. Further, by assuming a homogeneous particle size and a spherical shape for the nanoparticles, the 1-D filtration model was explored to elucidate the detachment of AgNPs under various experimental conditions.

6.2. Theoretical calculations

Energy of interaction. As introduced in Chapter 4, the sum of the repulsive energy (V_R), attractive energy (V_A) and Born repulsion (V_B) was used to calculate the energy of interaction (all variables in the following equations are defined in Appendix B).

$$V_R = \pi\varepsilon_0\varepsilon_r a_p \left(2\psi_{d_f}\psi_{d_p} \ln\left[\frac{1+\exp(-\kappa s)}{1-\exp(-\kappa s)}\right] + \left(\psi_{d_f}^2 + \psi_{d_p}^2\right)\ln\left[1-\exp(-2\kappa s)\right]\right) \quad (6\text{-}1)$$

$$V_A = \frac{Aa_p}{6s}\left(1 + \frac{14s}{\lambda}\right)^{-1} \quad (6\text{-}2)$$

$$V_B = \frac{A\sigma_c^6}{7560}\left(\frac{8a_p + s}{(2a_p + s)^7} + \frac{6a_p - s}{s^7}\right) \quad (6\text{-}3)$$

Filtration model. Filtration models typically start from a one dimensional advection-diffusion equation, as described in Equation 6-4, by assuming first order attachment kinetics (Li et al. 2008).

$$\frac{\partial N}{\partial t} = D\frac{\partial^2 N}{\partial x^2} - v_0\frac{\partial N}{\partial x} - k_{att}N \quad (6\text{-}4)$$

N is the effluent number concentration at steady-state condition ($\#/L^3$), t is the time period after filtration starts (T), x is the distance from the surface of filter bed parallel to flow (L), D is the diffusion (plus dispersion) coefficient (L^2/T), and v_0 is the filtration velocity (L/T).

The attachment coefficient (k_{att}) is calculated by Equation 6-5 (Wang et al. 2008a):

$$k_{att} = \frac{v_0}{L} \ln\left(\frac{N_0}{N}\right) \tag{6-5}$$

L is filter depth (L), and N_0 is the initial AgNP number concentration (#/L^3). To describe the detachment profile, the model was modified as shown in Equation 6-6 by adding a term to include detachment from the solid-phase, dependent on the amount captured on the filter media (Wang et al. 2008b).

$$\frac{\partial N}{\partial t} = D \frac{\partial^2 N}{\partial x^2} - v_0 \frac{\partial N}{\partial x} - k_{att} N + k_{det} \frac{\rho_b}{\varepsilon} S \tag{6-6}$$

k_{det} is the detachment coefficient (1/T), S is the specific deposit attached to the filter media (#/M), ρ_b is the bulk density of the filter media (M/L^3), and ε is the volumetric water content, i.e., the porosity (-). S can be expressed in a whole filter as shown in Equation 6-7:

$$S(x) = \frac{t_0 \varepsilon k_{att} N_0}{\rho_b} \exp\left(-\frac{k_{att}}{v_0} x\right) \tag{6-7}$$

where t_0 is the AgNP injection period.

To solve Equation 6-6, a numerical scheme that employs a finite difference method in space and the Crank-Nicolson method in time was used. In this study, the boundary and initial conditions were set as follows:

$$N(x=0,\ t<30\ \text{min}) = N_0$$

$$N(x=0,\ t \geq 30\ \text{min}) = 0$$

$$N(x,\ t=0) = 0$$

Using the first order finite difference scheme of backward facing steps, this equation can be solved numerically using MATLAB (The MathWorks, Natick, MA) (details are in Appendix C).

6.3. Materials and Methods

Citrate-capped AgNPs were purchased from Nanocomposix (San Diego, CA). Citrate was chosen because it is one of most commonly used capping agents in AgNP synthesis (Tolaymat et al. 2010). The laboratory analysis confirmed the spherical shape and the monodispersed size distribution of approximately 50 nm of AgNPs (refer to Section 4.2.1 for the details of the particle size determination). To prevent any changes in AgNPs characteristics, the solution was kept at 4˚C and away from light.

Spherical glass beads purchased from MO-SCI (St.Louis, MO) were used for filter media. The glass beads were mainly composed of SiO_2 (as shown in Table 3.2 in section 3.3 and more information is in Appendix D) and were sieved to a narrow size range between 300~350 μm. To remove impurities from the surface before use, the glass beads were subjected to an intensive washing procedure (Tobiason 1987).

Filtration experiments were conducted in a laboratory-scale acrylic cylindrical column. The inner diameter of the column was 3.81 cm and the depth of the filter bed was 10 cm. The porosity of the packed bed was determined gravimetrically to be 0.42. The two influent streams, AgNP suspension and background water, were separately prepared and pumped via a gear pump (Micropump, Cole Parmer) and a peristaltic pump (Easy-load II, Masterflex), respectively, and mixed immediately before entering into the column. The flow ratio of AgNP suspension to the background water was kept at 1:20 to maintain constant influent AgNP concentration.

The ionic strength was controlled by $NaNO_3$ or $Ca(NO_3)_2$ added to the background water. Since a sufficient amount of attachment is needed to achieve detachment, ionic strength of 100 mM with $NaNO_3$ and 10 mM with $Ca(NO_3)_2$ were

chosen. In the experiments with NOM, Suwannee River Fulvic Acid (International Humic Substances Society, MN) was used to have 3.5 mg TOC/L background water to coat AgNPs and filter media. pH was controlled with 0.025 mM bicarbonate buffer at pH 7 to prevent significant changes in surface charge by pH. The filtration velocity was controlled at 2 m/hr, which is in the range used in conventional drinking water treatment plants, but far faster than groundwater flow.

Six filtration tests were conducted with varying ion types, ionic strengths, and/or filtration velocities. Prior to the filtration test, the filter bed was flushed for 30 pore volumes by the background water. Each test consisted of three steps: 1) 25 pore volumes of filtration with AgNPs, 2) 25 pore volumes of flow at the same velocity and the same chemical conditions without AgNPs, and 3) 25 pore volumes of flow with either near zero ionic strength (deionized water) or with increased velocity. To achieve detachment of the captured AgNPs after 50 pore volumes, ionic strength was reduced to close to 0.025 mM or the filtration velocity was doubled from 2 to 4 m/hr. Samples were collected every 1 or 2 minutes during both filtration period and the detachment periods.

Table 6.1: Summary of the filtration tests.

Experiment #[a]	NOM coating	Ionic strength	Detachment
C50-I10-Ca-I	No	10 mM Ca(NO$_3$)$_2$	Decreasing ionic strength
C50-I10-Ca-FA-I	Yes	10 mM Ca(NO$_3$)$_2$	Decreasing ionic strength
C50-I100-Na-I	No	100 mM NaNO$_3$	Decreasing ionic strength
C50-I10-Ca-V	No	10 mM Ca(NO$_3$)$_2$	Increasing velocity
C50-I10-Ca-FA-V	Yes	10 mM Ca(NO$_3$)$_2$	Increasing velocity
C50-I100-Na-V	No	100 mM NaNO$_3$	Increasing velocity

[a] C refers to citrate, 50 is for 50 nm size, the I value is the ionic strength (mM), the chemical name is the source of the ionic strength, FA refers to fulvic acid coating, I refers to ionic strength reduction, and V refers to filtration velocity increase.

AgNP samples were immediately acidified with trace metal grade HNO$_3$ to dissolve AgNPs (sample pH < 0.5). The acidified samples were stored at 4˚C overnight. The dissolved Ag concentration was analyzed using an inductively coupled plasma-optical emission spectroscopy (ICP-OES, Varian). The surface charge of AgNPs and filter media was measured by dynamic light scattering (DLS, Malvern Zetasizer). Direct observations of AgNPs and filter media were conducted by transmission electron microscopy (TEM, FEI Tencai) and scanning electron microscopy (SEM, Zeiss).

6.4. Results and Discussion

The experimental breakthrough curves are presented in terms of the relative concentration by pore volume (Figure 6.1). Relative concentration is the normalized

effluent concentration, or the fraction of the influent concentration remaining in the effluent. The detachment was relatively insignificant in all but one of the filtration tests. The most significant detachment occurred when the ionic strength was reduced from 100 mM NaNO$_3$.
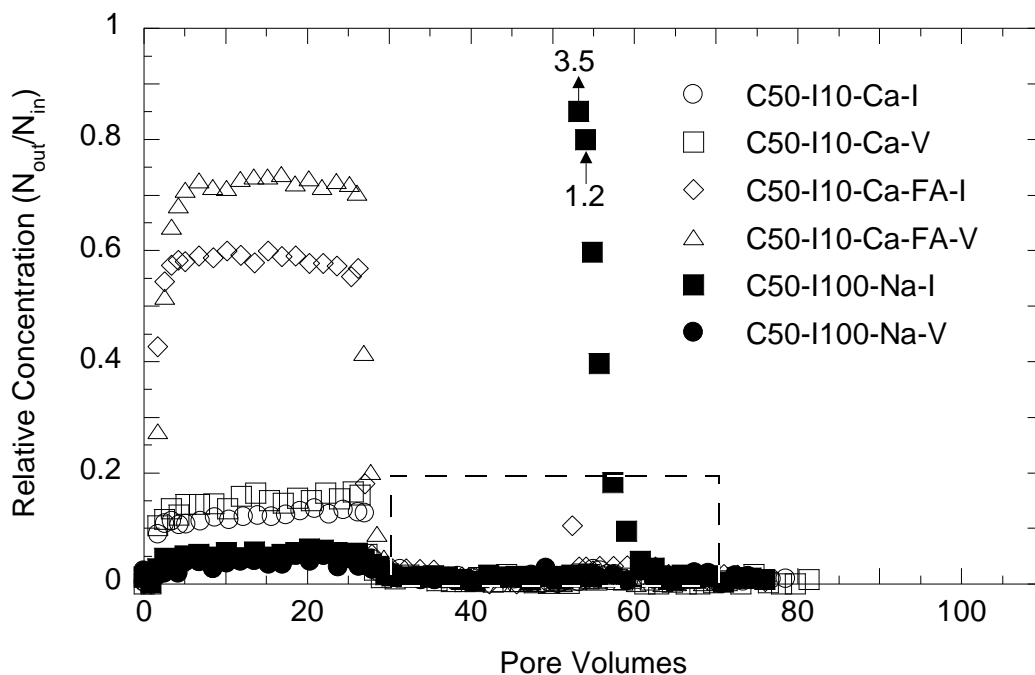
Figure 6.1:   Breakthrough curves of citrate AgNPs with detachment.

As shown in Figure 6.2 (the dashed area indicated in Figure 6.1), the insignificant detachment with Ca(NO$_3$)$_2$ is similar to the previous findings (Hahn and O'Melia 2004, Jaisi et al. 2008) in that the detachment was significantly reduced with Ca ions. It is likely that Ca ions lead AgNPs to the primary energy minimum where (essentially) irreversible attachment occurs. Since the surface charge of the citrate-capped nanoparticles can be neutralized by Ca ions (Saleh et al. 2008), the repulsive force between AgNPs and filter media can be quite low.
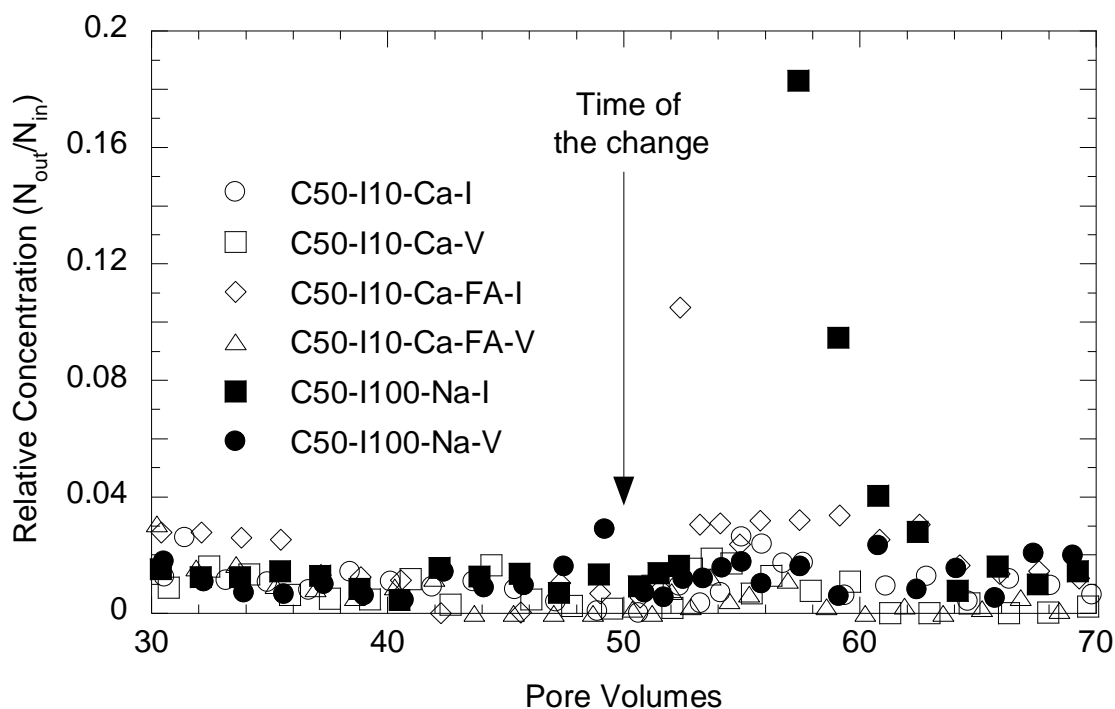
Figure 6.2: Detachment curves of citrate AgNPs.

When the filtration velocity was doubled to allow a greater hydrodynamic drag force on the AgNPs already captured in the filter, there was only a negligible amount of AgNP detachment regardless of ionic strength, ion type, or NOM presence. Note that the required velocity to detach nanoparticles is theoretically considered to be more than 100 m/hr (Zhang 2012) which is far greater than any of those used in this study. Even with a wide and deep secondary energy minimum at I=100 mM of $NaNO_3$, the deposition is expected to be strong enough to withstand the hydrodynamic force applied in this study (though there was a tiny amount of detached AgNPs by the velocity change). This result does not refute the fact that hydrodynamic shear can affect the AgNPs deposited probably in the secondary energy minimum. However, it provides an insight that detachment can occur more easily with a chemical change rather than a physical one.

129

It should be noted that these filtration experiments were relatively short and designed primarily to test whether some of the capture of particles was in the range of the secondary minimum of the energy curve. The small amount of detachment with the velocity change in these experiments does not mean that detachment would not occur to a significant degree with the same velocity change after filtration of thousands of pore volumes (as occurs in water treatment practice). In that case, deposits might have significant thickness, and a change in the velocity could induce more detachment than seen in these experiments.

Even after the detachment period, AgNPs remained in the filter, yielding the amount of AgNPs that withstood the detachment condition. When the ionic strength was reduced, the remaining AgNPs in the filter were considered to be irreversibly attached in the primary energy minimum. In all tests, the amount of AgNPs remaining in the filter (irreversibly attached) was quantified for the AgNP mass-balance. The ratio of the detached AgNPs to the originally attached AgNPs was calculated from the experimental data (and converted to a percent) and is shown in Table 6.2 for all of the experiments. The overall mass balance for each experiment is shown in Figure 6.3

Table 6.2: Percent of the originally attached AgNPs that became detached.

Experiment #	C50-I10-Ca-I	C50-I10-Ca-V	C50-I10-Ca-FA-I	C50-I10-Ca-FA-V	C50-I100-Na-I	C50-I100-Na-V
Detached AgNPs/ Attached AgNPs (%)	1.23	0.40	7.33	0.61	25.50	0.68
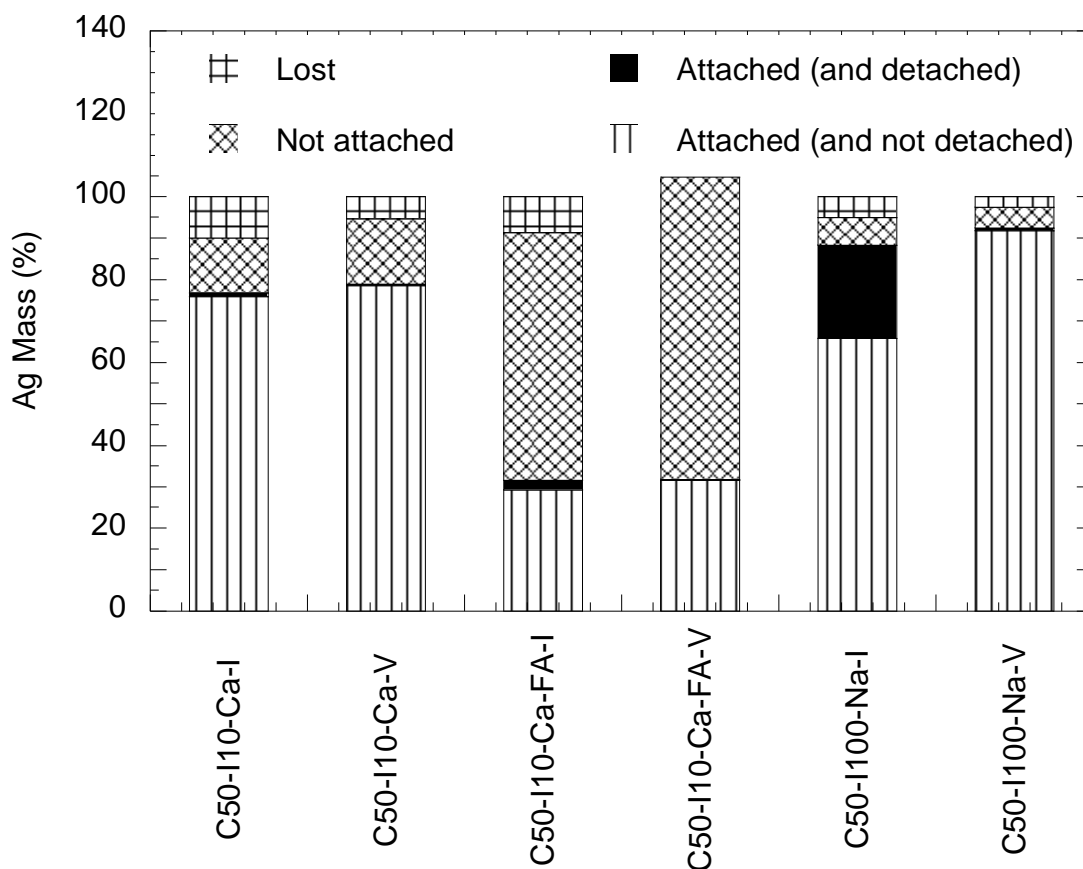
Figure 6.3:   Mass balance of Ag by mass in this study.

In the case of the I=100 mM NaNO$_3$ test, the ratio of the detached to the originally attached AgNP mass was approximately 1:4. Assuming the detachment occurred for all particles attached in the secondary energy minimum, it suggests that one-fourth of AgNPs which could approach the primary energy minimum were stopped in the secondary energy minimum. Though the distance to the secondary energy minimum from the filter media surface was calculated to be only 4.19 nm (Table 6.3), the release of AgNPs seemed affected by the degree of the change from attraction to repulsion energy despite the small physical distance from the filter media. Also, since the influent AgNP

131

concentration was in the low range (less than 100 µg/L), the number of the AgNPs injected to the filter was insufficient to fully cover every filter media surface. Therefore, multilayer AgNP deposition was unlikely to take place in this study. One might argue that I=100 mM of $NaNO_3$ could promote the aggregation of AgNPs in the suspension, leading to the deposition of AgNP aggregates on the filter media. However, the empty bed contact time was only approximately 1.18 min which is thought to be an insufficient time for AgNPs to be aggregated. Therefore, the significant amount of detachment is attributed to the detachment of the AgNPs that had been deposited in the secondary energy minimum.

With regard to the classical DLVO theory, the energy of the interaction between AgNPs and filter media was calculated (Figure 6.4a). This calculation was conducted assuming a spherical particle and a flat plane since the size ratio of AgNP to filter media was close to 0.00015. A relatively deep and wide secondary energy minimum was calculated for the 100 mM $NaNO_3$ case while the other conditions showed no such significant secondary energy minimum. The surface potentials of AgNPs and glass beads were more negative at I=100 mM of $NaNO_3$ in comparison to the other two conditions, and that caused the greater repulsive energy reflected in the figure 6.4a. The surface potentials for the three conditions were calculated from zeta-potential measurements and are shown in Table 6.3. It seems that the electric double layer suppression by the 100 mM ionic strength also led to the suppression of energy of interaction curves toward the filter media surface, resulting in a higher energy barrier and a deeper secondary energy minimum. Note that the secondary energy minimum disappeared when the ionic strength was greatly reduced, assuming the surface potentials of AgNPs and filter media were unaffected (Figure 6.4b). Considering the experimental results for detachment in light of

the energy interaction calculations, it is believed that the primary reason for AgNP detachment was their release from the secondary energy minimum.

A comparison of the detached AgNP amounts from C50-I10-Ca-FA-I and C50-I10-Ca-I (Figure 6.3) shows that the NOM coating on the AgNP caused measurable detachment when the ionic strength was reduced. Since the location and the depth of the secondary energy minimum were almost identical regardless of NOM presence (Table 6.3), it is assumed that the steric effect rather than electrostatic effect by NOM coating might cause a weak AgNP deposition which is vulnerable to the ionic strength decrease. At I=10 mM of $Ca(NO_3)_2$, the steric effect by NOM coating appears to be the main factor because the surface charge becomes equalized regardless of the NOM coating due to Ca-citrate complexation, considering the higher affinity of citrate to Ca than Na (Walser 1961). Nevertheless, the overall results highlighted that the change of ionic strength (which affects electrostatic repulsion) of Na ions had the most direct effect on the magnitude of detachment of AgNPs.

Table 6.3: Results of the energy of interaction calculations.

Experiment #	Surface potential at pH7 (mV)	Energy barrier height (J)	Energy barrier distance from surface (nm)	Secondary energy minimum depth (J)	Distance from the surface at the secondary energy minimum (nm)
C50-I10-Ca	-20.26	1.08×10^{-20}	3.22	-1.62×10^{-21}	15.08
C50-I10-Ca-FA	-16.20	7.01×10^{-21}	3.60	-1.70×10^{-21}	14.46
C50-I100-Na	-50.75	2.81×10^{-20}	0.99	-1.18×10^{-20}	4.19
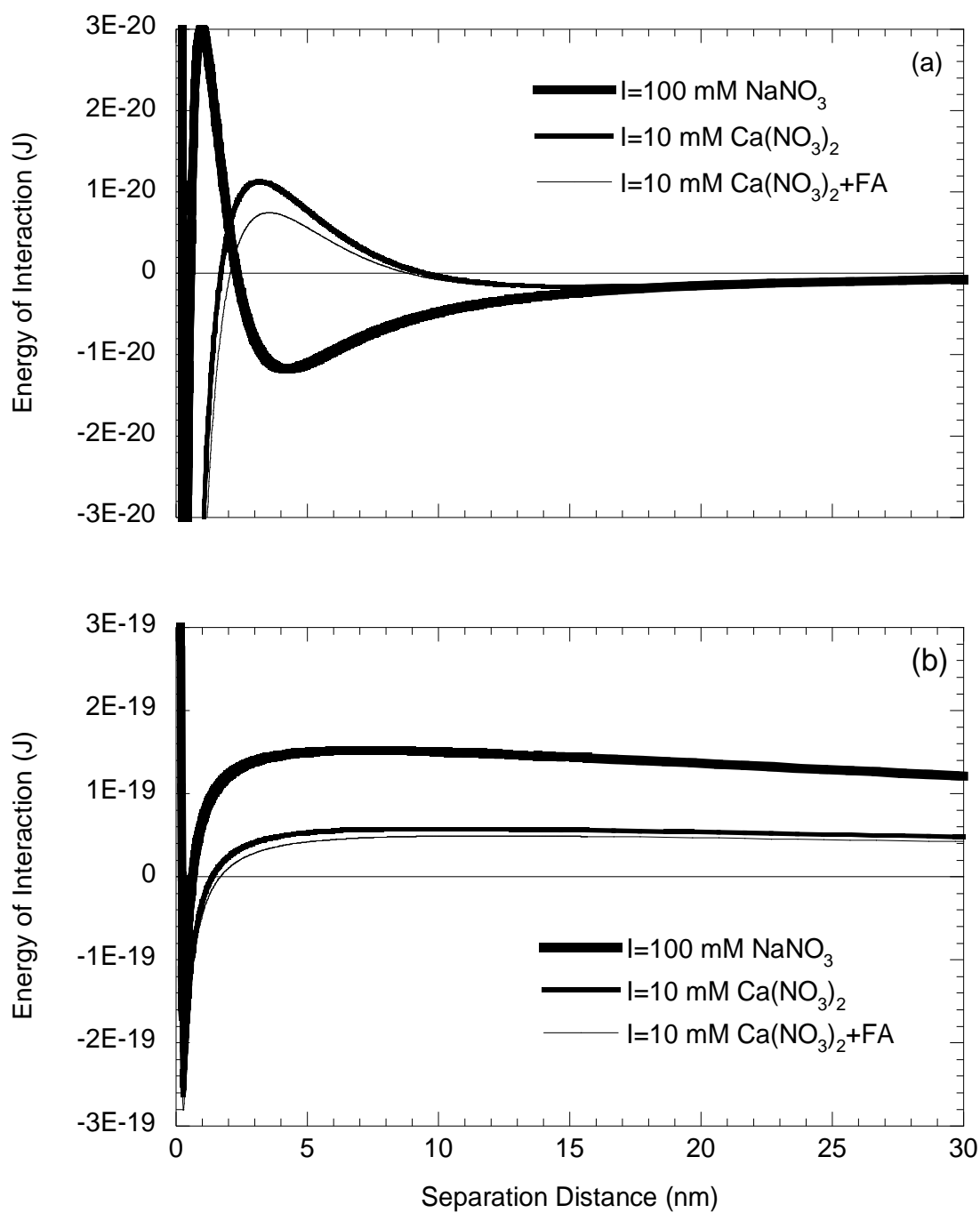
Figure 6.4: Energy of interaction between citrate AgNPs and filter media (a) at the ionic strength during filtration and (b) at the low (near zero) ionic strength during the detachment phase of the experiments (at pH 7).

134

The filtration model derived from 1-D advection-diffusion equation was used as a tool to model the effluent profile of AgNPs, and all model outputs in this study were the concentrations at the outlet of the filter. This model was run by using the known value of v_0 and calculating k_{att}, and S directly from the experimental results from the attachment period. The diffusion plus dispersion coefficient was taken to be the particle diffusion coefficient, even though dispersion was probably greater than this value; the primary reason for using the model was to estimate the detachment coefficient, so this choice for the diffusion coefficient was deemed unimportant. The remaining parameter, k_{det} was estimated to fit the model to the experimental result during the detachment period between 50 and 60 pore volumes. Overall, this model effectively simulated the sharp increase and decrease of citrate AgNPs in the experiments (Figure 6.5). The assumption of first order attachment kinetics was reasonable because the surface area of filter media is substantially greater than the surface area of injected AgNPs. Also, the k_{det} derived in each test condition allowed good agreement with experimental results. This result demonstrates that the transport of 50 nm AgNPs in granular media filtration was primarily affected by diffusion and advection and that I-D advection-diffusion equation was applicable to the conditions of the experiments.
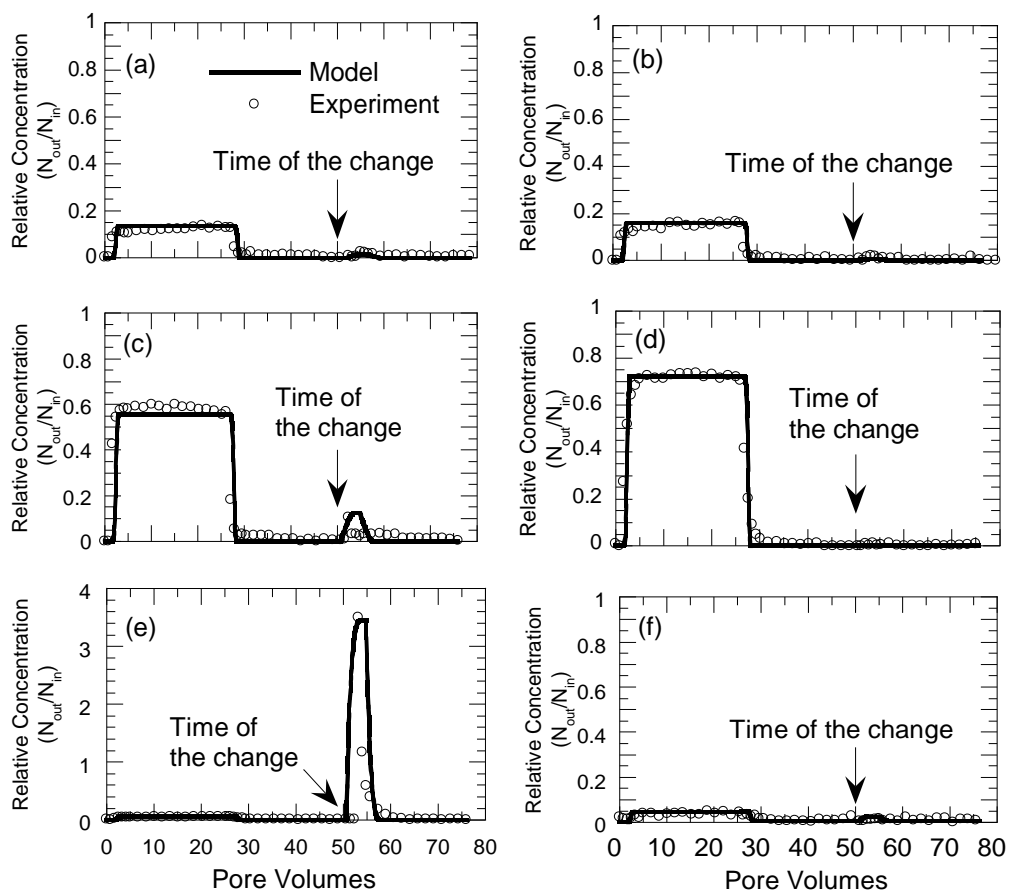
Figure 6.5: Comparison of experimental results and model predictions for all filtration tests. (Each column shows the cases of the detachment caused by ionic strength reduction (left) or by filtration velocity increase (right). Experimental condition varies from top to bottom (top: I=10 mM $Ca(NO_3)_2$, middle: I=10 mM $Ca(NO_3)_2$ with fulvic acid, bottom: I=100 mM $NaNO_3$)).

This model was fitted to the detachment profile for each experimental condition. Values of k_{det} were estimated using the root-mean-square error in the short detachment period (50~60 pore volumes), and they are shown in Table 6.4.

Table 6.4:   Estimated detachment coefficients from six filtration tests.

Experiment #	C50-I10 -Ca-I	C50-I10 -Ca-FA-I	C50-I100 -Na-I	C50-I10 -Ca-V	C50-I10 -Ca-FA-V	C50-I100 -Na-V
k_{det} $(10^{-4}\ s^{-1})$	0.018	0.69	0.82	0.016	0.17	0.0032

At higher pore volume values, the detachment coefficient was estimated to be as low as $10^{-7}\ s^{-1}$ which indicates almost no detachment. The likelihood of further detachment after the detachment period was insubstantial because the detachment might be caused solely by eliminating the secondary energy minimum whose effect appeared immediately, just as turning off a switch.

Interestingly, the detachment coefficients from the two tests with the most detachment (I=10 mM of $Ca(NO_3)_2$ with fulvic acid and I=100 mM of $NaNO_3$ without NOM) were estimated to be similar, even though the amount of detached AgNPs was significantly different between those tests. The seemingly identical detachment coefficient with different amount of detachment was attributed to the different amounts of attachment. In other words, the detachment coefficient is the parameter which determines the detachment rate of a system independent of the amount of attachment. The similarity of results in these two experiments suggests that the steric effect by NOM coating causes as much detachment potential as the elimination of secondary energy minimum. Thus, the detachment coefficient is a preferred parameter to interpret the detachment potential from different experimental conditions.

6.5. Conclusions

In this study, the detachment of AgNPs could be attributed mainly to the secondary energy minimum in terms of the amount of the detached AgNPs. The significant reduction in ionic strength resulted in effective detachment by eliminating the secondary energy minimum. Less detachment was observed with I=10 mM of $Ca(NO_3)_2$ than I=100 mM of $NaNO_3$ because Ca ions were able to effectively neutralize the surface charges, presumably by Ca-citrate complexation. The steric effect by NOM coating could lead to a weak AgNP deposition resulting in more detachment than in the absence of NOM. The velocity increase showed a negligible effect on the detachment because the velocity range applied here was much lower than the velocity level required to enable nanoparticle detachment. The remaining AgNPs after filtration and after a sudden decrease of the ionic strength was applied were considered to be irreversibly deposited in the primary energy minimum. The model derived from 1-D advection-diffusion equation with attachment and detachment terms was successfully used to fit to the experimental results and estimate the detachment coefficients. The detachment occurred rapidly in a brief period immediately after the ionic strength decreased or filtration velocity increased, and the detachment coefficients were estimated using data from that period. The comparison of the detachment coefficients demonstrated the contribution of the steric effect to detachment.

References

Benn, T., Cavanagh, B., Hristovski, K., Posner, J.D. and Westerhoff, P. (2010) The Release of nanosilver from consumer products used in the home. Journal of Environmental Quality 39(6), 1875-1882.

Bergendahl, J. and Grasso, D. (2000) Prediction of colloid detachment in a model porous media: hydrodynamics. Chemical Engineering Science 55(9), 1523-1532.

Cobb, M.D. and Macoubrie, J. (2004) Public perceptions about nanotechnology: Risks, benefits and trust. Journal of Nanoparticle Research 6(4), 395-405.

Farokhzad, O.C. and Langer, R. (2009) Impact of nanotechnology on drug Delivery. ACS Nano 3(1), 16-20.

Franchi, A. and O'Melia, C.R. (2003) Effects of natural organic matter and solution chemistry on the deposition and reentrainment of colloids in porous media. Environmental Science & Technology 37(6), 1122-1129.

Hahn, M.W. and O'Melia, C.R. (2004) Deposition and reentrainment of Brownian particles in porous media under unfavorable chemical conditions: Some concepts and applications. Environmental Science & Technology 38(1), 210-220.

Jaisi, D.P., Saleh, N.B., Blake, R.E. and Elimelech, M. (2008) Transport of single-walled carbon nanotubes in porous media: Filtration mechanisms and reversibility. Environmental Science & Technology 42(22), 8317-8323.

Lecoanet, H.F., Bottero, J.Y. and Wiesner, M.R. (2004) Laboratory assessment of the mobility of nanomaterials in porous media. Environmental Science & Technology 38(19), 5164-5169.

Lecoanet, H.F. and Wiesner, M.R. (2004) Velocity effects on fullerene and oxide nanoparticle deposition in porous media. Environmental Science & Technology 38(16), 4377-4382.

Li, Y.S., Wang, Y.G., Pennell, K.D. and Abriola, L.M. (2008) Investigation of the transport and deposition of fullerene (C_{60}) nanoparticles in quartz sands under varying flow conditions. Environmental Science & Technology 42(19), 7174-7180.

Mu, L. and Sprando, R.L. (2010) Application of nanotechnology in cosmetics. Pharmaceutical Research 27(8), 1746-1749.

Nowack, B. and Bucheli, T.D. (2007) Occurrence, behavior and effects of nanoparticles in the environment. Environmental Pollution 150(1), 5-22.

Petosa, A.R., Jaisi, D.P., Quevedo, I.R., Elimelech, M. and Tufenkji, N. (2010) Aggregation and deposition of engineered nanomaterials in aquatic environments: Role of physicochemical interactions. Environmental Science & Technology 44(17), 6532-6549.

Project on Emerging Nanotechnologies (2014) Consumer products inventory. Available at http://www.nanotechproject.org/cpi/about/analysis.

Ryan, J.N. and Elimelech, M. (1996) Colloid mobilization and transport in groundwater. Colloids and Surfaces A-Physicochemical and Engineering Aspects 107, 1-56.

Saleh, N., Kim, H.J., Phenrat, T., Matyjaszewski, K., Tilton, R.D. and Lowry, G.V. (2008) Ionic strength and composition affect the mobility of surface-modified Fe-0 nanoparticles in water-saturated sand columns. Environmental Science & Technology 42(9), 3349-3355.

Serrano, E., Rus, G. and Garcia-Martinez, J. (2009) Nanotechnology for sustainable energy. Renewable & Sustainable Energy Reviews 13(9), 2373-2384.

Shen, C.Y., Lazouskaya, V., Jin, Y., Li, B.G., Ma, Z.Q., Zheng, W.J. and Huang, Y.F. (2012) Coupled factors influencing detachment of nano- and micro-sized particles from primary minima. Journal of Contaminant Hydrology 134, 1-11.

Solovitch, N., Labille, J., Rose, J., Chaurand, P., Borschneck, D., Wiesner, M.R. and Bottero, J.Y. (2010) Concurrent aggregation and deposition of TiO_2 nanoparticles in a sandy porous media. Environmental Science & Technology 44(13), 4897-4902.

Tobiason, J.E. (1987) Physicochemical aspects of particle deposition in porous media, Johns Hopkins University, Baltimore, MD.

Tolaymat, T.M., El Badawy, A.M., Genaidy, A., Scheckel, K.G., Luxton, T.P. and Suidan, M. (2010) An evidence-based environmental perspective of manufactured silver nanoparticle in syntheses and applications: A systematic review and critical appraisal of peer-reviewed scientific papers. Science of the Total Environment 408(5), 999-1006.

Walser, M. (1961) Ion Association .5. Dissociation constants for complexes of citrate with sodium, potassium, calcium, and magnesium ions. Journal of Physical Chemistry 65(1), 159-161.

Wang, P., Shi, Q.H., Liang, H.J., Steuerman, D.W., Stucky, G.D. and Keller, A.A. (2008a) Enhanced environmental mobility of carbon nanotubes in the presence of humic acid and their removal from aqueous solution. Small 4(12), 2166-2170.

Wang, Y.G., Li, Y.S., Fortner, J.D., Hughes, J.B., Abriola, L.M. and Pennell, K.D. (2008b) Transport and retention of nanoscale C_{60} aggregates in water-saturated porous media. Environmental Science & Technology 42(10), 3588-3594.

Zhang, T. (2012) Modeling of nanoparticle transport in porous media, The University of Texas at Austin.

Zhu, W., Bartos, P.J.M. and Porro, A. (2004) Application of nanotechnology in construction - Summary of a state-of-the-art report. Materials and Structures 37(273), 649-658.

Chapter 7: CONCLUSIONS

Since it can be expected that an increasing number of engineered nanoparticles will be discharged into natural waters, the fate and transport of nanoparticles in waters has become an important research topic. This study focused on the transport and attachment of AgNPs in granular media filtration. Most of the previous work in this area was conducted to simulate groundwater flow conditions and used high nanoparticle concentration (in the mg/L range). In this research, high filtration velocity (~2 m/hr) and low influent AgNP concentration (~100 μg/L) were employed to emulate the presumed conditions that would be encountered in a drinking water treatment plant. The recovered Ag mass of all tests was above 90% of the injected AgNPs, verifying that the AgNP analytical method was appropriate. The significance of this study was to broaden the scientific understanding of attachment and transport of nanoparticles in granular media filtration. Further, the implicit aim of this study was to revisit the existing treatment technology as an option to treat emerging pollutants such as engineered nanoparticles instead of developing a novel technology. The main findings of the research are presented below.

In Chapter 3, the theoretical prediction of nanoparticle transport was evaluated using the experimental data obtained under favorable attachment conditions. The main findings from that work include the following:

- The interaction of positively charged BPEI AgNPs and negatively charged glass beads showed no energy barrier in terms of electrostatic interaction, and, therefore, the attachment efficiency (α) was assumed to be 1.

142

- Aggregation of the BPEI AgNPs was prevented at the chemical condition of I=1 mM of $NaNO_3$ and pH 7.

- The favorable attachment conditions between the positive BPEI AgNPs and the negative glass beads was true at all of the chemical conditions utilized, so that almost identical breakthrough curves were obtained at different ionic strengths (I=1~20 mM of $NaNO_3$) and pH values (7 and 9).

- The filtration efficiency decreased as the filter depth decreased (from 8 to 2 cm), the velocity increased (from 2 to 8 m/hr), and filter media size increased (from 325 to 776 μm).

- When using the mean (TEM) diameter for the model predictions, the transport of 100 nm BPEI AgNPs in granular media filtration showed good agreement with the expectations from the colloidal filtration model of Tufenkji and Elimelech (2004), proving the validity of the model. However, as the particles decreased to 50 and 10 nm, the experimental results tended to move toward the predictions using the (larger) hydrodynamic diameter.

To study the chemical effect on attachment or detachment of AgNPs onto glass beads in granular media filtration, a series of filtration tests was conducted at 10 cm filter depth, 2 m/hr filtration velocity, 325 μm filter media, and 50 nm citrate- or PVP-capped AgNPs in the remaining part of the research. In all cases, both the particles and the media were negatively charged (unless the chemical conditions caused charge neutralization).

In Chapter 4, the attachment of AgNPs onto glass beads was investigated under different ionic strengths and ion types in the background solution. The experimental results were described using the DLVO theory, and the major findings are as follows:

- The attachment of citrate AgNPs was enhanced as the ionic strength increased from 1 to 10 mM of $Ca(NO_3)_2$ or 10 mM to 100 mM of $NaNO_3$.

- At the same ionic strength, the attachment of citrate AgNPs was greater with Ca or Mg ions rather than Na ions, and this result suggests that charge neutralization occurred by Ca- or Mg-citrate complexation on the AgNP surface.

- Ripening was favored at the top of the filter bed when the ionic strength was high enough to cause AgNP aggregation. On the other hand, chemical conditions that led to stable AgNPs resulted in uniform AgNP capture throughout the filter bed.

- The attachment of PVP AgNPs was insignificantly affected by the electrostatic effect resulting from different ionic strengths and ion types, indicating the strong ability of PVP to stabilize particles.

In Chapter 5, the effect of NOM on the attachment of AgNPs was investigated. Suwannee River humic and fulvic acids were chosen as the representative types of NOM and were applied to yield 3.5 mg TOC/L background water. Both AgNPs and filter media were pre-coated with NOM for 24 hours prior to each test. The filtration tests were conducted under varying NOM type, capping agent type, and pH. The following conclusions were reached:

- The mixing of AgNPs with NOM for 24 hours resulted in a negligible size change. Monitoring the AgNP surface potential over 24 hours suggested that the NOM adsorption happened very rapidly.

- NOM coating led to more negative surface charge of AgNPs, but, surface charge neutralization occurred with I=10 mM of $Ca(NO_3)_2$ regardless of the capping agent and NOM type.

- Though the electrostatic effect was not enhanced by NOM coating, the overall removal efficiency was lowered by NOM coating, indicating a dominant steric effect.

- The humic acid coating resulted in lower removal efficiency than the fulvic acid coating, probably due to the greater steric hindrance caused by the greater molecular weight of humic acid.

- The removal efficiency of humic acid coated-AgNPs was similar regardless of capping agent type, implying a possible displacement of capping agent and/or a complete coverage by NOM coating.

- The effect of pH (between 7 and 9) was insignificant on the removal of NOM-coated AgNPs at I=10 mM of $Ca(NO_3)_2$, which demonstrates the decreased electrostatic repulsion by the Ca ion bindings with carboxylic groups.

In Chapter 6, the detachment of captured AgNPs (after a substantial period of attachment) was tested either by lowering ionic strength or by increasing filtration velocity. The one dimensional filtration model was incorporated with the experimental results to estimate the detachment coefficient (k_{det}). The conclusive statements are as follows:

- The most significant detachment occurred by lowering ionic strength from 100 mM to 0.025 mM of $NaNO_3$. Detachment was insignificant by lowing ionic strength from 10 mM to 0.025 mM of $Ca(NO_3)_2$. Both of these results were consistent with the concept that particles captured in the region of the

secondary energy minimum would become detached, but that those captured in the primary energy minimum would not detach.

- Detachment was enhanced in the presence of NOM, presumably due to a weak deposition caused by steric hindrance.

- The filtration velocity increase resulted in a negligible amount of detachment, indicating that the filtration velocity range adopted in this study was insufficient to cause a noticeable AgNP detachment.

- The experimental results were well-fitted by the 1-D model, and the estimated detachment coefficients from the model provided information that the detachment capacity was comparable regardless of the amount of captured AgNPs.

Significance

This study contributed to expanding the knowledge on the attachment and transport of nanoparticles in granular media filtration. The experimental evidence of the capture of AgNPs in granular media filtration indicated that the existing colloidal filtration theory is appropriate for nanoparticles greater than 50 nm, but it also pointed out the conceivable size dependent properties of nanoparticles, which change at smaller size such as 10 nm.

The findings in this study are relevant to the design and operation of a granular media filter that would encounter nanoparticles. Near-complete nanoparticle removal would be achievable by controlling the physical and/or chemical conditions. However, when the removal is high, most deposition could happen at the top of the filter bed due to

the aggregation-prone condition. As long as a long-term operation is concerned, the ripening aspect needs to be considered along with the sufficient removal efficiency.

This study employed a simplified analytical method compared to the well-known Standard Method, and the experimental results successfully demonstrated at least 90% Ag recovery. Since the sample dissolution in acid followed by ICP-OES could save time and reduce the possible experimental errors, this method can be adopted in studies of other types of metal-based nanoparticles.

Recommendations for future work

This study was originated on the prediction that increasing numbers of nanoparticles in surface waters would eventually reach the granular media filter in water treatment plants. As more research outcomes were released focusing on the fate of AgNPs in the environment, sulfidized AgNPs were proposed as a major form that would exist in the environment. Also, the presence of Cl ions in water could stimulate the dissolution and speciation of AgNPs. Therefore, more research efforts are needed to elucidate the fate of nanoparticles in both natural and engineered systems. It is also desirable to study the possible removal mechanisms of nanoparticles throughout their pathway in the environment.

Regarding experimental materials, ensuring a consistent surface property of nanoparticles and filter media is critical to obtaining reproducible results. Normally, filter media are washed and reused for a subsequent test. However, depending on the filter media rinsing process, the surface property of filter media could be changed and eventually affect the attachment efficiency (α). In addition, it is difficult to have an identical surface property from nanoparticles synthesized in different batches. If the

147

attachment efficiency (α) is affected only by the experimental variables being tested but also by the particle surface property resulting from the preparation, it would be difficult to estimate the accurate attachment efficiency (α) under unfavorable attachment conditions. Therefore, it is highly recommended to prepare sufficient amount of nanoparticles and filter media at once and use them for a series of tests without re-synthesizing or reusing.

As discussed in Chapter 3, the size dependent nanoparticle property was suggested and it would be critical for the further applications of nanoparticles. In terms of granular media filtration of nanoparticles, more experimental results of nanoparticles in the range of 10 to 30 nm are required to update the colloidal filtration model in such a small size. A successful update would extend the applicability of the colloidal filtration model toward nanoparticles, providing more accurate prediction on the transport of nanoparticles.

In terms of nanoparticle characterization, multiple instruments have been adopted to measure nanoparticle size and surface properties. However, the surface property of particles such as adsorbed macromolecule thickness has relied on theoretical estimation rather than experimental measurement. Therefore, more advances in analytical technology, especially in direct observation using microscopy are required to precisely analyze the surface of nanoparticles.

Appendix A: Research of nanoparticle transport in porous media

Table A1:   List of articles on nanoparticle transport in porous media.

Reference	Nanoparticle Kind	Nanoparticle Size (nm)	Media Kind	Media Size (μm)	Filter Diameter (mm)	Filter Depth (cm)	Filtration velocity[a] (m/hr)	pH	Ionic strength (M)	Influent concentration (mg/L)	NOM
(Cornelis et al. 2013)	AgNPs	10	Soil	~2000	15	12	0.3384	7, 9	10^{-3}	1.7	No
(El Badawy et al. 2013)	AgNPs	10 ~ 12	Quartz sand	360	11	10	0.63	7.0	5×10^{-3}	10	No
(Flory et al. 2013)	AgNPs	15.6	Glass bead	425~600	25	5	0.1224	4, 6.5, 9, 11	10^{-5}	15	No
(Li et al. 2013)	AgNPs	10, 12	Sand	500, 700	25	15	2.322	7.2	5.5×10^{-3}	45,55	No
(Liang et al. 2013a)	AgNPs	45 ~ 78	Soil	N.A.	80	10	0.0036 , 0.0119	6 ~ 7	10^{-3}, 5×10^{-3},10^{-2}	1, 10	No
(Liang et al. 2013b)	AgNPs	15 ~ 20	Quartz sand	240, 350, 607	30	12	0.018 ~ 0.421	6 ~ 7	10^{-3}, 2.5×10^{-3}, 5×10^{-3}	10, 30	No
(Lin et al. 2011)	AgNPs	12	Glass bead	409	10	6	0.72	5.0, 8.3	10^{-3} ~ 5×10^{-2}	N.A.	No
(Lin et al. 2012)	AgNPs	5.4 ~ 27.7	Glass bead	360	10	4	0.72	6.9 ~7.2	10^{-3} ~ 10^{-1}	N.A.	No
(Neukum et al. 2014)	AgNPs	25	Sandstone	100~200	50	3	$3.03*10^{-5}$ ~ 0.0896	6~7 ,6	10^{-5}, 10^{-4}, 10^{-3} 10^{-2}	441~800	No
(Ren and Smith 2013)	AgNPs	49.8	Ottawa sand	180, 340, 550	10	15	0.4572	6.7	~ 5×10^{-2}	50	No
(Sagee et al. 2012)	AgNPs	30	Quartz sand	210-300	31	10	0.396 ~ 0.102	7.5	N.A.	N.A.	No
(Song et al. 2011)	AgNPs	10	Glass bead	350	10	10	0.72	8.1	2×10^{-2}	50	No
(Taghavy et al. 2013)	AgNPs	12	Ottawa sand	360	25	16	0.1224	4, 7	10^{-2}	2.51 ~ 3.17	No
(Tian et al. 2010)	AgNPs	52.4	Quartz sand	500	25	15	0.1188	N.A.	N.A.	100	No
(Xiao and Wiesner 2013)	AgNPs	19, 36	Glass bead	N.A.	10	10	0.3816	N.A.	10^{-3}	N.A.	No
(Yang et al. 2014)	AgNPs	40	Glass bead	360	10	N.A.	N.A.	7.0	10^{-3}, 10^{-2},3×10^{-1}	1.5	Yes
(Rahman et al. 2013)	AlO	18.4	Quartz sand	250	15	7	0.072 ~ 0.864	4.8	10^{-3}, 10^{-2},10^{-1}	50, 150, 400	No
(Liu et al. 2009b)	Boron	10 ~ 20	Quartz sand	212-270	15	15	1.368	5.6	10^{-2} ~ 4×10^{-1}	50	No
(Brant et al. 2005)	C_{60}	168	Glass bead	355	N.A.	9.25	1.44	7	10^{-3} ~ 10^{-1}	10	No
(Cai et al. 2013)	C_{60}	135 ~ 505	Quartz sand	417~600	20	10	0.0576	5, 7	10^{-4} ~ 10^{-2}	10	No
(Cheng et al. 2005)	C_{60}	~ 100	Surface soil	250	9	5	0.0158 ~ 0.475	6.7 ~ 7.2	2×10^{-2}	48	No
(Espinasse et al. 2007)	C_{60}	92	Glass bead	360	26.5	10	1.44 ~ 4.32	6.5 ~ 7.5	0.01 ~ 0.6	7 ~ 25	No
(Jaisi and Elimelech 2009)	C_{60}	122, 50.5	Surface soil	420~1000	16	4.3	0.792	5.6 ~ 5.8	10^{-3}	N.A.	No
(Lecoanet and Wiesner 2004)	C_{60}	168	Glass bead	355	25	9.25	1.44 ~ 5.04	7	10^{-2}	10	No
(Li et al. 2008)	C_{60}	120	Ottawa sand	125, 165, 355, 710	25	15	0.0183 ~ 0.139	7	0.003065	3	No
(Qu et al. 2012)	C_{60}	162	Quartz sand	250 ~ 300	15	5	0.03397	6	10^{-3} ~ 2×10^{-2}	5	Yes
(Wang et al. 2008b)	C_{60}	95	Ottawa sand, glass bead	360	25	15	0.307	7	10^{-3}	1.3 ~ 3.1	No
(Wang et al. 2008c)	C_{60}	92	Quartz sand	125, 335	25	15	0.126 ~ 0.133	7	3×10^{-3} ~ 3×10^{-2}	2.5 ~ 3.27	No
(Wang et al. 2012b)	C_{60}	94.2	Ottawa sand	360	25	15	0.122	7	5×10^{-5} ~ 10^{-3}	3.9 ~ 5.0	Yes

Reference	Material	Size (nm)	Porous media	Grain size				pH	Ionic strength	Concentration	Coated
(Zhang et al. 2012b)	C_{60}	172	Quartz sand	361	15	7	0.168 ~ 0.258	7.5 ~8	10^{-2}	0.06 ~ 10.3	No
(Zhang et al. 2012a)	C_{60}	175	Ottawa sand	250	6.6	6.0~6.8	0.0292 ~ 0.292	6.5 ~ 7.5	$10^{-3} \sim 10^{-2}$	N.A..	Yes
(Li et al. 2011)	CeO_2	62.6	Silica sand	717	25.4	45	6.948	3, 6, 9	$10^{-1} \sim 10^{-}$	10, 50	No
(Liu et al. 2012)	CeO_2	4.6	Ottawa sand	250-300	25	15	0.475	4, 6, 8.5	10^{-2}	1 ~ 6	Yes
(Busch et al. 2014)	C-nZVI	2400	Quartz sand / Glass bead	100~500 / 250~510	35	10	5.004	4, 6, 7.5, 10, 12	3×10^{-2}, 5×10^{-2}, 2×10^{-1}, 4×10^{-1}	500	No
(Jones and Su 2012)	Cu^0	25	Sand	256	15	30	0.940	7, 9.1	$10^{-3} \sim 10^{-}$	4.32 ~ 11.15	Yes
(Jeong and Kim 2009)	CuO	372	Etched glass	870	N.A.	11.3	0.072 ~ 0.72	7.0	10^{-2}	9	No
(Hydutsky et al. 2007)	Fe^0	50 ~ 100	Sand	160	16	71	1.512 ~ 3.024	N.A.	N.A.	5000	No
(Kanel et al. 2007)	Fe^0	10 ~ 160	Sand	425-600	25	10	0.220	7.0	10^{-2}	0.2, 0.5, 1	No
(Kim et al. 2009)	Fe^0	~ 20	Silica sand	300	10.9	12.5	3.96	N.A.	5×10^{-3}	1000	No
(Kim et al. 2012)	Fe^0	20	Silica sand	300	12.5	15	1.152	6, 7, 8	$10^{-3} \sim 10^{-2}$	300	No
(Phenrat et al. 2009)	Fe^0	41 ~ 63	Silica sand	300	10.9	25.5	0.562	8.0	10^{-2}	30 ~ 6000	No
(Saleh et al. 2007)	Fe^0	146	Silica sand	300	10.9	12.5	3.96	7.4	$10^{-3} \sim 10^{-}$	3000	No
(Saleh et al. 2008)	Fe^0	146	Silica sand	300	11	61.3	1.152	7.7	$10^{-5} \sim 1$	30	No
(Schrick et al. 2004)	Fe^0	30 ~ 100	Ottawa sand	200~700	12	13	7.2 ~ 10.8	6.7	N.A.	5000	No
(Tiraferri and Sethi 2009)	Fe^0	357	Quartz sand	263	16	7	0.0994 ~ 0.497	7.4	$10^{-3} \sim 10^{-}$	154	No
(Zhan et al. 2008)	Fe^0	30 ~ 70	Ottawa sand	300	1.5-1.8	3	3.00	N.A.	N.A.	3000	No
(He et al. 2007)	Fe-Pd nanoparticles	4.3, 14.1	Soil	N.A.	10	3.4	0.150	N.A.	N.A.	1000	No
(Lecoanet et al. 2004)	Ferroxane, etc.	300	Glass bead	355	25	9.25	1.44	7	10^{-2}	10	No
(Tosco et al. 2012)	Ferrihydrite	106.7	Quartz sand	194	16	11.2	0.279 ~ 0.839	8	$\sim 10^{-2}$	7.5	No
(Espinasse et al. 2007)	Fullerols	120	Glass bead	360	26.5	10	1.44, 4.32	6.5 ~ 7.5	$10^{-5} \sim 1$	18	No
(Lecoanet and Wiesner 2004)	Fullerols	1.2	Glass bead	355	25	9.25	1.44 ~ 5.04	7	10^{-2}	10	No
(Lecoanet et al. 2004)	Fullerols	1.2	Glass bead	355	25	9.25	1.44	7	10^{-2}	10	No
(Kasel et al. 2013)	MWNT	170 ~ 210	Quartz sand	240, 350, 607	30	12	0.371 ~ 0.396	8.5	10^{-3}	0.005, 0.01, 1	No
(Liu et al. 2009a)	MWNTs	7 ~ 70	Quartz sand	476	50	10	0.0175	10	$10^{-4} \sim 10^{-2}$	N.A.	No
(Tian et al. 2012)	MWNT	175	Quartz sand	100~200, 500~600	25	15	0.244	5.6, 10	$10^{-3} \sim 10^{-}$	N.A.	No
(Doshi et al. 2008)	nAl	100	Silica sand	N.A.	15	16	0.0850	4, 7	10^{-2}	50	No
(Elimelech and Omelia 1990)	Polystyrene latex	46	Glass bead	200, 400	N.A.	20	5.04	6.7	$3 \times 10^{-3} \sim 3 \times 10^{-2}$	1 ~ 4	No
(Franchi and O'Melia 2003)	Polystyrene latex	98	Glass bead	200	25	25	4.572	7.2	$10^{-3} \sim 5 \times 10^{-1}$	1	Yes
(Hahn and O'Melia 2004)	Polystyrene latex	80, 308	Glass bead	400	25	20	4.896	5 ~ 10	10^{-2}	1	No
(Huber et al. 2000)	Polystyrene latex	53~193	Munich gravel	250	100	20	0.174 ~ 0.187	N.A.	$10^{-3} \sim 10^{-}$	N.A.	No
(Pelley and Tufenkji 2008)	Polystyrene latex	50, 110, 1500	Quartz sand	256	10	15	0.763	5.7	$10^{-3} \sim 10^{-}$	N.A.	Yes
(Shani et al. 2008)	Polystyrene latex	20	Dune sand	310-320	54	20	0.0601	7 ~ 8	$3 \times 10^{-3} \sim 4 \times 10^{-3}$	N.A.	No
(Shen et al. 2008)	Polystyrene latex	30.66	Glass bead	110, 220, 720	38	10	0.223	10	2×10^{-4}	10, 40	No
(Tripathi et al. 2012)	Polystyrene latex	20, 1000	Quartz sand	763	16	8	0.238	7.2	10^{-2}	N.A.	No
(Tufenkji and Elimelech 2005)	Polystyrene latex	63	Glass bead	330	16	12.6	0.299	8, 11	$2 \times 10^{-2} \sim 2 \times 10^{-1}$	N.A.	No
(Zhuang et al. 2005)	Polystyrene latex	20, 100	Quartz sand	300-355	45	10	0.0652 ~ 0.172	7.5	10^{-3}	100	No
(Torkzaban et	Quantum	1 ~	Sand	270	25	10	0.522	8.0	2×10^{-3},	N.A.	No

al. 2013)	dot	10							10^{-2}		
(Wang et al. 2013)	Quantum dot	5 ~ 18	Ottawa sand	354	25	10	0.122	5, 7, 9	3×10^{-3}, 3×10^{-2}, 10^{-2}	0.0013 ~ 0.0025	No
(Lecoanet et al. 2004)	SiO_2	47, 103	Glass bead	355	25	9.25	1.44	7	10^{-2}	10	No
(Lecoanet and Wiesner 2004)	SiO_2	57	Glass bead	355	25	9.25	1.44 ~ 5.04	7	10^{-2}	10	No
(Wang et al. 2012a)	SiO_2	8, 52	Silica sand	220	38.5	10	0.0526	10	10^{-3} ~ 2×10^{-1}	60 ~ 6000	No
(Jaisi and Elimelech 2009)	SWNTs	244	Glass bead	420~1000	16	4.3	0.792	5.6 ~ 5.8	10^{-3}	N.A.	No
(Jaisi et al. 2008)	SWNTs	1.25	Quartz sand	263	16	6.3	0.655	7.0	10^{-4} ~ 5.5×10^{-2}	87	Yes
(Lecoanet and Wiesner 2004)	SWNTs	0.7 ~ 1.1	Glass bead	355	25	9.25	1.44 ~ 5.04	7	10^{-2}	10	No
(Lecoanet et al. 2004)	SWNTs	0.7 ~ 1.1	Glass bead	355	25	9.25	1.44	7	10^{-2}	10	No
(Wang et al. 2008a)	SWNTs, MWNTs	1.4, 35	Quartz sand	350	25	15	0.119	N.A.	10^{-4} ~ 10^{-2}	25 ~ 53	Yes
(Ben-Moshe et al. 2010)	TiO_2	190	Glass bead	1000	35	20	0.0371 ~ 0.312	7, 10, 12	10^{-3} ~ 10^{-1}	N.A.	Yes
(Cai et al. 2013)	TiO_2	25	Quartz sand	417~600	20	10	0.0576	5, 7	10^{-4} ~ 10^{-2}	50	No
(Chen et al. 2008)	TiO_2	21	Glass bead	500	25.4	1.27	0.000308 ~ 0.0225	10	2×10^{-4}	25	No
(Chen et al. 2012)	TiO_2	10 ~ 40	Sand	275	25	10	0.1836	5.7, 9	3×10^{-3} ~ 2×10^{-1}	20	Yes
(Chowdhury et al. 2011)	TiO_2	18.4	Quartz sand	275	48	15	0.684, 3.42	5, 7	10^{-3} ~ 10^{-2}	100 ~ 800	No
Choy et al., 2008	TiO_2	< 100	Quartz sand	200	15	30	1.8 ~ 8.46	4.5	10^{-5}	50, 75, 100	No
(Fang et al. 2009)	TiO_2	35	Surface soil (12 kinds)	30 ~ 132	25	10	0.00108 ~ 0.0504	6.15 ~ 8.58	2×10^{-4} ~ 5×10^{-3}	2000	No
(Godinez et al. 2013)	TiO_2	19	Sand	307	9	15	1.739, 3.481	9	10^{-3}, 10^{-2}, 10^{-1}	25	No
(Guzman et al. 2006)	TiO_2	5 ~ 12	Pyrex wafer	700	30	7	0.54 ~ 0.576	1, 3, 7, 10, 12	N.A.	70 ~ 140	No
(Han et al. 2014)	TiO_2	25	Quartz sand	510	20	10	0.0225	5, 7	10^{-4} ~ 10^{-2}	50	Yes
(Joo et al. 2009)	TiO_2	10	Quartz sand	290	11	10	0.316	5.5, 7.0	10^{-3} ~ 3×10^{-2}	20	No
(Lecoanet et al. 2004)	TiO_2	40	Glass bead	355	25	9.25	1.44	7	10^{-2}	10	No
(Petosa et al. 2012)	TiO_2	5	Quartz sand	256	16	3, 10	0.1501	7, 8	10^{-4} ~ 1	N.A.	No
(Rottman et al. 2013)	TiO_2	21	Quartz sand	190	15	15	0.882	7	10^{-3}	50	No
(Solovitch et al. 2010)	TiO_2	32	Silica sand	650	47	7	0.0000216	3.5 ~ 8.0	10^{-3} ~ 10^{-1}	50	No
(Wang et al. 2012c)	TiO_2	30	Quartz sand	550	25	16.5	0.299	7.3, 8.3, 10.3	10^{-4} ~ 10^{-1}	10	No
(Jiang et al. 2012)	ZnO	20	Quartz sand	510	40	20	0.588	8	10^{-4} ~ 2×10^{-2}	5	Yes
(Jiang et al. 2013)	ZnO	20	Quartz sand	510	40	20	0.166, 0.335	8	10^{-4} ~ 2×10^{-2}	5	No
(Kanel and Al-Abed 2011)	ZnO	~ 100	Quartz sand	150 ~ 425	11	10	0.63	3, 7, 9, 11	1×10^{-4}	20	No

[a]filtration velocity (v_0) = volumetric flow rate (Q) / cross sectional area of filter bed (A_c)

Appendix B: Parameters and symbols

$$A_S = \frac{2(1-\gamma^5)}{2-3\gamma+3\gamma^2-2\gamma^6}$$ Porosity-dependent parameter

$$D_\infty = \frac{kT}{6\pi\mu a_p}$$ Diffusion coefficient

$$N_A = \frac{A}{12\pi\mu a_p^2 v_0}$$ Attraction number

$$N_{col} = \frac{\kappa A}{\varepsilon_0 \varepsilon_r \zeta_p \zeta_c}$$ Stability parameter

$$N_{DL} = \kappa d_p$$ Double layer force parameter

$$N_{E1} = \frac{\varepsilon_0 \varepsilon_r (\zeta_p^2 + \zeta_c^2)}{3\pi\mu v_0 d_p}$$ 1st electrokinetic parameter

$$N_{E2} = \frac{2\zeta_p \zeta_c}{(\zeta_p^2 + \zeta_c^2)}$$ 2nd electrokinetic parameter

$$N_G = \frac{2a_p^2 (\rho_p - \rho_f) g}{9\mu v_0}$$ Gravity number

$$N_{Gi} = \frac{1}{N_G + 1}$$ Revised gravity number (Nelson and Ginn, 2011)

$$N_{LEK} = \frac{d_p d_M^2 v_0 \Gamma N_a \rho_p}{\mu M_W}$$ Layer electrokinetic parameter

$$N_{Lo} = \frac{4A}{9\pi\mu d_p^2 v_0}$$ London number

$$N_{Pe} = \frac{v_0 d_c}{D_\infty}$$ Peclet number

$$N_R = \frac{d_p}{d_c}$$ Aspect ratio

$$N_{vdW} = \frac{A}{kT}$$ van der Waals number

A	Hamaker constant (J)
A_c	Cross section area of differential slice of a packed bed (cm^2)
a_c	Media radius (μm)
a_p	Particle radius (nm)
C	Fluid-phase particle mass concentration (mg/L)
D	Particle diffusion coefficient (cm^2/s)
d_c	Media diameter (μm)
d_M	Macromolecule adsorbed layer thickness (nm)
d_p	Particle diameter (nm)
dz	Height of differential slice of a packed bed (cm)
g	Gravitational acceleration (cm/s^2)
I	Ionic strength (mM)
K	Boltzmann constant ($g \cdot cm^2/s^2$-K)
M_w	Macromolecule molecular weight
N	Fluid-phase particle number concentration (#/L)
N_a	Avogadro's number (#/mol)
Q	Volumetric flow rate (mL/min)
s	Separation distance (nm)
S	Solid-phase particle concentration (μg/g)
T	Absolute temperature (K)
v_0	Fluid velocity (m/hr)

α	Attachment efficiency (-)
ε	Porosity (-)
$\varepsilon_0\,\varepsilon_r$	Permittivity in water (C^2/J-m)
ζ_c	Zeta potential of a media (mV)
ζ_p	Zeta potential of a particle (mV)
η	Single collector removal efficiency (-)
η_0	Single collector contact efficiency (-)
κ	Inverse characteristic length of diffuse layer (1/nm)
λ	Characteristic wavelength (nm)
μ	Fluid viscosity (g/cm-s)
ρ_c	Media density (g/cm^3)
ρ_f	Fluid density (g/cm^3)
ρ_p	Particle density (g/cm^3)
Ψ_c	Surface potential of a media (mV)
Ψ_p	Surface potential of a particle (mV)
Γ	Surface excess concentration (mg/m^2)

Appendix C: Supporting information for 1-D advection-diffusion model

Using a finite difference scheme, equation 6-6 can be written as:

$$
\begin{aligned}
\frac{N_i^{n+1} - N_i^n}{\Delta t} &= \frac{D}{2\Delta x^2}\left(N_{i+1}^{n+1} - 2N_i^{n+1} + N_{i-1}^{n+1} + N_{i+1}^{n} - 2N_i^{n} + N_{i-1}^{n}\right) \\
&\quad - \frac{v_0}{2\Delta x}\left(N_i^{n+1} - N_{i-1}^{n+1} + N_i^{n} - N_{i-1}^{n}\right) \\
&\quad - \frac{k_{att}}{2}(N_i^{n+1} + N_i^{n}) + k_{att}k_{det}t_0 N_0 \exp\left(-\frac{k_{att}}{v_0}\Delta x(i-1)\right)
\end{aligned}
\tag{C1}
$$

where n is number of time step, i is number of space step, Δt is time step (5 sec) and Δx is space step (0.1 cm). The effluent concentration at the outlet of the filter was simulated until 90 min.

This model used the first order attachment kinetics assuming that the available deposition area on the filter media was greater than the total surface area of AgNPs injected. The total surface area of 325 μm filter media in 10 cm filter depth was compared to the total surface area of 50 nm AgNPs injected during the filtration test (Table C1).

Total surface area = Number of particle × Surface area of a particle

The AgNP number concentration was adopted from the product details (Appendix D) and the porosity of filter bed was assumed to be 0.42.

Table C1:   Comparison of total surface areas of filter media and AgNPs.

	Number of particles used	Surface area (cm^2)	
		Single particle	Total
Filter media	3.68×10^6	3.32×10^{-3}	1.22×10^4
Citrate AgNPs	6.60×10^{13}	8.99×10^{-11}	5.93×10^3
PVP AgNPs	9.00×10^{13}	7.82×10^{-11}	7.04×10^3

Appendix D: Product information of silver nanoparticles (AgNPs) and glass beads

Table D1:   Product information of citrate- and PVP-capped AgNPs (from Nanocomposix, Inc.).

	Citrate AgNPs	PVP AgNPs
Diameter (TEM)	53.5±4.4 nm	49.9±4.6 nm
Hydrodynamic diameter (DLS)	56.0 nm	63.6 nm
Zeta potential	-53.6 mV (at pH 6.9)	-53.5 mV (at pH 6.2)
Particle concentration	$1.1×10^{12}$ particles/mL	$1.5×10^{12}$ particles/mL
Solvent	2 mM citrate water	Milli-Q water

Table D2:   Product information of 10, 50, and 100 nm BPEI-capped AgNPs (from Nanocomposix, Inc.).

	10 nm BPEI AgNPs	50 nm BPEI AgNPs	100 nm BPEI AgNPs
Diameter (TEM)	8.3±2.2 nm	45.8±3.8 nm	99.4±8.2 nm
Hydrodynamic diameter (DLS)	32.9 nm	90.4 nm	142.0 nm
Zeta potential	12.4 mV (at pH 9.8)	39.3 mV (at pH 9.6)	40.0 mV (at pH 9.3)
Particle concentration	$3.3×10^{14}$ particles/mL	$2.1×10^{12}$ particles/mL	$2.0×10^{11}$ particles/mL
Solvent	Milli-Q water	Milli-Q water	Milli-Q water

Product information of glass beads is as follows (from MO-SCI, Inc.).

pH in water	7.8
Bulk density of dry beads (specific gravity)	1.3 g/cm^3 (2.5 g/cm^3)
Softening temperature	650 ˚C
Coefficient of thermal expansion	90×10^{-7} /˚C
Compression strength	29 kg/mm^2 (39,875 psi)
Vicker hardness	550 kg/mm^2 (760,250 psi)
Index of refraction	1.51 (n_D)

Appendix E: Particle size analysis from TEM images

The image processing software "ImageJ" was employed to analyze particle size from TEM images.   ImageJ is a public domain software and free download is available at http://imagej.nih.gov/ij/download.html. The particle size analysis can be performed as follows.

1) Open a TEM image file by selecting File-Open in ImageJ menu. An open image is shown in part (a) of Figure E1.

2) At the bottom of the image, a scale bar is imported with the TEM image. To set the scale in ImageJ, locate the cursor on the scale bar and zoom in the scale bar by hitting 'Ctrl'+'+' until the scale bar is about to fill the image screen. Then, select Straight Line tool from the toolbar and make an identical length on the scale bar by clicking and dragging. Select Analyze-Set scale in menu and Set scale pop-up window comes up. Enter the known distance and unit of length, respectively (e.g., 100 and nm).

3) After closing Set scale pop-up window, right click on the image and select Original scale to return to the original size.

4) Select Image-Adjust-Threshold from the menu and close Threshold pop-up window. If particles are aggregated, the bottom slider which controls maximum brightness can be moved slightly to the left before closing the window.

5) Select Analyze-Analyze Particles from the menu. When Analyze Particle window comes up, enter an appropriate size range and circularity (e.g., 100-5,000 nm^2 and 0.50-1.00). Select Overlay Masks in the Show dropdown box.

6) By clicking Ok in the Analyze window, the Results table opens with particle size analysis data (as shown in part (b) of Figure E1). If two or multiple particles are recognized as one big particle in the image, manually clear the row of such particles in Results table by identifying the corresponding numbers in the image. The second column of the results is the particle area which can be converted into particle diameter in a separate calculation. (Author's note: The particle diameter of each particle was averaged and used as a mean diameter of the TEM image in this study.)

7) Repeat 1) to 6) for two other images taken from the same sample. Average diameters from three images to obtain a representative mean diameter of a sample.
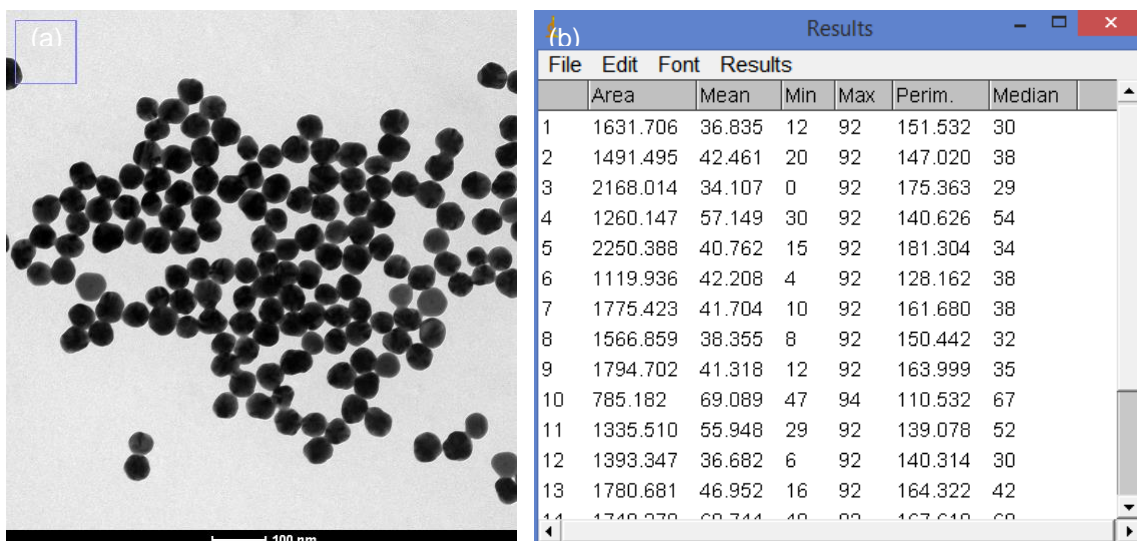
Figure E1: (a) TEM image file opened in ImageJ and (b) an example of particle size analysis in Results window.

Appendix F: Experimental case name conventions

B10	BPEI 10 nm AgNPs
B50	BPEI 50 nm AgNPs
B100	BPEI 100 nm AgNPs
C50	citrate 50 nm AgNPs
P50	PVP 50 nm AgNPs
M325	Media size 325 μm
M463	Media size 463 μm
M776	Media size 776 μm
L2	Filter depth 2 cm
L4	Filter depth 4 cm
L8	Filter depth 8 cm
V2	Filtration velocity 2 m/hr
V4	Filtration velocity 4 m/hr
V8	Filtration velocity 8 m/hr
I1-Ca	Ionic strength 1 mM by $Ca(NO_3)_2$
I5-Ca	Ionic strength 5 mM by $Ca(NO_3)_2$
I10-Ca	Ionic strength 10 mM by $Ca(NO_3)_2$
I10-Mg	Ionic strength 10 mM by $Mg(NO_3)_2$
I10-Na	Ionic strength 10 mM by $NaNO_3$
I100-Na	Ionic strength 100 mM by $NaNO_3$
HA	Coated with humic acid
FA	Coated with fulvic acid
pH 9	Tested at pH 9
I	Detached by ionic strength reduction
V	Detached by filtration velocity increase

REFERENCES

Akaighe, N., MacCuspie, R.I., Navarro, D.A., Aga, D.S., Banerjee, S., Sohn, M. and Sharma, V.K. (2011) Humic acid-induced silver nanoparticle formation under environmentally relevant conditions. Environmental Science & Technology 45(9), 3895-3901.

Anandarajah, A. and Chen, J. (1995) Single correction function for computing retarded van der Waals attraction. Journal of Colloid and Interface Science 176(2), 293-300.

Bai, R.B. and Tien, C. (1999) Particle deposition under unfavorable surface interactions. Journal of Colloid and Interface Science 218(2), 488-499.

Baker, M.N. (1948) Quest for pure water: the history of water purification from the earliest records to the twentieth century, American Water Works Association, New York.

Barisik, M., Atalay, S., Beskok, A. and Qian, S.Z. (2014) Size dependent surface charge properties of silica nanoparticles. Journal of Physical Chemistry C 118(4), 1836-1842.

Beckett, R., Jue, Z. and Giddings, J.C. (1987) Determination of molecular-weight distributions of fulvic and humic acids using flow field-flow fractionation. Environmental Science & Technology 21(3), 289-295.

Benjamin, M.M. and Lawler, D.F. (2013) Water quality engineering: Physical and chemical treatment processes, Wiley.

Ben-Moshe, T., Dror, I. and Berkowitz, B. (2010) Transport of metal oxide nanoparticles in saturated porous media. Chemosphere 81(3), 387-393.

Benn, T.M. and Westerhoff, P. (2008) Nanoparticle silver released into water from commercially available sock fabrics. Environmental Science & Technology 42(18), 7025-7026.

Benn, T., Cavanagh, B., Hristovski, K., Posner, J.D. and Westerhoff, P. (2010) The release of nanosilver from consumer products used in the home. Journal of Environmental Quality 39(6), 1875-1882.

Bergendahl, J. and Grasso, D. (2000) Prediction of colloid detachment in a model porous media: hydrodynamics. Chemical Engineering Science 55(9), 1523-1532.

Bhatt, P.A., Pratap, A. and Jha, P.K. (2013) Size and dimension dependent diffusion coefficients of SnO$_2$ nanoparticles. International Conference on Recent Trends in Applied Physics and Material Science 1536, 237-238.

Bhattacharjee, S., Ko, C.H. and Elimelech, M. (1998) DLVO interaction between rough surfaces. Langmuir 14(12), 3365-3375.

Bian, S.W., Mudunkotuwa, I.A., Rupasinghe, T. and Grassian, V.H. (2011) Aggregation and dissolution of 4 nm ZnO nanoparticles in aqueous environments: influence of pH, ionic strength, size, and adsorption of humic acid. Langmuir 27(10), 6059-6068.

Blaser, S.A., Scheringer, M., MacLeod, M. and Hungerbuhler, K. (2008) Estimation of cumulative aquatic exposure and risk due to silver: Contribution of nano-functionalized plastics and textiles. Science of the Total Environment 390(2-3), 396-409.

Boyd, R.D., Pichaimuthu, S.K. and Cuenat, A. (2011) New approach to inter-technique comparisons for nanoparticle size measurements; using atomic force microscopy, nanoparticle tracking analysis and dynamic light scattering. Colloids and Surfaces A: Physicochemical and Engineering Aspects 387(1), 35-42.

Bradford, S.A., Torkzaban, S. and Walker, S.L. (2007) Coupling of physical and chemical mechanisms of colloid straining in saturated porous media. Water Research 41(13), 3012-3024.

Brant, J., Lecoanet, H. and Wiesner, M.R. (2005) Aggregation and deposition characteristics of fullerene nanoparticles in aqueous systems. Journal of Nanoparticle Research 7(4-5), 545-553.

Busch, J., Meißner, T., Potthoff, A. and Oswald, S.E. (2014) Transport of carbon colloid supported nanoscale zero-valent iron in saturated porous media. Journal of Contaminant Hydrology 164, 25-34

Cai, L., Tong, M.P., Ma, H. and Kim, H. (2013) Cotransport of titanium dioxide and fullerene nanoparticles in saturated porous media. Environmental Science & Technology 47(11), 5703-5710.

Carlson, C., Hussain, S.M., Schrand, A.M., Braydich-Stolle, L.K., Hess, K.L., Jones, R.L. and Schlager, J.J. (2008) Unique cellular interaction of silver nanoparticles: size-dependent generation of reactive oxygen species. Journal of Physical Chemistry B 112(43), 13608-13619.

Chae, S.R., Badireddy, A.R., Budarz, J.F., Lin, S.H., Xiao, Y., Therezien, M. and Wiesner, M.R. (2010) Heterogeneities in fullerene nanoparticle aggregates affecting reactivity, bioactivity, and transport. ACS Nano 4(9), 5011-5018.

Chen, L.X., Sabatini, D.A. and Kibbey, T.C.G. (2008) Role of the air-water interface in the retention of TiO_2 nanoparticles in porous media during primary drainage. Environmental Science & Technology 42(6), 1916-1921.

Chen, G.X., Liu, X.Y. and Su, C.M. (2012) Distinct effects of humic acid on transport and retention of TiO_2 rutile nanoparticles in saturated sand columns. Environmental Science & Technology 46(13), 7142-7150.

Cheng, X.K., Kan, A.T. and Tomson, M.B. (2005) Study of C_{60} transport in porous media and the effect of sorbed C_{60} on naphthalene transport. Journal of Materials Research 20(12), 3244-3254.

Chinnapongse, S.L., MacCuspie, R.I. and Hackley, V.A. (2011) Persistence of singly dispersed silver nanoparticles in natural freshwaters, synthetic seawater, and simulated estuarine waters. Science of the Total Environment 409(12), 2443-2450.

Choi, O. and Hu, Z.Q. (2008) Size dependent and reactive oxygen species related nanosilver toxicity to nitrifying bacteria. Environmental Science & Technology 42(12), 4583-4588.

Chowdhury, I., Hong, Y., Honda, R.J. and Walker, S.L. (2011) Mechanisms of TiO_2 nanoparticle transport in porous media: Role of solution chemistry, nanoparticle concentration, and flowrate. Journal of Colloid and Interface Science 360(2), 548-555.

Cobb, M.D. and Macoubrie, J. (2004) Public perceptions about nanotechnology: Risks, benefits and trust. Journal of Nanoparticle Research 6(4), 395-405.

Cornelis, G., Doolette, C., Thomas, M., McLaughlin, M.J., Kirby, J.K., Beak, D.G. and Chittleborough, D. (2012) Retention and dissolution of engineered silver nanoparticles in natural soils. Soil Science Society of America Journal 76(3), 891-902.

Cornelis, G., Pang, L.P., Doolette, C., Kirby, J.K. and McLaughlin, M.J. (2013) Transport of silver nanoparticles in saturated columns of natural soils. Science of the Total Environment 463, 120-130.

Curley, R. (2010) New thinking about pollution, The Rosen Publishing Group, New York.

Darby, J.L. and Lawler, D.F. (1990) Ripening in depth filtration - Effect of particle-size on removal and head loss. Environmental Science & Technology 24(7), 1069-1079.

Debnath, D., Kim, C., Kim, S.H. and Geckeler, K.E. (2010) Solid-state synthesis of silver nanoparticles at room temperature: Poly(vinylpyrrolidone) as a tool. Macromolecular Rapid Communications 31(6), 549-553.

Delay, M., Dolt, T., Woellhaf, A., Sembritzki, R. and Frimmel, F.H. (2011) Interactions and stability of silver nanoparticles in the aqueous phase: Influence of natural organic matter (NOM) and ionic strength. Journal of Chromatography A 1218(27), 4206-4212.

DePaolis, F. and Kukkonen, J. (1997) Binding of organic pollutants to humic and fulvic acids: Influence of pH and the structure of humic material. Chemosphere 34(8), 1693-1704.

Domingos, R.F., Baalousha, M.A., Ju-Nam, Y., Reid, M.M., Tufenkji, N., Lead, J.R., Leppard, G.G. and Wilkinson, K.J. (2009) Characterizing manufactured nanoparticles in the environment: multimethod determination of particle sizes. Environmental Science & Technology 43(19), 7277-7284.

Doshi, R., Braida, W., Christodoulatos, C., Wazne, M. and O'Connor, G. (2008) Nano-aluminum: Transport through sand columns and environmental effects on plants and soil communities. Environmental Research 106(3), 296-303.

Edzwald, J.K. and Tobiason, J.E. (1999) Enhanced coagulation: US requirements and a broader view. Water Science and Technology 40(9), 63-70.

El Badawy, A.M., Luxton, T.P., Silva, R.G., Scheckel, K.G., Suidan, M.T. and Tolaymat, T.M. (2010) Impact of environmental conditions (pH, ionic strength, and electrolyte type) on the surface charge and aggregation of silver nanoparticles suspensions. Environmental Science & Technology 44(4), 1260-1266.

El Badawy, A.M., Scheckel, K.G., Suidan, M. and Tolaymat, T. (2012) The impact of stabilization mechanism on the aggregation kinetics of silver nanoparticles. Science of the Total Environment 429, 325-331.

El Badawy, A.M., Hassan, A.A., Scheckel, K.G., Suidan, M.T. and Tolaymat, T.M. (2013) Key factors controlling the transport of silver nanoparticles in porous media. Environmental Science & Technology 47(9), 4039-4045.

163

Elimelech, M. (1990) The effect of particle size on the kinetics of deposition of Brownian particles in porous media, The Johns Hopkins University, Baltimore.

Elimelech, M. (1992) Predicting collision efficiencies of colloidal particles in porous-media. Water Research 26(1), 1-8.

Elimelech, M. and Omelia, C.R. (1990) Kinetics of deposition of colloidal particles in porous-media. Environmental Science & Technology 24(10), 1528-1536.

Elimelech, M., Jia, X., Gregory, J. and Williams, R. (1998) Particle deposition & aggregation: Measurement, Modeling and Simulation, Butterworth-Heinemann.

Elzey, S. and Grassian, V.H. (2010) Agglomeration, isolation and dissolution of commercially manufactured silver nanoparticles in aqueous environments. Journal of Nanoparticle Research 12(5), 1945-1958.

Environmental_Working_Group (2014). Available at http://www.ewg.org/tap-water/whatsinyourwater/1050/CA/California/Silver-total/.

EPA (1990) Technologies for upgrading existing or designing new drinking water treatment facilities. EPA/625/4-89/023

EPA (1999) Guidance manual for compliance with the interim enhanced water treatment rule: Turbidity provisions. EPA/815/R-99/010

EPA (2014) Integrated Risk Information System. Available at http://www.epa.gov/iris/subst/0099.htm.

Espinasse, B., Hotze, E.M. and Wiesner, M.R. (2007) Transport and retention of colloidal aggregates of C_{60} in porous media: Effects of organic macromolecules, ionic composition, and preparation method. Environmental Science & Technology 41(21), 7396-7402.

Fabrega, J., Luoma, S.N., Tyler, C.R., Galloway, T.S. and Lead, J.R. (2011) Silver nanoparticles: Behaviour and effects in the aquatic environment. Environment International 37(2), 517-531.

Fang, J., Shan, X.Q., Wen, B., Lin, J.M. and Owens, G. (2009) Stability of titania nanoparticles in soil suspensions and transport in saturated homogeneous soil columns. Environmental Pollution 157(4), 1101-1109.

Farokhzad, O.C. and Langer, R. (2009) Impact of nanotechnology on drug delivery. ACS Nano 3(1), 16-20.

Fleischer, M. (1963) Data of Geochemistry (6th ed.), U.S. Government printing office, Washington.

Flory, J., Kanel, S.R., Racz, L., Impellitteri, C.A., Silva, R.G. and Goltz, M.N. (2013) Influence of pH on the transport of silver nanoparticles in saturated porous media: laboratory experiments and modeling. Journal of Nanoparticle Research 15(3), 1484

Foldbjerg, R., Olesen, P., Hougaard, M., Dang, D.A., Hoffmann, H.J. and Autrup, H. (2009) PVP-coated silver nanoparticles and silver ions induce reactive oxygen species, apoptosis and necrosis in THP-1 monocytes. Toxicology Letters 190(2), 156-162.

Franchi, A. and O'Melia, C.R. (2003) Effects of natural organic matter and solution chemistry on the deposition and reentrainment of colloids in porous media. Environmental Science & Technology 37(6), 1122-1129.

Godinez, I.G., Darnault, C.J.G., Khodadoust, A.P. and Bogdan, D. (2013) Deposition and release kinetics of nano-TiO_2 in saturated porous media: Effects of solution ionic strength and surfactants. Environmental Pollution 174, 106-113.

Gondikas, A.P., Morris, A., Reinsch, B.C., Marinakos, S.M., Lowry, G.V. and Hsu-Kim, H. (2012) Cysteine-induced modifications of zero-valent silver nanomaterials: implications for particle surface chemistry, aggregation, dissolution, and silver speciation. Environmental Science & Technology 46(13), 7037-7045.

Gottschalk, F., Sonderer, T., Scholz, R.W. and Nowack, B. (2009) Modeled environmental concentrations of engineered nanomaterials (TiO_2, ZnO, Ag, CNT, fullerenes) for different regions. Environmental Science & Technology 43(24), 9216-9222.

Grassian, V.H. (2008) When size really matters: Size-dependent properties and surface chemistry of metal and metal oxide nanoparticles in gas and liquid phase environments. Journal of Physical Chemistry C 112(47), 18303-18313.

Griffitt, R.J., Luo, J., Gao, J., Bonzongo, J.C. and Barber, D.S. (2008) Effects of particle composition and species on toxicity of metallic nanomaterials in aquatic organisms. Environmental Toxicology and Chemistry 27(9), 1972-1978.

Gueguen, C. and Cuss, C.W. (2011) Characterization of aquatic dissolved organic matter by asymmetrical flow field-flow fractionation coupled to UV-Visible diode array and excitation emission matrix fluorescence. Journal of Chromatography A 1218(27), 4188-4198.

Guzman, K.A.D., Finnegan, M.P. and Banfield, J.F. (2006) Influence of surface potential on aggregation and transport of titania nanoparticles. Environmental Science & Technology 40(24), 7688-7693.

Hahn, M.W. and O'Melia, C.R. (2004) Deposition and reentrainment of Brownian particles in porous media under unfavorable chemical conditions: Some concepts and applications. Environmental Science & Technology 38(1), 210-220.

Han, P., Wang, X.T., Cai, L., Tong, M.P. and Kim, H. (2014) Transport and retention behaviors of titanium dioxide nanoparticles in iron oxide-coated quartz sand: Effects of pH, ionic strength, and humic acid. Colloids and Surfaces A-Physicochemical and Engineering Aspects 454, 119-127.

Hassett, J.P. and Anderson, M.A. (1979) Association of hydrophobic organic-compounds with dissolved organic-matter in aquatic systems. Environmental Science & Technology 13(12), 1526-1529.

He, F., Zhao, D.Y., Liu, J.C. and Roberts, C.B. (2007) Stabilization of Fe-Pd nanoparticles with sodium carboxymethyl cellulose for enhanced transport and dechlorination of trichloroethylene in soil and groundwater. Industrial & Engineering Chemistry Research 46(1), 29-34.

Hepplewhite, C., Newcombe, G. and Knappe, D.R.U. (2004) NOM and MIB, who wins in the competition for activated carbon adsorption sites? Water Science and Technology 49(9), 257-265.

Hofmeister, H., Tan, G.L. and Dubiel, M. (2005) Shape and internal structure of silver nanoparticles embedded in glass. Journal of Materials Research 20(6), 1551-1562.

Hogg, R., Healy, T.W. and Fuersten, D.W. (1966) Mutual coagulation of colloidal dispersions. Transactions of the Faraday Society 62(522P), 1638-1651.

Huber, N., Baumann, T. and Niessner, R. (2000) Assessment of colloid filtration in natural porous media by filtration theory. Environmental Science & Technology 34(17), 3774-3779.

166

Hunter, R.J. (1981) Zeta potential in colloid science, Academic Press, New York.

Huynh, K.A. and Chen, K.L. (2011) Aggregation kinetics of citrate and polyvinylpyrrolidone coated silver nanoparticles in monovalent and divalent electrolyte solutions. Environmental Science & Technology 45(13), 5564-5571.

Hydutsky, B.W., Mack, E.J., Beckerman, B.B., Skluzacek, J.M. and Mallouk, T.E. (2007) Optimization of nano- and microiron transport through sand columns using polyelectrolyte mixtures. Environmental Science & Technology 41(18), 6418-6424.

IHSS (2013) Source materials for International Humic Substances Society samples. Available at http://www.humicsubstances.org/sources.html.

Jaisi, D.P., Saleh, N.B., Blake, R.E. and Elimelech, M. (2008) Transport of single-walled carbon nanotubes in porous media: Filtration mechanisms and reversibility. Environmental Science & Technology 42(22), 8317-8323.

Jaisi, D.P. and Elimelech, M. (2009) Single-walled carbon nanotubes exhibit limited transport in soil columns. Environmental Science & Technology 43(24), 9161-9166.

Jeong, S.W. and Kim, S.D. (2009) Aggregation and transport of copper oxide nanoparticles in porous media. Journal of Environmental Monitoring 11(9), 1595-1600.

Jiang, X.J., Tong, M.P., Lu, R.Q. and Kim, H. (2012) Transport and deposition of ZnO nanoparticles in saturated porous media. Colloids and Surfaces A-Physicochemical and Engineering Aspects 401, 29-37.

Jiang, X.J., Wang, X.T., Tong, M.P. and Kim, H. (2013) Initial transport and retention behaviors of ZnO nanoparticles in quartz sand porous media coated with Escherichia coli biofilm. Environmental Pollution 174, 38-49.

Johnson, W.P., Tong, M. and Li, X. (2007) On colloid retention in saturated porous media in the presence of energy barriers: The failure of alpha, and opportunities to predict eta. Water Resources Research 43(12), W12S13.

Jones, E.H. and Su, C.M. (2012) Fate and transport of elemental copper (Cu-0) nanoparticles through saturated porous media in the presence of organic materials. Water Research 46(7), 2445-2456.

Joo, S.H., Al-Abed, S.R. and Luxton, T. (2009) Influence of carboxymethyl cellulose for the transport of titanium dioxide nanoparticles in clean silica and mineral-coated sands. Environmental Science & Technology 43(13), 4954-4959.

Kaegi, R., Voegelin, A., Sinnet, B., Zuleeg, S., Hagendorfer, H., Burkhardt, M. and Siegrist, H. (2011) Behavior of metallic silver nanoparticles in a pilot wastewater treatment plant. Environmental Science & Technology 45(9), 3902-3908.

Kaegi, R., Voegelin, A., Sinnet, B., Zuleeg, S., Siegrist, H. and Burkhardt, M. (2012) Fate and behavior of silver nanoparticles in urban wastewater systems, Berlin, Germany.

Kanel, S.R., Nepal, D., Manning, B. and Choi, H. (2007) Transport of surface-modified iron nanoparticle in porous media and application to arsenic(III) remediation. Journal of Nanoparticle Research 9(5), 725-735.

Kanel, S.R., Goswami, R.R., Clement, T.P., Barnett, M.O. and Zhao, D. (2008) Two dimensional transport characteristics of surface stabilized zero-valent iron nanoparticles in porous media. Environmental Science & Technology 42(3), 896-900.

Kanel, S.R. and Al-Abed, S.R. (2011) Influence of pH on the transport of nanoscale zinc oxide in saturated porous media. Journal of Nanoparticle Research 13(9), 4035-4047.

Kasel, D., Bradford, S.A., Simunek, J., Heggen, M., Vereecken, H. and Klumpp, E. (2013) Transport and retention of multi-walled carbon nanotubes in saturated porous media: Effects of input concentration and grain size. Water Research 47(2), 933-944.

Key, F.S. and Maass, G. (2001) Ions, atoms and charged particles. Silver Colloids, 1-6.

Khanna, P.K., Singh, N., Kulkarni, D., Deshmukh, S., Charan, S. and Adhyapak, P.V. (2007) Water based simple synthesis of re-dispersible silver nano-particles. Materials Letters 61(16), 3366-3370.

Kim, H.J., Phenrat, T., Tilton, R.D. and Lowry, G.V. (2009) Fe-0 nanoparticles remain mobile in porous media after aging due to slow desorption of polymeric surface modifiers. Environmental Science & Technology 43(10), 3824-3830.

Kim, B., Park, C.S., Murayama, M. and Hochella, M.F. (2010) Discovery and characterization of silver sulfide nanoparticles in final sewage sludge products. Environmental Science & Technology 44(19), 7509-7514.

Kim, H.J., Phenrat, T., Tilton, R.D. and Lowry, G.V. (2012) Effect of kaolinite, silica fines and pH on transport of polymer-modified zero valent iron nano-particles in heterogeneous porous media. Journal of Colloid and Interface Science 370, 1-10.

Kittler, S., Greulich, C., Diendorf, J., Koller, M. and Epple, M. (2010) Toxicity of silver nanoparticles increases during storage because of slow dissolution under release of silver ions. Chemistry of Materials 22(16), 4548-4554.

Laban, G., Nies, L.F., Turco, R.F., Bickham, J.W. and Sepulveda, M.S. (2010) The effects of silver nanoparticles on fathead minnow (*Pimephales promelas*) embryos. Ecotoxicology 19(1), 185-195.

Lau, B.L.T., Hockaday, W.C., Ikuma, K., Furman, O. and Decho, A.W. (2013) A preliminary assessment of the interactions between the capping agents of silver nanoparticles and environmental organics. Colloids and Surfaces a-Physicochemical and Engineering Aspects 435, 22-27.

Lawler, D.F., Mikelonis, A.M., Kim, I., Lau, B.L.T. and Youn, S. (2013) Silver nanoparticle removal from drinking water: flocculation/sedimentation or filtration? Water Science and Technology: Water Supply 13(5), 1181-1187.

Lead, J.R., Wilkinson, K.J., Balnois, E., Cutak, B.J., Larive, C.K., Assemi, S. and Beckett, R. (2000) Diffusion coefficients and polydispersities of the Suwannee River fulvic acid: Comparison of fluorescence correlation spectroscopy, pulsed-field gradient nuclear magnetic resonance, and flow field-flow fractionation. Environmental Science & Technology 34(16), 3508-3513.

Lecoanet, H.F. and Wiesner, M.R. (2004) Velocity effects on fullerene and oxide nanoparticle deposition in porous media. Environmental Science & Technology 38(16), 4377-4382.

Lecoanet, H.F., Bottero, J.Y. and Wiesner, M.R. (2004) Laboratory assessment of the mobility of nanomaterials in porous media. Environmental Science & Technology 38(19), 5164-5169.

Levard, C., Reinsch, B.C., Michel, F.M., Oumahi, C., Lowry, G.V. and Brown, G.E. (2011) Sulfidation processes of PVP-coated silver nanoparticles in aqueous solution: Impact on dissolution rate. Environmental Science & Technology 45(12), 5260-5266.

Levard, C., Hotze, E.M., Lowry, G.V. and Brown, G.E. (2012) Environmental transformations of silver nanoparticles: Impact on stability and toxicity. Environmental Science & Technology 46(13), 6900-6914.

Li, Y.S., Wang, Y.G., Pennell, K.D. and Abriola, L.M. (2008) Investigation of the transport and deposition of fullerene (C_{60}) nanoparticles in quartz sands under varying flow conditions. Environmental Science & Technology 42(19), 7174-7180.

Li, Z., Sahle-Demessie, E., Hassan, A.A. and Sorial, G.A. (2011) Transport and deposition of CeO_2 nanoparticles in water-saturated porous media. Water Research 45(15), 4409-4418.

Li, X. and Lenhart, J.J. (2012) Aggregation and dissolution of silver nanoparticles in natural surface water. Environmental Science & Technology 46(10), 5378-5386.

Li, Z., Hassan, A.A., Sahle-Demessie, E. and Sorial, G.A. (2013) Transport of nanoparticles with dispersant through biofilm coated drinking water sand filters. Water Research 47(17), 6457-6466.

Liang, Z.H., Das, A. and Hu, Z.Q. (2010) Bacterial response to a shock load of nanosilver in an activated sludge treatment system. Water Research 44(18), 5432-5438.

Liang, Y., Bradford, S.A., Simunek, J., Heggen, M., Vereecken, H. and Klumpp, E. (2013a) Retention and remobilization of stabilized silver nanoparticles in an undisturbed loamy sand soil. Environmental Science & Technology 47(21), 12229-12237.

Liang, Y., Bradford, S.A., Simunek, J., Vereecken, H. and Klumpp, E. (2013b) Sensitivity of the transport and retention of stabilized silver nanoparticles to physicochemical factors. Water Research 47(7), 2572-2582.

Liau, S.Y., Read, D.C., Pugh, W.J., Furr, J.R. and Russell, A.D. (1997) Interaction of silver nitrate with readily identifiable groups: relationship to the antibacterial action of silver ions. Letters in Applied Microbiology 25(4), 279-283.

Lin, S.H., Cheng, Y.W., Bobcombe, Y., Jones, K.L., Liu, J. and Wiesner, M.R. (2011) Deposition of silver nanoparticles in geochemically heterogeneous porous media: Predicting affinity from surface composition analysis. Environmental Science & Technology 45(12), 5209-5215.

Lin, S.H., Cheng, Y.W., Liu, J. and Wiesner, M.R. (2012) Polymeric coatings on silver nanoparticles hinder autoaggregation but enhance attachment to uncoated surfaces. Langmuir 28(9), 4178-4186.

Liu, J.J., Xu, Z.H. and Masliyah, J. (2003) Studies on bitumen-silica interaction in aqueous solutions by atomic force microscopy. Langmuir 19(9), 3911-3920.

Liu, X.Y., Wazne, M., Christodoulatos, C. and Jasinkiewicz, K.L. (2009a) Aggregation and deposition behavior of boron nanoparticles in porous media. Journal of Colloid and Interface Science 330(1), 90-96.

Liu, X.Y., O'Carroll, D.M., Petersen, E.J., Huang, Q.G. and Anderson, C.L. (2009b) Mobility of multiwalled carbon nanotubes in porous media. Environmental Science & Technology 43(21), 8153-8158.

Liu, J.Y. and Hurt, R.H. (2010) Ion release kinetics and particle persistence in aqueous nano-silver colloids. Environmental Science & Technology 44(6), 2169-2175.

Liu, X.Y., Chen, G.X. and Su, C.M. (2012) Influence of collector surface composition and water chemistry on the deposition of cerium dioxide nanoparticles: QCM-D and column experiment approaches. Environmental Science & Technology 46(12), 6681-6688.

Long, W. and Hilpert, M. (2009) A correlation for the collector efficiency of Brownian particles in clean-bed filtration in sphere packings by a Lattice-Boltzmann method. Environmental Science & Technology 43(12), 4419-4424.

Lowry, G.V., Espinasse, B.P., Badireddy, A.R., Richardson, C.J., Reinsch, B.C., Bryant, L.D., Bone, A.J., Deonarine, A., Chae, S., Therezien, M., Colman, B.P., Hsu-Kim, H., Bernhardt, E.S., Matson, C.W. and Wiesner, M.R. (2012) Long-term transformation and fate of manufactured Ag nanoparticles in a simulated large scale freshwater emergent wetland. Environmental Science & Technology 46(13), 7027-7036.

Lubick, N. (2008) Nanosilver toxicity: ions, nanoparticles-or both? Environmental Science & Technology 42(23), 8617-8617.

Ma, H.L., Pedel, J., Fife, P. and Johnson, W.P. (2009) Hemispheres-in-cell geometry to predict colloid deposition in porous media. Environmental Science & Technology 43(22), 8573-8579.

MacCuspie, R.I., Rogers, K., Patra, M., Suo, Z.Y., Allen, A.J., Martin, M.N. and Hackley, V.A. (2011) Challenges for physical characterization of silver nanoparticles under pristine and environmentally relevant conditions. Journal of Environmental Monitoring 13(5), 1212-1226.

Malynych, S., Luzinov, I. and Chumanov, G. (2002) Poly(vinyl pyridine) as a universal surface modifier for immobilization of nanoparticles. Journal of Physical Chemistry B 106(6), 1280-1285.

Morones, J.R., Elechiguerra, J.L., Camacho, A., Holt, K., Kouri, J.B., Ramirez, J.T. and Yacaman, M.J. (2005) The bactericidal effect of silver nanoparticles. Nanotechnology 16(10), 2346-2353.

Mu, L. and Sprando, R.L. (2010) Application of nanotechnology in cosmetics. Pharmaceutical Research 27(8), 1746-1749.

NARA (2014) e-CFR Title-40 Part 143.3 Secondary maximum contaminant level. Available at http://www.ecfr.gov/cgi-bin/text-idx?SID=5c2f71fbc4c7e6fc033d5ad9787e0e61&node=40:23.0.1.1.5.0.39.3&rgn=div8.

Nelson, K.E. and Ginn, T.R. (2011) New collector efficiency equation for colloid filtration in both natural and engineered flow conditions. Water Resources Research 47(5), W05543.

Neukum, C., Braun, A. and Azzam, R. (2014) Transport of stabilized engineered silver (Ag) nanoparticles through porous sandstones. Journal of Contaminant Hydrology 158, 1-13.

Nowack, B. and Bucheli, T.D. (2007) Occurrence, behavior and effects of nanoparticles in the environment. Environmental Pollution 150(1), 5-22.

Nowack, B. (2010) Nanosilver revisited downstream. Science 330(6007), 1054-1055.

Panyala, N.R., Pena-Mendez, E.M. and Havel, J. (2008) Silver or silver nanoparticles: a hazardous threat to the environment and human health? Journal of Applied Biomedicine 6(3), 117-129.

Pelley, A.J. and Tufenkji, N. (2008) Effect of particle size and natural organic matter on the migration of nano- and microscale latex particles in saturated porous media. Journal of Colloid and Interface Science 321(1), 74-83.

Petosa, A.R., Jaisi, D.P., Quevedo, I.R., Elimelech, M. and Tufenkji, N. (2010) Aggregation and deposition of engineered nanomaterials in aquatic environments: Role of physicochemical interactions. Environmental Science & Technology 44(17), 6532-6549.

Petosa, A.R., Brennan, S.J., Rajput, F. and Tufenkji, N. (2012) Transport of two metal oxide nanoparticles in saturated granular porous media: Role of water chemistry and particle coating. Water Research 46(4), 1273-1285.

Phenrat, T., Kim, H.J., Fagerlund, F., Illangasekare, T., Tilton, R.D. and Lowry, G.V. (2009) Particle size distribution, concentration, and magnetic attraction affect transport of polymer-modified Fe-0 nanoparticles in sand columns. Environmental Science & Technology 43(13), 5079-5085.

Phenrat, T., Song, J.E., Cisneros, C.M., Schoenfelder, D.P., Tilton, R.D. and Lowry, G.V. (2010) Estimating attachment of nano- and submicrometer-particles coated with organic macromolecules in porous media: Development of an empirical model. Environmental Science & Technology 44(12), 4531-4538.

Project on Emerging Nanotechnologies (2014) Consumer products inventory. Available at http://www.nanotechproject.org/cpi/about/analysis.

Qu, X.L., Alvarez, P.J.J. and Li, Q.L. (2012) Impact of sunlight and humic acid on the deposition kinetics of aqueous fullerene nanoparticles (nC_{60}). Environmental Science & Technology 46(24), 13455-13462.

Rahman, T., George, J. and Shipley, H.J. (2013) Transport of aluminum oxide nanoparticles in saturated sand: Effects of ionic strength, flow rate, and nanoparticle concentration. Science of the Total Environment 463, 565-571.

Rai, M., Tadav, A. and Gade, A. (2008) Silver nanoparticles as a new generation of antimicrobials. Biotechnology Advances 27(1), 76-83.

Raimondi, F., Scherer, G.G., Kotz, R. and Wokaun, A. (2005) Nanoparticles in energy technology: Examples from electrochemistry and catalysis. Angewandte Chemie-International Edition 44(15), 2190-2209.

Rajagopalan, R. and Tien, C. (1976) Trajectory analysis of deep-bed filtration with sphere-in-cell porous-media model. AICHE Journal 22(3), 523-533.

Regulations (2014). Available at http://www.regulations.gov/#!documentDetail;D=CDC-2012-0014-0001.

Rejeski, D., Kulken, T., Pollschuk, P. and Pauwels, E. (2014) The project on emerging nanotechnologies.

Ren, D.J. and Smith, J.A. (2013) Proteinate-capped silver nanoparticle transport in water-saturated sand. Journal of Environmental Engineering-ASCE 139(6), 781-787.

Roalson, S.R., Kweon, J., Lawler, D.F. and Speitel, G.E. (2003) Enhanced softening: Effects of lime dose and chemical additions. Journal American Water Works Association 95(11), 97.

Rottman, J., Sierra-Alvarez, R. and Shadman, F. (2013) Real-time monitoring of nanoparticle retention in porous media. Environmental Chemistry Letters 11(1), 71-76.

Ryan, J.N. and Elimelech, M. (1996) Colloid mobilization and transport in groundwater. Colloids and Surfaces A-Physicochemical and Engineering Aspects 107, 1-56.

Sagee, O., Dror, I. and Berkowitz, B. (2012) Transport of silver nanoparticles (AgNPs) in soil. Chemosphere 88(5), 670-675.

Saleh, N., Sirk, K., Liu, Y.Q., Phenrat, T., Dufour, B., Matyjaszewski, K., Tilton, R.D. and Lowry, G.V. (2007) Surface modifications enhance nanoiron transport and NAPL targeting in saturated porous media. Environmental Engineering Science 24(1), 45-57.

Saleh, N., Kim, H.J., Phenrat, T., Matyjaszewski, K., Tilton, R.D. and Lowry, G.V. (2008) Ionic strength and composition affect the mobility of surface-modified Fe-0 nanoparticles in water-saturated sand columns. Environmental Science & Technology 42(9), 3349-3355.

Schrick, B., Hydutsky, B.W., Blough, J.L. and Mallouk, T.E. (2004) Delivery vehicles for zerovalent metal nanoparticles in soil and groundwater. Chemistry of Materials 16(11), 2187-2193.

Schulz, C.R. and Okun, D.A. (1984) Surface water treatment for communities in developing countries, Wiley, New York.

Serrano, E., Rus, G. and Garcia-Martinez, J. (2009) Nanotechnology for sustainable energy. Renewable & Sustainable Energy Reviews 13(9), 2373-2384.

Shani, C., Weisbrod, N. and Yakirevich, A. (2008) Colloid transport through saturated sand columns: Influence of physical and chemical surface properties on deposition. Colloids and Surfaces A-Physicochemical and Engineering Aspects 316(1-3), 142-150.

Sharp, E.L., Parsons, S.A. and Jefferson, B. (2006) Seasonal variations in natural organic matter and its impact on coagulation in water treatment. Science of the Total Environment 363(1-3), 183-194.

Shen, C.Y., Huang, Y.F., Li, B.G. and Jin, Y. (2008) Effects of solution chemistry on straining of colloids in porous media under unfavorable conditions. Water Resources Research 44(5), W05419

Shen, C.Y., Lazouskaya, V., Jin, Y., Li, B.G., Ma, Z.Q., Zheng, W.J. and Huang, Y.F. (2012) Coupled factors influencing detachment of nano- and micro-sized particles from primary minima. Journal of Contaminant Hydrology 134, 1-11.

Siddiqui, M.S., Amy, G.L. and Murphy, B.D. (1997) Ozone enhanced removal of natural organic matter from drinking water sources. Water Research 31(12), 3098-3106.

Sloane, N.J.A. (1998) Kepler's conjecture confirmed. Nature 395(6701), 435-436.

Solomon, S.D., Bahadory, M., Jeyarajasingam, A.V., Rutkowsky, S.A., Boritz, C. and Mulfinger, L. (2007) Synthesis and study of silver nanoparticles. Journal of Chemical Education 84(2), 322-325.

Solovitch, N., Labille, J., Rose, J., Chaurand, P., Borschneck, D., Wiesner, M.R. and Bottero, J.Y. (2010) Concurrent aggregation and deposition of TiO_2 nanoparticles in a sandy porous media. Environmental Science & Technology 44(13), 4897-4902.

Song, J.E., Phenrat, T., Marinakos, S., Xiao, Y., Liu, J., Wiesner, M.R., Tilton, R.D. and Lowry, G.V. (2011) Hydrophobic interactions increase attachment of gum arabic- and PVP-coated Ag nanoparticles to hydrophobic surfaces. Environmental Science & Technology 45(14), 5988-5995.

Song, Y.J., Wang, M.L., Zhang, X.Y., Wu, J.Y. and Zhang, T. (2014) Investigation on the role of the molecular weight of polyvinyl pyrrolidone in the shape control of high-yield silver nanospheres and nanowires. Nanoscale Research Letters 9(1), 17.

Stankus, D.P., Lohse, S.E., Hutchison, J.E. and Nason, J.A. (2011) Interactions between natural organic matter and gold nanoparticles stabilized with different organic capping agents. Environmental Science & Technology 45(8), 3238-3244.

Sun, Y.G. and Xia, Y.N. (2002) Shape-controlled synthesis of gold and silver nanoparticles. Science 298(5601), 2176-2179.

Suresh, L. and Walz, J.Y. (1996) Effect of surface roughness on the interaction energy between a colloidal sphere and a flat plate. Journal of Colloid and Interface Science 183(1), 199-213.

Taghavy, A., Mittelman, A., Wang, Y.G., Pennell, K.D. and Abriola, L.M. (2013) Mathematical modeling of the transport and dissolution of citrate-stabilized silver nanoparticles in porous media. Environmental Science & Technology 47(15), 8499-8507.

Tejamaya, M., Romer, I., Merrifield, R.C. and Lead, J.R. (2012) Stability of citrate, PVP, and PEG coated silver nanoparticles in ecotoxicology media. Environmental Science & Technology 46(13), 7011-7017.

Tian, Y., Gao, B., Silvera-Batista, C. and Ziegler, K.J. (2010) Transport of engineered nanoparticles in saturated porous media. Journal of Nanoparticle Research 12(7), 2371-2380.

Tian, Y., Gao, B., Wang, Y., Morales, V.L., Carpena, R.M., Huang, Q.G. and Yang, L.Y. (2012) Deposition and transport of functionalized carbon nanotubes in water-saturated sand columns. Journal of Hazardous Materials 213, 265-272.

Tiraferri, A. and Sethi, R. (2009) Enhanced transport of zerovalent iron nanoparticles in saturated porous media by guar gum. Journal of Nanoparticle Research 11(3), 635-645.

Tobiason, J.E. (1987) Physicochemical aspects of particle deposition in porous media, Johns Hopkins University, Baltimore, MD.

Tolaymat, T.M., El Badawy, A.M., Genaidy, A., Scheckel, K.G., Luxton, T.P. and Suidan, M. (2010) An evidence-based environmental perspective of manufactured silver nanoparticle in syntheses and applications: A systematic review and critical appraisal of peer-reviewed scientific papers. Science of the Total Environment 408(5), 999-1006.

Torkzaban, S., Bradford, S.A., Wan, J.M., Tokunaga, T. and Masoudih, A. (2013) Release of quantum dot nanoparticles in porous media: Role of cation exchange and aging time. Environmental Science & Technology 47(20), 11528-11536.

Tosco, T., Bosch, J., Meckenstock, R.U. and Sethi, R. (2012) Transport of ferrihydrite nanoparticles in saturated porous media: Role of ionic strength and flow rate. Environmental Science & Technology 46(7), 4008-4015.

Tripathi, S., Champagne, D. and Tufenkji, N. (2012) Transport behavior of selected nanoparticles with different surface coatings in granular porous media coated with *Pseudomonas aeruginosa* biofilm. Environmental Science & Technology 46(13), 6942-6949.

Tufenkji, N. and Elimelech, M. (2004) Correlation equation for predicting single-collector efficiency in physicochemical filtration in saturated porous media. Environmental Science & Technology 38(2), 529-536.

Tufenkji, N. and Elimelech, M. (2005) Breakdown of colloid filtration theory: Role of the secondary energy minimum and surface charge heterogeneities. Langmuir 21(3), 841-852.

Vanoss, C.J., Giese, R.F. and Costanzo, P.M. (1990) DLVO and Non-DLVO interactions in hectorite. Clays and Clay Minerals 38(2), 151-159.

Vincent, B., Edwards, J., Emmett, S. and Jones, A. (1986) Depletion flocculation in dispersions of sterically-stabilized particles (soft spheres). Colloids and Surfaces 18(2-4), 261-281.

Wagener, P., Schwenke, A. and Barcikowski, S. (2012) How citrate ligands sffect nanoparticle adsorption to microparticle supports. Langmuir 28(14), 6132-6140.

Walser, M. (1961) Ion association .5. Dissociation constants for complexes of citrate with sodium, potassium, calcium, and magnesium ions. Journal of Physical Chemistry 65(1), 159-161.

Wang, H.C. and Kasper, G. (1991) Filtration efficiency of nanometer-size aerosol-particles. Journal of Aerosol Science 22(1), 31-41.

Wang, Y.G., Li, Y.S., Fortner, J.D., Hughes, J.B., Abriola, L.M. and Pennell, K.D. (2008a) Transport and retention of nanoscale C_{60} aggregates in water-saturated porous media. Environmental Science & Technology 42(10), 3588-3594.

Wang, Y.G., Li, Y.S. and Pennell, K.D. (2008b) Influence of electrolyte species and concentration on the aggregation and transport of fullerene nanoparticles in quartz sands. Environmental Toxicology and Chemistry 27(9), 1860-1867.

Wang, P., Shi, Q.H., Liang, H.J., Steuerman, D.W., Stucky, G.D. and Keller, A.A. (2008c) Enhanced environmental mobility of carbon nanotubes in the presence of humic acid and their removal from aqueous solution. Small 4(12), 2166-2170.

Wang, L.L., Huang, Y., Kan, A.T., Tomson, M.B. and Chen, W. (2012a) Enhanced transport of 2,2',5,5'-polychlorinated biphenyl by natural organic matter (NOM) and surfactant-modified fullerene nanoparticles (nC_{60}). Environmental Science & Technology 46(10), 5422-5429.

Wang, C., Bobba, A.D., Attinti, R., Shen, C.Y., Lazouskaya, V., Wang, L.P. and Jin, Y. (2012b) Retention and transport of silica nanoparticles in saturated porous media: Effect of concentration and particle size. Environmental Science & Technology 46(13), 7151-7158.

Wang, Y., Gao, B., Morales, V.L., Tian, Y., Wu, L., Gao, J., Bai, W. and Yang, L.Y. (2012c) Transport of titanium dioxide nanoparticles in saturated porous media under various solution chemistry conditions. Journal of Nanoparticle Research 14(9), 1095.

Wang, Y.G., Zhu, H.G., Becker, M.D., Englehart, J., Abriola, L.M., Colvin, V.L. and Pennell, K.D. (2013) Effect of surface coating composition on quantum dot mobility in porous media. Journal of Nanoparticle Research 15(8), 1805.

Wen, L.S., Santschi, P.H., Gill, G.A. and Tang, D.G. (2002) Silver concentrations in Colorado, USA, watersheds using improved methodology. Environmental Toxicology and Chemistry 21(10), 2040-2051.

WHO (2003) Silver in drinking-water. Available at http://www.who.int/water_sanitation_health/dwq/chemicals/silver.pdf.

Wijnhoven, S.W.P., Peijnenburg, W.J.G.M., Herberts, C.A., Hagens, W.I., Oomen, A.G., Heugens, E.H.W., Roszek, B., Bisschops, J., Gosens, I., Van de Meent, D., Dekkers, S., De Jong, W.H., Van Zijverden, M., Sips, A.J.A.M. and Geertsma, R.E. (2009) Nano-silver - a review of available data and knowledge gaps in human and environmental risk assessment. Nanotoxicology 3(2), 109-138.

Wood, C.M., Playle, R.C. and Hogstrand, C. (1999) Physiology and modeling of mechanisms of silver uptake and toxicity in fish. Environmental Toxicology and Chemistry 18(1), 71-83.

Xiao, Y. and Wiesner, M.R. (2013) Transport and retention of selected engineered nanoparticles by porous media in the presence of a biofilm. Environmental Science & Technology 47(5), 2246-2253.

Xiu, Z.M., Zhang, Q.B., Puppala, H.L., Colvin, V.L. and Alvarez, P.J.J. (2012) Negligible particle-specific antibacterial activity of silver nanoparticles. Nano Letters 12(8), 4271-4275.

Yang, J., Bitter, J.L., Smith, B.A., Fairbrother, D.H. and Ball, W.P. (2013) Transport of oxidized multi-walled carbon nanotubes through silica based porous media: Influences of aquatic chemistry, surface chemistry, and natural organic matter. Environmental Science & Technology 47(24), 14034-14043.

Yang, X.Y., Lin, S.H. and Wiesner, M.R. (2014) Influence of natural organic matter on transport and retention of polymer coated silver nanoparticles in porous media. Journal of Hazardous Materials 264, 161-168.

Yao, K.M., Habibian, M.M. and Omelia, C.R. (1971) Water and waste water filtration - Concepts and applications. Environmental Science & Technology 5(11), 1105-1112.

Zhan, J.J., Zheng, T.H., Piringer, G., Day, C., McPherson, G.L., Lu, Y.F., Papadopoulos, K. and John, V.T. (2008) Transport characteristics of nanoscale functional zerovalent iron/silica composites for in situ remediation of trichloroethylene. Environmental Science & Technology 42(23), 8871-8876.

Zhang, W., Yao, Y., Li, K.G., Huang, Y. and Chen, Y.S. (2011) Influence of dissolved oxygen on aggregation kinetics of citrate-coated silver nanoparticles. Environmental Pollution 159(12), 3757-3762.

Zhang, T. (2012) Modeling of nanoparticle transport in porous media, The University of Texas at Austin.

179

Zhang, W., Isaacson, C.W., Rattanaudompol, U.S., Powell, T.B. and Bouchard, D. (2012a) Fullerene nanoparticles exhibit greater retention in freshwater sediment than in model porous media. Water Research 46(9), 2992-3004.

Zhang, L.L., Hou, L., Wang, L.L., Kan, A.T., Chen, W. and Tomson, M.B. (2012b) Transport of fullerene nanoparticles (nC_{60}) in saturated sand and sandy soil: Controlling factors and modeling. Environmental Science & Technology 46(13), 7230-7238.

Zhu, W., Bartos, P.J.M. and Porro, A. (2004) Application of nanotechnology in construction - Summary of a state-of-the-art report. Materials and Structures 37(273), 649-658.

Zhuang, J., Qi, J. and Jin, Y. (2005) Retention and transport of amphiphilic colloids under unsaturated flow conditions: Effect of particle size and surface property. Environmental Science & Technology 39(20), 7853-7859.

Zularisam, A.W., Ismail, A.F. and Salim, R. (2006) Behaviours of natural organic matter in membrane filtration for surface water treatment - a review. Desalination 194(1-3), 211-231.

Vita

Ijung Kim was born in Seoul, Korea in 1980. After graduating from Daewon Foreign Language High School in 1999, he received a bachelor's and master's degree in Civil and Environmental Engineering from Korea Advanced Institute of Science and Technology, Daejeon, Korea in 2003 and 2005, respectively. He worked as a research scientist at Korea Institute of Science and Technology, Seoul, Korea from 2005 to 2009. He started his Ph.D. study in the Department of Civil, Architectural and Environmental Engineering at the University of Texas at Austin in the fall of 2009.

Permanent address: 566 Sangdo 1 dong, Dongjak gu, Seoul, Korea (156-830)

Email address: kistkij@gmail.com or ijungkim@utexas.edu

This dissertation was typed by the author.